VALIDATION AND ASSESSMENT OF A CFD METHODOLOGY FOR FIRE SAFETY ENGINEERING APPLICATIONS

LUCA IANNANTUONI

Doctoral Programme in Energy

Department of Energy
Politecnico di Milano

March 2012 – XXIII Cycle

Tutor
Prof. Pierangelo Andreini
Supervisor
Prof. Alfonso Niro
Chair of Doctoral Programme
Prof. Carlo E. Bottani

Luca Iannantuoni: *Validation and assessment of a CFD methodology for Fire Safety Engineering applications,* Doctoral Programme in Energy, © March 2012

Version 1.0 - This thesis was typeset with LaTeX, running on GNU/Linux. Graphics were produced with python using chaco, matplotlib and mayavi libraries.

A man is but the product of his thoughts,
what he thinks, he becomes.

— **Mahatma Gandhi**

Expect problems,
and eat them for breakfast.

— A.M.

ACKNOWLEDGMENTS

I want to say thanks to all the people that gave me strength, motivation and any kind of support during this years, especially to my colleague Ing. Daniele Ettorre and Prof. Lucio Araneo for the contributions in spray modeling and experimental activities that was of paramount importance for this work; PhD. Giovanni Manzini and Prof. Pierangelo Andreini for the opportunity given to me to apply in such fascinating field of research, starting with my Master Thesis in Mechanical Engineering; Prof. Carlo Ortolani and Prof. Adriano Muzzio for chattering upon crucial topics related to my activity; Ing. Eugenio Galli and Ing. Donato Andrea Paradiso of Metropolitana Milanese S.p.a. for the work done together and for the confidence shown all along; Yi Wang from Factory Mutual for the help with OpenFOAM™, Ing. Andrea Ferrari from Hughes Associates Europe and Luciano Nigro from Marioff Italy for having promoted this research concretely.

CONTENTS

LIST OF FIGURES

LIST OF TABLES

Part I

SETTING THE SCENE

1

INTRODUCTION

In the Fire Safety Engineering (FSE), when standard requirements do not provide a good establishment, the Performance Based Design (PDB) approach is the most effective solution to design protection systems for civil buildings and infrastructures. This circumstance often occurs for historical buildings, for huge or complex buildings and for tunnels. The present work focuses in particular about road and subway tunnels, because of the rapid increase of underground transportation systems demand and of their emergency management due to the high risk of fires.

There are two major areas of interest for FSE analysis of that systems: the thermal response of structures and the efficacy of smoke management strategies. In fact, smoke can travel within a tunnel rapidly and it is the most hazardous factor to human beings and structures; therefore the main focus is on smoke management. Three different kinds of methodologies have been classified as basic tools to study the smoke propagation in case of fire: pseudo-thermal scale models, full scale tests and numerical models.

Experimental activities are difficult because they are expensive. It is expensive designing smoke management systems with full-scale fire tests because these systems would require covering all possible scenarios including all necessary computational design tools.

There is an increasing demand for performance-based design in this field, due to the various benefits from this approach. Fire performance strategy is highly assessed to maintain a safe environment for occupants to escape and to preserve structures.

To determine whether the system is effective the criteria is defined and scrutinized. Anytime the hypothesis significantly changes during

its lifecycle, the system's performance needs be checked to verify that the safety criteria are met.

Up to now, there are not well established guidelines for applying the PBD approach to address the huge variety of system design optimizations, but it is well known that among other computational techniques, CFD methodologies are more promising to forecast the evolution of a given fire scenario to verify, maintain or improve the required safety levels of the proposed fire-fighting strategy; they play a significant role when analyzing fire consequences, specifically where complex flows need to be resolved.

The International Standard Organization (ISO) published the ISO/TR 13387 as a guideline to such methodologies, since the PBD approach in FSE it is an effective way to improve safety levels in civil buildings and infrastructures, overcoming obsolete or unsuitable practices, and to give an impulse to research in the field, but the standard explicitly don't cover all the needed aspects and so a strong effort is needed to achieve confidence.

The present work deals with this class of problems, which is commonly identified as fire dynamic simulation, and it aims to address typical fire scenarios of interest in FSE, regarding some of the main aspects connected with design purposes.

Emergency strategies assessment is of primary importance and since the strategies involve one or more active systems to provide smoke and fire control, a deep understanding of their own and mutual influences on the consequences of the fire is of paramount interest. This is hardly done by experiments, since ventilation systems and water spray systems effectiveness depends upon a great number of parameters.

Water mist systems are very interesting because they are a promising and innovative technology for tunnel applications (they are effective in pool fires suppression, air disruption and oxygen depletion, etc..) but up to now few experiments were carried out and there are no standards for their application in tunnel fire fighting design.

The other important aspect which is not well covered by standards and for which CFD simulation come in help, and that is investigated in the present work, is the design of ventilation shafts for smoke management (with a focus on natural ventilation, since it is a good opportunity because it doesn't require mechanical equipment to be installed and started to evacuate hot combustion products). Different smoke strategies are used to keep clean from smokes emergency evacuation paths and it is unpractical to carry on experiments determining the influence of the all parameters that affects, for instance, the estimation of the Available Safe Egress Time (ASET) in a particular configuration of a subway station during its design stage, because of the great number of them and the fact that may vary significantly.

Hence, CFD simulations are carried on with the primary intent to help the lack of experiments in the design and optimization of these systems.

A particular attention is given to water mist systems, since they seem to be very efficient for tunnel applications, despite of common sprinkler systems. Within this research a common commercial water mist spray model's performance is investigated after a previous evaluation of the nozzle and spray characteristics. Through the validation of a proper numerical set-up it is possible to minimize the high uncertainty that affect the description of the scenario, in particular regarding wall layer resolution, thermal exchange and spray characteristic, mass and momentum exchange. To do such analysis, the characterization, validation and assessment of the model is of paramount importance and the literature available on the subject is unsatisfactory to carry on an analysis on stratification of smoke due to water discharge, which may implicate danger for people evacuating due to water cooling. These scenario can be split into two areas, those related to natural ventilation design in subway systems, and those related to water mist effect on smoke in road tunnel fire fighting strategies. These two scenarios are selected because they state a comprehensive description of all the relevant phenomena involved

in fire simulations. As few experimental data exist relating to water mist and there is no established empirical understanding concerning them, this thesis will use a series of related scenarios to validate the numerical set-up for fire simulations and through experimental activity to characterize a water mist spray for further assess its numerical description.

There is not one simple procedure when evaluating different operating conditions because of the many variables involved; therefore a comprehensive overview of all aspects involved is out of the scope of this work. Although, the presented methodologies are capable to evaluate the consequences of design parameters in order to be applied as a tool for system's performance optimization. A rigorous approach have been applied in order to ensure, where possible: grid independence, reproducibility, sensitivity of the model (with particular reference to water spray simulation) and results were backed by experimental validation whenever it was possible. In fact, buoyancy driven flows induced by fire require a validated numerical set up to forecast natural ventilation scenarios to assure the minimum possible uncertainty. For this reason small-scale and large scale compartment fire tests are used to support simulation results.

2

CFD FIRE MODELING

2.1 CFD FIRE SIMULATION

The ISO/TR 13387 distinguish numerical codes essentially in zone models and field models and remand to other sources for details on their specific evaluation of capabilities [2, 3]. The zone models are based generally upon a simplified description of geometries and physics and are not considered in the present study, since the degree of uncertainty is much more high than with fields models. Fields models attempt to represent the real geometries and accurate description of the phenomena involved in the scenario and are synonymous for CFD codes. A realistic CFD model might represent in fact all the relevant phenomena involved, and to do so many sub-models are needed, according to basic assumptions and approaches whose refer to different kind of methods. In this study the Finite Volume approach is adopted for the gas phase description; a turbulence model is needed because the combustion processes involved with typical fire scenarios occur as diffusive turbulent combustion processes; a Lagrangian Discrete Phase Model (DPM) is used to model a water mist spray, a radiation model is needed because of its relative importance, although it may be very difficult to resolve it, (as the finite volume discrete ordinance model, fvDOM) and of course a combustion model (the Eddy Break-up Model, EBU). An open source CFD toolbox called OpenFOAM™ was chosen, which own all its features and, even more, allow an easy customization of the solver and of the sub-models. During the work the version 1.7 was used, which differs for minor changes respect to the up-to-date 2.1 version, for what regards the applications presented in this thesis. The applied solver,

which since 2010 belong to the standard distribution of the code, is called fireFoam and has been interested also in recent publications Pro [38].

2.2 GOVERING EQUATIONS

To deal with a compressible multiphase turbulent flow a set of governing equations is needed to represent the continuity equation, the momentum equation, the energy equation plus the equation of state and interphase modeling equation (i.e. to account evaporation and drag). The model resolve a set of transport equation for every species that is needed to be accounted for, and each of them can be represented with the generalized equation for the transport of a generic scalar, as stated in Equation 1.

$$\frac{\partial(\rho\phi)}{\partial t} + \nabla(\rho\phi\mathbf{u}) = \nabla(\Gamma\nabla\phi) + S_\phi + S_\phi^d \tag{1}$$

where

$\frac{\partial(\rho\phi)}{\partial t}$	rate of increase
$\nabla(\rho\phi\mathbf{u})$	net rate of flow
$\nabla(\Gamma\nabla\phi)$	rate of increase due to diffusion
Γ	molecular (kinematic) diffusion coefficient
ρ	density
S_ϕ	rate of increase due to sources
S_ϕ^d	rate of increase due to interphase change

2.3 COMBUSTION MODELING

Fire is an eso-thermal reaction process (combustion) that occurs when a fuel and an oxidiser (oxygen) are bought together in certain concentrations and an ignition occours that lead in some point a sufficient amount of energy to activate an extremely complex chemestry. For a

given quantity of fuel, the minimum quantity of oxigen required is determined by the balanced global chemical equation for the considered specie.

$$CH_4 + 2O_2 \rightarrow 2H_2O + CO_2 \tag{2}$$

Usually the oxygen which takes part to the combustion process is atmospheric oxygen – which constitutes approximately the 20.9 by volume and it is common to express the stoichiometric ratio as an air to fuel ratio. (e.g. for methane $17.2 kg_{air}/kg_{fuel}$ as calculated from equation 2). The global equations should be very useful to describe the most important phenomena related to heat exchange and smoke production, but the underlaying mechanisms for the oxidation of methane contains 177 separate reaction steps. A further 67 steps can be added if atmospheric nitrogen is also considered. For example, carbon monoxide is converted to carbon dioxide in a temperature dependent reversible reaction. Fires where the air supply is less than stoichiometric are said to be rich in fuel or ventilation controlled, and the overall rate of combustion is determined by the ventilation rate. The lack of oxygen means that some of the reaction steps will not complete, and the products of combustion will contain partly burnt fuel, and compounds such as carbon monoxide or NO_X (various nitrogen oxides). Fires where the air supply is greater than stoichiometric are said to be air rich or fuel controlled. The rate of reaction is determined by the rate of fuel release. Fires are usually classified according to the heat release rate and the species mixture of the fuel involved. Although combustion is a process that occur where substances are in the gaseous phase, the mass source of the fuel is more often a liquid or a solid material. Heat feedback from the flames allows the pyrolisys reactions which lead to the volatilization of fuel creating a self-sustaining process. The term volatilize in fact refers to a complex of inter-dependent processes such as evaporation, sublimation and chemical decomposition. Pool fires and jet fires are

the most used kind of fires in research and experimentation because of their well defined and scalable behavior, where usually a pure substance is burned respectively with a fixed surface area or a fixed mass flux, in order to assure a near constant RHR. In the presented applications, because design fire were prescribed in order to account for a certain RHR without any indication about the materials involved, a methane reaction was used to describe the combustion process. Fires where the fresh air supply (rich in oxydizer) is less than stoichiometric are said to be fuel rich or ventilation controlled fires, and the overall rate of combustion is then determined by the ventilation rate. The lack of oxydizer signify that the reaction mechanism won't complete and so the products of combustion will contain partly burnt fuel and compounds such as carbon monoxide. High temperature rates also involve the usual inert nitrogen that constitutes the ambient air leading to the production of NOx (various nitrogen oxides). Fires where the air supply is greater than stoichiometric values are defined sustained by a rich mixture or fuel controlled. Ignition is defined as the onset or initiation of combustion, while the extinction correspond to the end of the process. In FSE referring to fire-fighting systems, control and suppression of combustion are defined as phenomena related to the efficacy of a certain strategy to contain or reduce the RHR of a prescribed fire. Control and suppression are not addressed in the present study due to the high uncertanty involved in detailed combustion chemistry. In non pre-mixed combustion the reaction is mixing-controlled and the non-dimensional Damköhler number is the ratio of the mixing time (or turbulence timescale) and reaction time (or chemical timescale). Mixing controlled reactions so as that of diffusive combustion correspond to $Da \gg 1$.

$$Da = \frac{\tau_t}{\tau_c} \tag{3}$$

where

τ_t turbulence time scale

τ_c chemical time scale

The most important phenomena of fire dynamics are of course related to the buoyancy forces generated. Since a quasi-stationary low momentum flow, buoyancy forces increase due to the density gradient and this intensity is accounted for usually with the Froude number, which measures the ratio of kinetic forces to buoyancy forces. This might be a way to classify a certain structure of the plume for a particular kind fire, usually represented divided into three parts: a persistent flame, an intermittent flame and the buoyant plume [12].

The turbulent combustion of a typical design fire (usually a pool fire of liquid or gasous equivalent single component species) for typical FSE applications may be described sufficiently well with the Eddy Dissipation Model (EDM) proposed originally by Magnussen and Hjertager[31].

The chimestry of the combustion, since the design fire for many purposes it's usually described with an equivalent fire of a single component specie, to avoid the uncertainty associated with pyrolysis modeling of complex materials, is a infinitly-fast one step reaction, in order to assure the heat release rate would be its nominal value (of course if oxygen is available fro the combustion to occur), without pretending to predict the formation of intermediate products, which very difficult to validate because of the lack of experimental data, and difficult to resolve, due to the small time and space scale of chemistry and the inherent complexity of combustion reaction chains.

In the model of Magnussen, the consumption rate of reactants is basically determined upon turbulence mixing hypothesis and its given by the Equation 4

$$\overline{\rho\dot{\omega}} = C\overline{\rho}\frac{1}{\tau_t} min\left(\tilde{Y}_F, \frac{\tilde{Y}_O}{s}, \beta\frac{\tilde{Y}_P}{(1+s)}\right) = C\overline{\rho}\frac{\epsilon}{k} min\left(\tilde{Y}_F, \frac{\tilde{Y}_O}{s}, \beta\frac{\tilde{Y}_P}{(1+s)}\right) \tag{4}$$

where

$\overline{\rho\dot{\omega}}$ fuel consumption rate

Y_O oxygen mass fraction

Y_F fuel mass fraction

Y_P product mass fraction

s stoichiometric ratio

τ_t turbulent mixing time scale

ϵ turbulence dissipation rate

k turbulence kinetic energy

Ce β are empirical constant set respectively to 4 and 1 according to the author and the tilde states for Favre averages notation, Reynolds averages may be used as well. The chemical reactions so take place controlled by the turbulence mixing for values of $k/\varepsilon > 0$, limited by the species with the lower concentration, according to the global reaction of combustion that describe the species involved. The model is strongly dependent on turbulent resolution and the limitations are essentially due to the fact that there is no temperature dependence, so it is valid where the temperatures is sufficiently high for the chemical timescale to be far shorter than the mixing timescale. It is suitable only for one or two-step reaction mechanisms and the model constant are not well understood and the values used here refer to methane combustion and usually they varies form 1 to 7. The mixture fraction combustion model (usually with PDF approach), the Arrhenius model are other well established model that are not considered in this research.

2.4 RADIATION MODELING

Radiative heat transfer plays a significant role in the thermal behavior of the fire scenario, particularly nearby the plume, where the highest temperatures are reached. The surfaces surrounding the fire may be properly characterized in terms of optical properties, and a soot

model may provide a nearly acceptable representation of the smoke in terms of radiative emission, absorption and scattering. During the literature review the most significant work were found in the field of the internal combustion engine modeling, which has different purposes an analysis and fairly small domains to mesh. In fact the radiation transmission is computationally expensive, and in large domains often it has to be limited to certain regions of interest or neglected, because of its relative small impact in the most common fire scenarios. When radiative exchange is neglected (and this is very common in CFD analysis for average temperatures generally below the 500 K because of its relatively small impact, often radiation is accounted as a fraction of the heat release rate that is confined in a relatively small portion of the domain, the great part of it sustaining a combustion which is indeed imposed by the design fire. Usually values of the radiation fraction of energy release vary in literature from around 30 to 35%. If radiation is neglected to assure energy balance the energy released during the combustion process determines higher gas temperatures with the consequence of overestimate the spread of smoke. This issue has found to be overcome in literature by reducing the fire size of the radiative quota, and thus prescribing an equivalent "convective" heat release rate. It is important to point out that if such approach is followed, then also the smoke production is reduced proportionally, leading to a counter-underestimation of the spread of smoke and of the concentration of combustion products. In all of the application presented in this study radiation has been taken into account. Radiative heat transfer is calculated with the intention not to arbitrary account for the radiation losses avoid the uncertain strategy of imposing an "equivalent" convective heat release rate, and not to pretend to accurately predict radiative heat fluxes. In fact radiation acts through electromagnetic waves and is function of many parameters, such as surface reflectivity, emissivity, temperature, and geometric properties and orientation with respect to other thermally participating objects (as flames and soot). Moreover, the optical properties of

the surfaces are function of other surface properties as roughness, finish and composition, whose may vary in an unpredictable manner while the fire occurs. There are two different radiation models available in OpenFOAM (TM) up to now, the well known P1 model and the finite volume Discrete Ordinate Method (fvDOM). They are both based upon the Radiative Transport Equation (RTE) which is described and eventually numerically optimized in a convenient general abstract class, while just the determination of the source terms is demanded to the specific radiation model of choice. In case that no radiation is computed, the source terms are set to zero in the RTE equations. While the fvDOM method may be more computationally expensive that the P1 model, it is more comprehensive, allowing for the account of scattering, semi-transparent media, specular surfaces, and wavelength-dependent transmission using banded-gray optical properties evaluation of gas mixtures. The fvDOM is the radiation model applied in this study, and since the radiative heat transfer equation is solved for a finite number of solid angles which has to be defined in advance, sensitivity study was conducted in order to assess a good compromise, since the computational cost increases a lot with big meshes, that often occur in the analysis of complex fire scenarios. The model uses the same spatial and temporal discretization as the fluid domain, but with additional arbitrary angular discretizations to calculate radiation intensity, which increases due to emission within the cell, and internal scattering from other directions, but decreases due to absorption and scattering from the outside.

2.5 TURBULENCE MODELING

Turbulence aspects of CFD simulations fairly exceed the purpose of the present work, and because of the fundamental influence of turbulence modeling in fire simulations and the fact that Direct Numerical Simulations (DNS) cannot be performed, the most used models in the

field (the standard $k-\epsilon$ and the LES) were tested in under to compare them among the same grid resolutions, adapted to achieve good and comparable results from the both. The standard $k-\epsilon$ model refer to the Reynolds Averaged Navier-Stokes (RANS) approach, which is well-established and was proposed by Launder and Spalding (1974), and belong to the class of two-equation models. Two-equation models are based on the assumption of isotropic turbulence, and therefore only need two additional equations to be mathematically complete. The theory behind is based on the fact that turbulence causes an increase in the effective viscosity of the fluid, and this extra-viscosity is derived and calculated from turbulent kinetic energy, k, and its rate of dissipation ϵ. The weakness of this model is that, as a RANS model, it only captures the average characteristics of the flow, and it is very difficult to adapt numerical constant to address the specific problem. Large Eddy Simulations (LES) are conceptually in between DNS and RANS approach. Large eddies (accordingly to the grid resolution) are resolved directly, whilst small eddies are modeled similar that in the RANS approach (or in the same way in Detached-LES). There are many reason because this approach is much more promising (despite the higher computational cost) and the most important one is that large eddies are directly correlated with the geometries surrounding the fluid field, and the main characteristic of the flow are in fact affected mostly by large eddies. LES simulations allow to still have informations about the fluctuation of the variables and perform undoubtably better for transient simulations.

2.6 WATER SPRAYS

In order to characterize and describe water sprays with CFD codes, many different break-up models have been developed to account for atomization process, both for primary and secondary instabilities that may rise from liquid-gas interactions. The validation of these mod-

els has been performed backed up with experimental data for non-evaporating, evaporating and reacting sprays under controlled conditions, most of all for combustion processes. These models need to be adapted for a particular spray description and are not generally applicable just on the basis of the geometries and operating parameters of the water spray nozzle of interest. So the initial condition for the spray are set usually after the primary atomization process, prescribing a size distribution and velocities based on experimental data, according to the fact that the atomization process won't be accounted at all, avoid all the uncertainty associated to capture the first break-up, fundamental to reproduce the spray patterns.

There are two main approaches to two-phase flow computation with the finite volume method: the Eulerian-Eulerian (EE) and the Eulerian-Lagrangian (EL). They both involve usually a fully two-way coupling of the separate sets of equations that describe the continuum and the dispersed phase dynamic, in order to account for the momentum exchange in between them and the mass exchange due to phase transition. The both approaches have been demonstrated to be equivalent to simulate spray dynamic, although there are strong differences on their respective fundamental hypothesis and assumptions. In fact according to Sirignano Sirignano [42] the EE approach, however the formulation, assumes that the volumetric concentration of the dispersed phase is sufficiently high, and this critical value has been set around 10^{-4}, which is much more that the estimated local concentrations that a sprinkler or a water mist sprays may produce in the volume of the ideal cone occupied by the droplets, since few centimeters from the orifices. It is also sufficiently far from the nozzle that measurements can be done with the most common techniques and where the droplets dynamic becomes of primary importance for the evolution of the fire scenario. So for this kind of application the standard approach ios the EL approach. Alternative approaches that may reduce compitational costs, such as EE method with the Method of Moments that are often applied for the description of the flow

dynamics need closure models, for example related to phase interactions, that are not straightforward and not based on a deterministic approach. So the EL approach seems undoubtedly the one of choice. The most widely used EL formulation is known as the Discrete Droplet Model (DDM) or Discrete Particle Model (DPM) [11], in which the carrier gas is described by the eulerian fluid equations of section 2.2 and a new system of equations is resolved to track the trajectory of representative particles.

In fact in the DDM the physical particles are accounted in representative numerical droplets, called parcels, for whose the trajectory is determined by the solution of a momentum balance equation which is largely dominated by gravity, buoyancy and aerodynamic drag, as in equation 5.

$$\frac{du_d}{dt} = F_D\,(u - u_d) + \frac{g(\rho_d - \rho)}{\rho_d} + F_s \tag{5}$$

where

$\frac{du_p}{dt}$ particle acceleration

F_D friction factor

g gravitational acceleration

u gas velocity

u_d droplet velocity

ρ gas density

ρ_d droplet density

The drag coefficient C_D which determine the friction factor is calculated on the hypothesis of sferical particles according to the a specific drag model. The drag coefficient is calculated from the Stoke's law, which ignores inertial terms and it is defined in Equation and it gives the drag force for a particle of radius r in a stationary fluid, while the drag force opposes the motion of the droplets. A spherical drop may be significantly affected by deformation due to acceleration, because it may be flattened by the drag forces. The deformation induced by

drag forces leads to a larger frontal area and tends to increase the drag coefficient.

$$C_D = \frac{F_D}{\frac{1}{2}\rho U^2 A} \tag{6}$$

where

F_D fricion factor

A frontal area

u relative velocity

ρ gas density

ρ_d droplet density

The prediction of the motion of a drop in these time-dependent problems should not be treated based on correlation for spheres in steady flows obtained for isolated drops, whose may be correct for very dilute sprays, in configurations where each drop can be assumed isolated. It has to be pointed out, however, that a part from considerations regarding the deformation, which has a low impact for very small droplets, a group of drops is considered as a whole with the PDM approach, making more difficult to treat the interaction of drops in the systems from a modeling point of view. At high Re numbers, flow separation occurs because of the boundary layer that envelope the droplet may act in order to generate a pressure gradient and when it becomes to separate, instabilities in vortex formation appear at low scale, and the buoyancy effect may have an impact on further break-up and estimating C_D. Experimental investigations on isolated droplet have shown that the drag coefficient changes a little at high Re numbers when the drag may be affected by the boundary layer. Some authors discussed about how these effects may be incorporated into spray calculations, and the commonly used correlations

for spray models are the one of Shiller and Neumann, reported in Equations 7and 8, as reported in detail by O'Rourke et al. [33].

$$C_D = \frac{24}{Re}\left(1 + 0.15Re^{0.687}\right) \quad Re \leq 10^3 \tag{7}$$

$$C_D = 0.44 \quad Re > 10^3 \tag{8}$$

A distortion parameter is then used to account for deformation and so to modify the drag coefficient, and this can be doneusing the relation proposed by Liu et al. [29] and written in Equation 9.

$$C_{D,y} = C_D\left(1 + 2.63y\right) \tag{9}$$

where

$C_{D,y}$ drag of the deformed drop

y dropet distortion

$C_{Dy}$is the drag coefficient estimated for the drop affected by deformation, despite that of the initially spherical drop, and y measure the deformation and varies between 0 and 1. In dense sprays, when spacings between the droplets are small, the drag coefficient of each drop is significantly altered by mutual interactions of the multidimensional coupling between the two phases. Studies conducted among the drag of multiple drops together have shown that the ratio of the modified drag due to the presence of other droplets to drag force acting on the single one, is not very sensitive to the Reynolds number, as reported in different studies [18, 37, 47].

If many drops are present as the case of water mist systems, the drag coefficient may be significantly altered, and this is mainly due to the effect due to the surrounding gas and the mutual momentum exchange. In fact it was found that in sprays some drops move much faster than one would could expect if the conventional isolated drop drag coefficient is used to estimate drag force. This is true also for

the smaller droplets and it is due to the increased velocity of the surrounding gas resulting from the mutual momentum exchange. Hence a two way coupling approach is very important to capture the water mist spray pattern, while drop deformation may play a secondary role. Another approach, different from tacking into account the momentum exchange source terms, is that of modify the drag coefficient estimation to take into account the enhanced velocity effect, called "effective drag" approach, usually applied estimating the new drag coefficient by multiplying it by a function of the local void fraction.

The mass exchange between the two phases due to evaporation is taken into account with proper source terms in the water vapor transport equation and evaporation is modeled properly to account for the effect of the presence of a mixture of gases surrounding the droplet. The problem may be in distinguish a forced convection mechanism which may affect thermal exchange. Effect of relative humidity on heat transfer across the surface of an evaporating water droplet in air flow was experimentally investigated. The results showed that the droplet temperature decreases in the low-relative-humidity condition, whereas it increases in the high-relative-humidity condition, which agree well with the DNS results by Kurose et al. (2009) and it was also found that the Nusselt number on the droplet surface is not affected by the relative humidity [5].

Water spray nozzles are devices that hold one or more iniector to convert a continuous flow of water into discrete fragments of fluid which are lead to instabilities due to the air friction that turn them into droplets of different sizes (first break-up). This atomization process is non-deterministic, and there are just a physical finite maximum and non-zero minimum diameter limit to the sizes produced due to fluid properties and aerodynamic forces that lead large droplets into small ones (second break-up). The second break-up is due to essentially two main mechanisms: the bag break-up and the stripping breack-up. The first refer to the droplet split into two or more doprlets of comparable sizes and the latter in a small droplet that leave the sur-

face of a larger one. Second break-up may be modelled according to the criteria of Parra (2004) with the Weber number which measure the ratio between drag force and surface tension (equation 10) and the Eötvōs number which measure the ratio between the acceleration force and the surface tension (equation 11).

$$We = \frac{\rho \left(u - u_d\right)^2 D}{\sigma} \tag{10}$$

$$Eö = \frac{\rho_d \frac{ds}{dt} D^2}{\sigma} \tag{11}$$

where

ρ air density

ρ_d droplet density

σ surface tension

u air velocity

u_d droplet velocity

Bag break-up occurs for Weber number greater than 12, or Eötvōs number greater than 16 and stripping break-up for We > 0.5 and Eo > 100 [27]. Secondary break-up is not accounted for, but of course a significant reduction in the droplet diameter is due to evaporation, which occur in fire scenario and it is of paramount importance. For a cluster of droplets, the evaporation process that affect the single drop it is influences by the neighboring, in function of their relative distance and location. For dense droplet clusters it was found that evaporation occurs most of all due to diffusion effects (as for Sherwood equal to 2 for zero convection flows), while the convection contribution plays a significant role in more dilute regions of the spray. The mass and heat transfer due to evaporation determine the final drop size and drop temperature when steady conditions are reached and in order to be allow the computation of millions of representative droplets in the simulation, simplifying assumptions are needed and the common most important one is the one referred as the lumped

capacitance assumption. The lamp capacitance assumption states that the temperature within the droplet may be considered uniform and not spacial dependent. This assumption is considered satisfied when the Biot number, defined in Equation 12, is sufficiently small, so that droplet temperature and radius will be just time dependent.

$$Bi = \frac{hd}{k_l} < 0.1 \tag{12}$$

where

h heat transfer coefficient

d droplet diameter

k_l liquid thermal conductivity

For spray simulations that involves drop sizes at most a couple of hundreds of micrometers the Biot number criterion is always well satisfied, and that is the case of water mist systems. Ranz-Marhall correlation [45] reported in Equation 13.

$$Nu = 2 + 0.6 Pr^{1/3} Re^{0.5} \tag{13}$$

where

Nu Nusselt number

Pr Prantl number

Re Reynolds number

The water vapor film influence on droplet thermal exchange is neglected, and the the drop surface temperature T_s is not solved for explicitly to evaluate the vapor and gas properties, but it is determined by using the two-thirds weighted temperature as stated in Equation.

$$T_s = \frac{T_g + 2T_d}{3} \tag{14}$$

where

T_s surface temperature

T_g gas temperature

T_d droplet temperature

Although more sophisticated evaporation models may be scrutinized, it was not possible during this research to find out how to evaluate them because of the lack of experimental data and the high sensitivity of evaporation sub-modeling in CFD simulations.

Another important aspect is about the contribution of turbulence to dispersion which may be very important for small droplets, because the velocity fluctuations in any directions may speed up the droplet dispersion. Usually the Stokes number is used to describe this phenomenon, which is the ratio of two characteristic times: the relaxation time of the droplet (as written in Equation 15 for a spherical droplet) and the vortex life time (estimated depending on the turbulence model adopted).

$$\tau = \frac{2}{9}\frac{\rho_d r_d^2}{\mu_g} \tag{15}$$

where

τ characteristic time

r droplet radius

ρ_d droplet density

μ_g surrounding gas dynamic viscosity

Also droplet collision has observed experimentally to have an impact due to consequent coalescence, bouncing, reflexive or stretching separation, but modeling the complex phenomena in binary droplet collisions that occur in spray flows is very hard due to the great variety of interconnected potential outcomes due to a collision [13, 28, 6]. First it is necessary to predict the stability regime of possible separations and then to correcly predict the resulting drop sizes. This kind of modeling in EL approach usually refer to an estimation of the probability that coalescence occur after the collision which can be expressed in a very general form but it is really time consuming, and that has been extended an improved since the base formulation of O'Rourke et al. in order to run several order of magnitude faster, as the one implemented in the KIVA code developed by Zhang et al [32].

Droplet wall interactions were considered negligible for the intent of this analysis, although they could be taken into account and may lead to significant secondary phenomena as secondary atomization, film formation, affecting considerably the thermal exchange of surfaces [9]. The activation of the water spray nozzle may be controlled, as in diluge systems, or automatic, in the latter case an activation model has to be implemented, based on the Responce Time Index (RTI) correlation. The RTI approach assumes that it possible to correlate the thermal responce of a sensible elementm as the one which control the nozzle activation, to the surrounding gas temperatures, by integrating a simple differential equation. The sensitivity of the automatic nozzle is characterized by the value of the RTI and some empirical constants have to be determined experimentally.

2.7 HEAT DETECTORS

The Responce Time Index correlation, was derived from a heat balance analysis on sprinkler's thermal link during operation, but could be extended to many other devices. The main assuptions rely on the fact that forced convection is the dominan heat transfer mechanism and that the element heats isothermally. The constant RTI was defined as in equation 16 (Heskestad et al., 1976).

$$RTI = \frac{-t_a u^{1/2}}{ln\left(1 - \frac{\Delta T_a}{\Delta T_g}\right)} \tag{16}$$

where

t_a activation time

ΔT_a activation temperature minus ambient temperature

ΔT_g duct temperature minus ambient temperature

u gas velocity

The activation of the heat detector is then governed by Equation 17.

$$\frac{dT}{dt} = \frac{|u|^{1/2}}{RTI}\left(T_g - T\right) \tag{17}$$

where

T	Temperture of the element
RTI	Responce Time Index
T_g	gas temperature
u	gas velocity

The RTI of a thermally activated device is determined by plunging the unit into a hot air duct until activation occurs, and the current standard test condition employs a temperature of 200°C and a velocity of 2.5 m/s for ordinary temperature sprinklers and a temperature of 200°C and a velocity of 1.5 m/s for ordinary temperature heat detectors. The validity of the RTI correlation has not been sufficiently investigated, but since it is now the standard parameter to refer to the responsiveness of heat detectors, it is also used to model the activation of water spray nozzles, in the form of Equation 18 as stated by Heskestad and Bill and modified by Di Marzo [25].

$$\frac{dT}{dt} = \frac{|u|^{1/2}}{RTI}\left(T_g - T\right) - \frac{C_1}{RTI}\left(T - T_a\right) - \frac{C_2}{RTI}\beta|u| \tag{18}$$

where

T	temperture of the element
RTI	Responce Time Index
T_g	gas temperature
T_a	ambient temperature
u	gas velocity
β	volume fraction of liquid in the gas stream
C_1, C_2	empirical constants

2.8 VENTILATION

Ventilation plays a role of paramount importance in fire-fighting strategies and also in the behaviour of the fire. Ventilation supplies the combustion with new oxydizer and affect the movement, stratification and dilution of the smoke, which also contain hazardous products of combustion. A well-established understanding of the interaction between ventilation and fire is crucial in developing fire safety strategies and both natural and forced ventilation are commonly utilised during tunnel fires in order to maintain safe escape routes for the occupants and rescue personnel with a proper smoke management. When the movement of smoke is versus the desired direction, the phenomenon is called back-layering, that is avoided assuring that a certain critical velocity is achieved. The critical velocity definition refers usualy to the one of Wu and Bakar [46] define the critical velocity as reported in equation 19 and 20 defined on the basis of a adimentional fire size Q^* (equation 21 and an adimentional ventilation rate V^* (equation 22).

$$V^* = 0.4\,(Q^*)^{-\frac{1}{3}} \quad Q^* \leq 0.2 \tag{19}$$

$$V^* = 0.4 \quad Q^* > 0.2 \tag{20}$$

$$Q^* = \frac{Q}{\rho_0 c_p T_0 \sqrt{g\overline{H}^5}} \tag{21}$$

$$V^* = \frac{V}{\sqrt{g\overline{H}}} \tag{22}$$

where

$\overline{H}$ hydraulic tunnel height

ρ_0 ambient density

T_0 ambient temperature

g gravity acceleration

c_p specific heat capacity of air

This results are extrapolated from small-scale experiments, but was shown to be in good agreement with well known full scale tests and are so commonly used for design porpuses. The constant critical velocity is reached when the plume and the flames, no matter if intermittent or persistent, reach the ceiling without a minimun backlayering. Carvel et al. investigated the effect of forced ventilation on the rate of combustion and fire spread for different types of fire. The study highlights that for some fires, increased ventilation will provide a greater supply of oxygen and thus increase the rate of burning. For other fires, the ventilation will have a cooling effect which will reduce the severity of the fire, or perhaps put the fire out entirely.

2.8.1 *Numerical schemes and solution strategies*

FireFoam like almost any solver written with the OpenFOAM™ toolbox uses the Finite Vol- ume Method to solve the system of equations upon an unstructured mesh, giving the opportu- nity to treat complex geometries with the optimal amount of cells for the given problem. The solution is searched with second order fully implicit schemes and the pressure based segregated solution method PISO or PIMPLE (PISO + SIMPLE) as suggested, the latter may give a sufficient stability to speed up simulations with maximum Courant numbers up to 2 [38]. The strategy adopted is to always perform unsteady simulation in order to have a complete descritpion of the evolution of the fire

since steady state condition is achieved, with reference of the most important physical propetries of gas, surfaces and water droplets evaporation rate. The solution schemes are always second-order in time and space, and since an implicit solver is used, the Couront number need to be assigned to assure convergence. A maximum value of 0.6 was used in order to assure that combustion is well resolved with PISO solution schemes. The Courant number expresses a relationship between the physical properties of the flow and the grid and time step size and is reported in Equation 23.

$$C = \overline{v}\frac{\Delta t}{\Delta x} \tag{23}$$

where

C Courant number

$\overline{v}$ average fluid linear velocity

Δx dimention of the grid at each cell location

Δt maximum time step

s stoichiometric ratio

ϵ turbulence dissipation rate

k turbulence kinetic energy

When advection dominates diffusion, a small value of the Courant number will decrease oscillations, improve accuracy and decrease numerical dispersion.

Part II

MODEL VALIDATION AND ASSESSMENT

Literature experiments for small scale and large scale compartment fires are compared with numerical simulations in order to achieve optimization of grid resolutions and numerical parameters. A model of a single-fluid multi-injector water mist nozzle is validated through experimental measurements. The model is capable to simulate the bulb thermal responce in order to allow the comparison between deluge and automatic systems and a sensitivity analisys is done in order to assess grid resolution and spray parameters to simulate the relevant phenomena involved in the most common fire scenarios.

3

SMALL-SCALE COMPARTMENT FIRE VALIDATION

3.1 DESCRIPTION OF THE STECKLER ROOM FIRE TESTS

The Steckler room fire test K.D. Steckler [26] cases are commonly used for validation purposes and benchmarking of numerical tools and CFD methodologies. The experiments focused on the buoyancy driven flows induced by fire in small compartments in many configurations in order to capture the influences of different parameters such the location of the fire, the heat release rate, the geometrical properties of the openings. In the selected experimental test the fire was created using a centrally located 62.9kW methane burner of a diameter of 0.3m at a height of 0.3m, in a compartment measuring 2.8m x 2.8m in plane and 2.18m in height, with a doorway centrally located in one of the walls measuring 0.74m wide by 1.83m high (corresponding to the 6/6 A series test). The burner was realized using a porous media, so the inlet gas mixture spread from the burner surface with approximately uniform concentration and velocity. During the experiments hot layer temperatures were measured at 11 locations in the centerline of the doorway by thermocouples at equal distances. In Figure a representation of the compratment is compared with a simulation output to give an overview of the kind of experiments, showing the flame geometry affected by induced air flows. The diffusive turbulent combustion take place in a relatively small region, but an extended region for the doorway is required to ensure that the airflow through the door is correctly resolved and this region is as an emi-cylinder region of 4m of radius that extends 1m long in the z-direction over the compartment. The comparisons between experimental and numerical results are shown for three different representative meshes plus

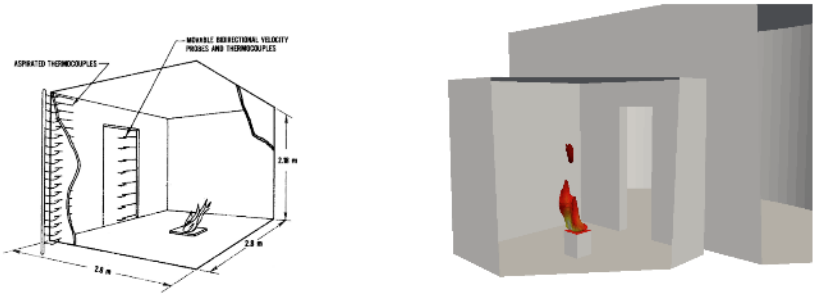

Figure 1: Steckler room fire test illustrations, as reported in publication compared with a simulation carried out in this analysis.

the one with the adapted wall layer, which results the better choice, despite the turbulent model that is used. The overall analysis allow to show that LES simulations perform well even on the same grid compared to RANS simulations also when analysing discretisation errors.

The fine grid is made by hex-cells of $5cm$ of length a medium grid with hex-cells of $7cm$ and a coarse grid of $10cm$ of length (of course this is not true for non-orthogonal cells far from the fire source). This work shows that a grid sensitivity analysis and a grid adaptation for the given problem is crucial in fire simulation, furthermore for predicting purposes it is very important to assure grid independence, for which we applied the GCI method, based on Richardson extrapolation proposed by Roache [39, 1], one of the most common method available in literature to assure grid independence evaluation, also applied for LES modeling [22, 23].

3.2 NUMERICAL SET-UP

The different meshes are illustrated in Figure 2 applied to evaluate grid sensitivity. A wall refinement is also tested in order to avoit standard wall function treatment. The simulated cases are reported in table 1 and they involve different meshes and different turbulence

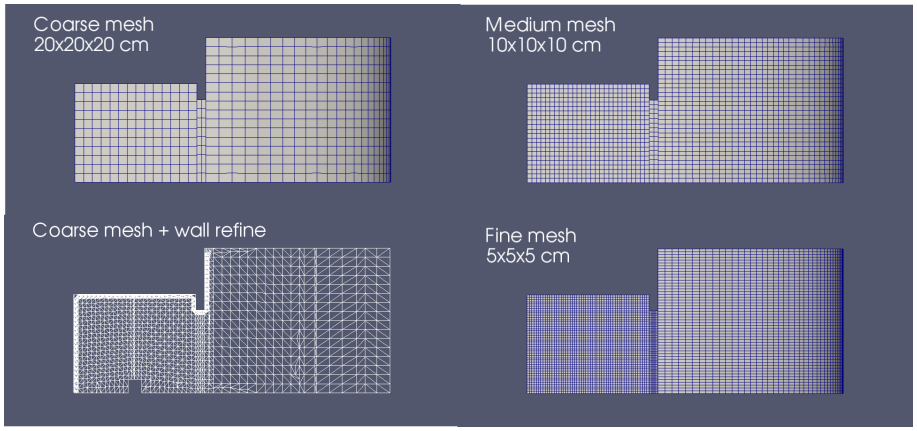

Figure 2: Comparisons of the meshes applied for the Steckler validation.

Case	Grid	Turbulence
1	Coarse	RANS
2	Medium	RANS
3	Fine	RANS
4	Wall refine	RANS
5	Coarse	LES
6	Medium	LES
7	Fine	LES
8	Wall refine	LES

Table 1: Simulations carried out to validate the Steckler compartment fire (6/6A series).

models. The mesh was adapted in order to assure physical convergence of the results and boundary conditions are reported in table 2and illustrated in Figure 3.

3.3 RESULTS

First has to be noticed that RANS and LES simulations perform quite well upon the same adapted meshes applied, while with LES simulations an average 30% more time is required to carry out computations,

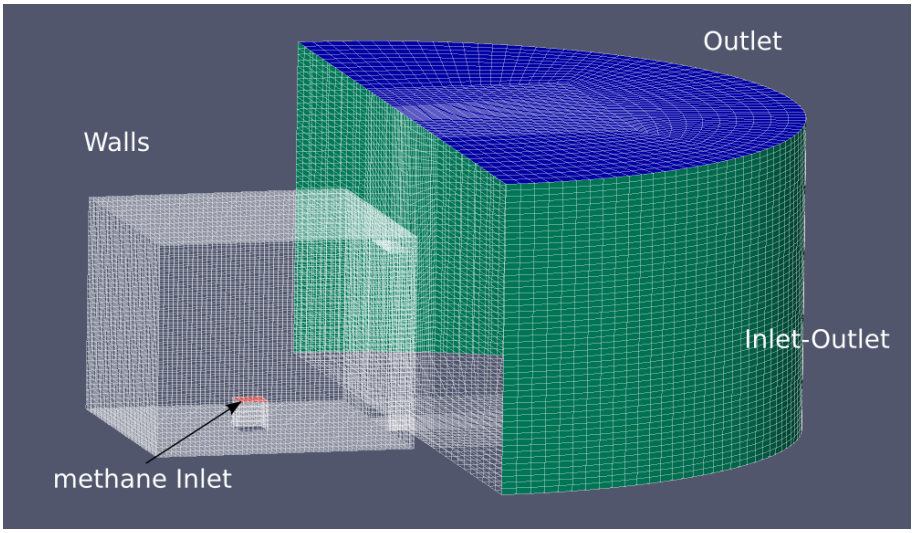

Figure 3: Representation of the domain and patches used to describe the fire compartment.

Patch	Type	Value
Fire	Mass flow rate (methane)	0.00128 kg/s
InletOutlet	U: pressureInletOutlet p: TotalPressure	-
Outflow	U: InletOutlet p: buoyancyPressure	-
Walls	Adiabatic	-

Table 2: Measured flow rates f, at different operating pressures for single injector C.

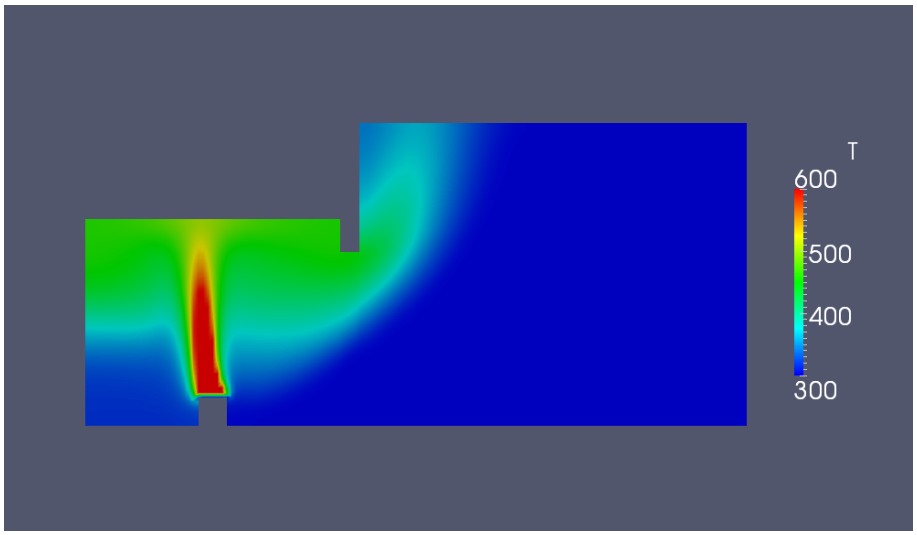

Figure 4: Temperature contours at steady state for a representative RANS simulation of the Steckler coompartment (6/6A).

the flame structure is much more well resolved in the LES case, as clearly illustraded by comparing the temperatures contour at steady state in Figures 4and 5. In oreder to assure that complete combustion occurs and the prescriber heat release rate is resolved the heat from combustion is monitored and a part of verysmall numerical obscillations they confirmed the nominal value of around $63kW$.

Comparisons beetwen experimental and numerical results are shown in terms of temperatures and velocity averages at the door centerline for LES simulations for the three standard meshes in Figure 6 and in Figure 7 comparing the coarse mesh with the same one with wall refinement for temperatures and in the same way in Figures 8 and 9 for velocities. The same plots are given for RANS calculations in Figures.

Since in this kind of buoyancy driven flows at low Mach Reynolds number, wall boundary flows does have a relevant impact in determining the flow field, and it is possible from this study to evince how a coarser grid with wall refinement can resolve sufficienlty well the combustion as well as the flow field, allowing a significan optimization for required computational resources. This is not so true for temperatures resolution in the hot layer zone due to the more complex physics involved, but always temepratures show a trend in the

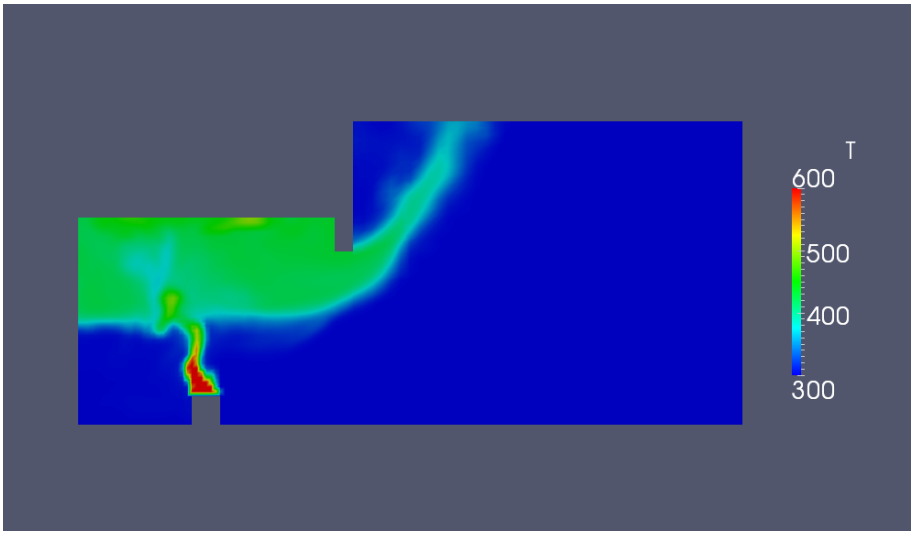

Figure 5: Temperature contours at steady state for a representative RANS simulation of the Steckler coompartment (6/6A).

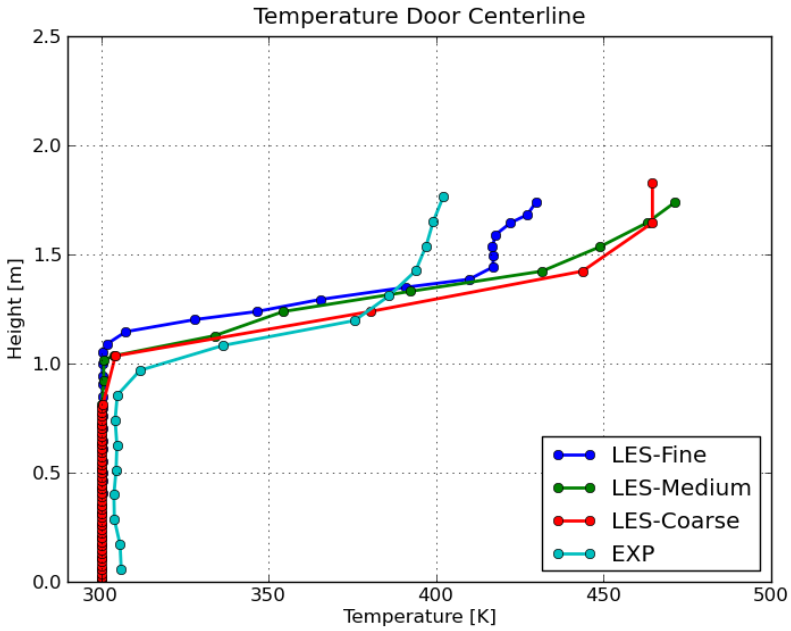

Figure 6: Comparison beetwen results from experiments and the meshes of different grid size in the temperature profile for LES simulation.

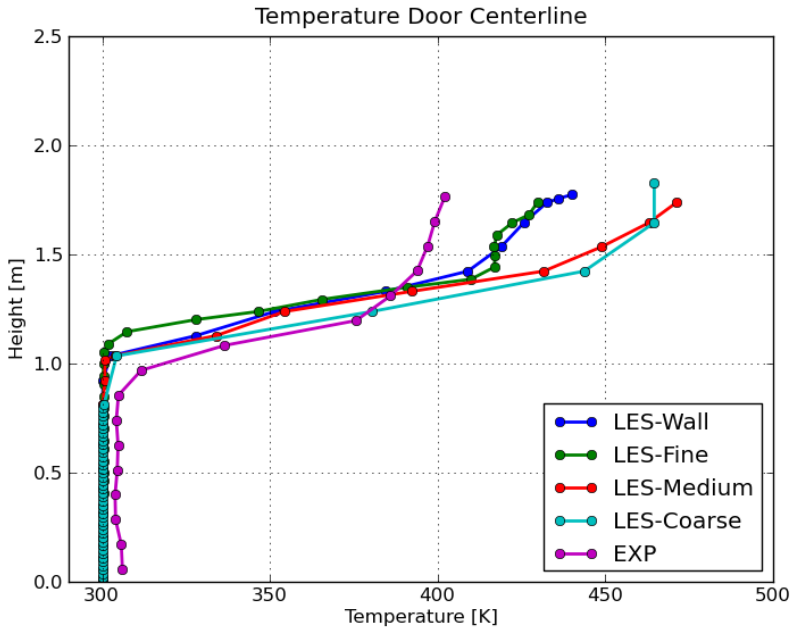

Figure 7: Comparison beetwen results from experiments, the coarse mesh and the mesh with wall refinement in the temperature profile for LES simulation.

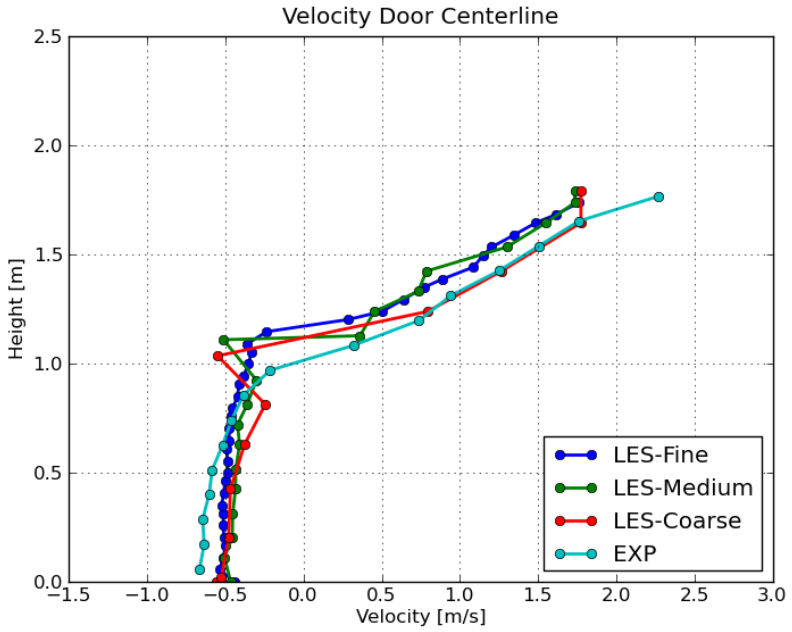

Figure 8: Comparison beetwen results from experiments and the meshes of different grid size in the velocity horizontal profile for LES simulation.

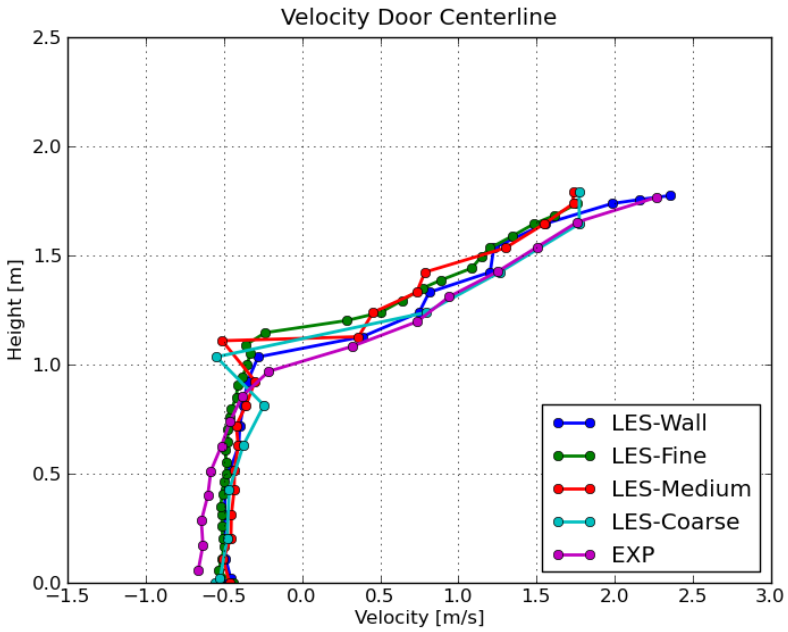

Figure 9: Comparison beetwen results from experiments, the coarse mesh and the mesh with wall refinement in the velocity horizontal profile for LES simulation.

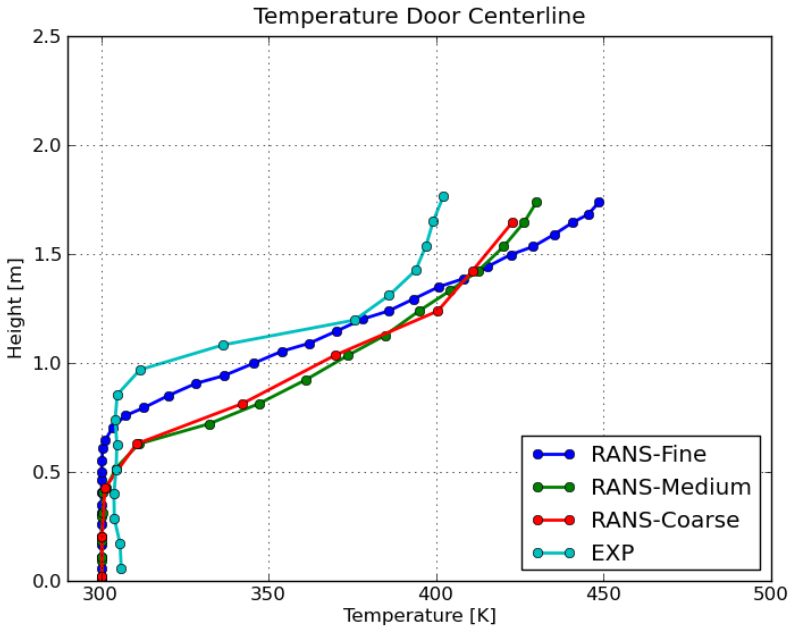

Figure 10: Comparison beetwen results from experiments and the meshes of different grid size in the temperature profile for LES simulation.

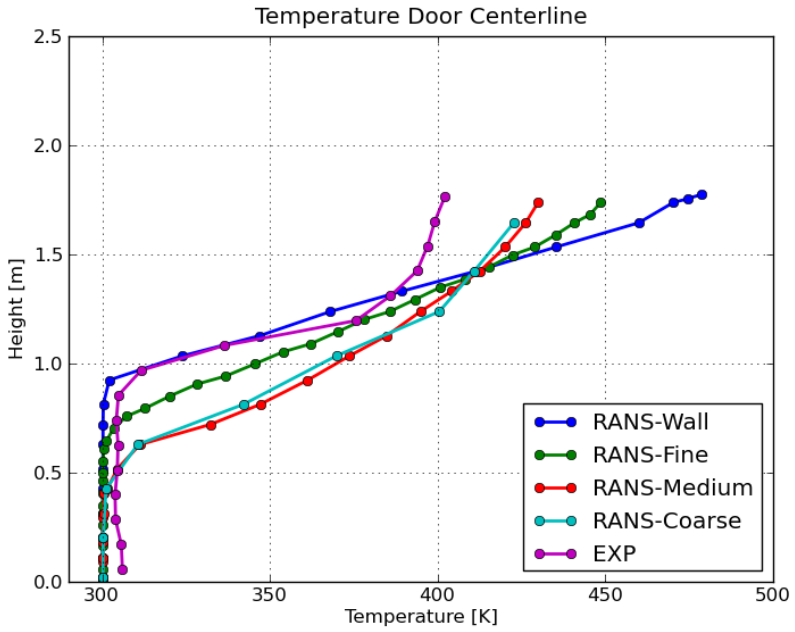

Figure 11: Comparison beetwen results from experiments, the coarse mesh and the mesh with wall refinement in the temperature profile for LES simulation.

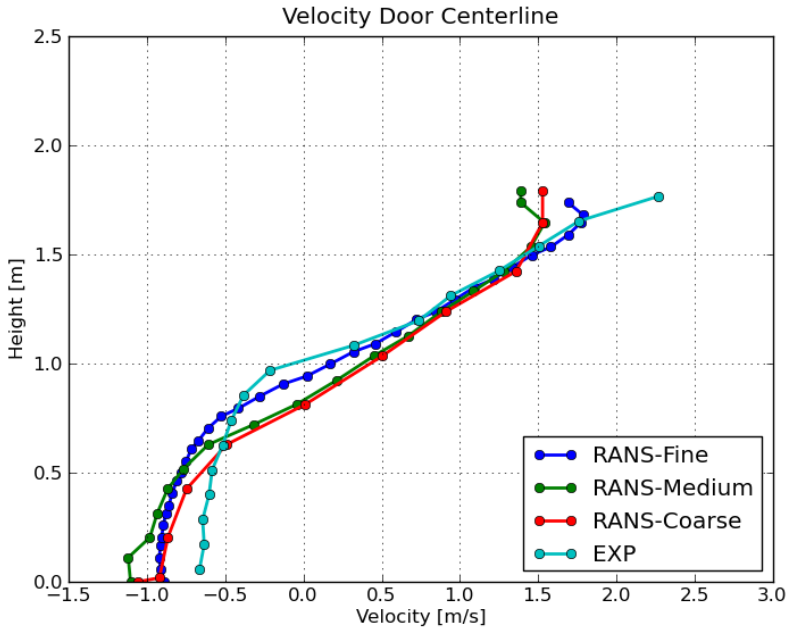

Figure 12: Comparison beetwen results from experiments and the meshes of different grid size in the velocity horizontal profile for LES simulation.

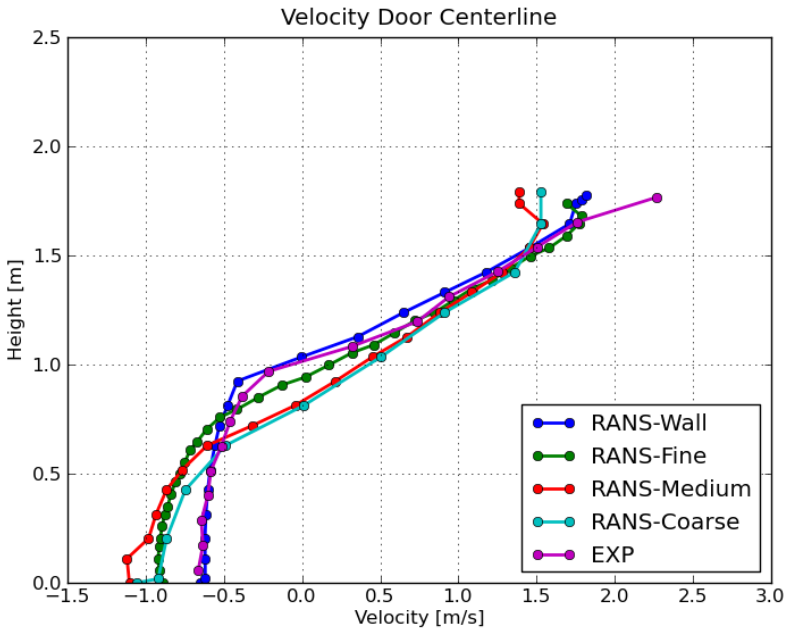

Figure 13: Comparison beetwen results from experiments, the coarse mesh and the mesh with wall refinement in the velocity horizontal profile for LES simulation.

safety direction, with a slight or pronounced overestimation. Since an adiabatic wall was considered that temperature overestimation is partially accounted in the overall energy balance. It is important to point out that experimental measurments of incoming air flow are much higher that the ambient temperatures. This is possibly due to thermal exchange between the hot plume exiting the room because thermocouples where not shielded in that direction, or radiative transfert may play a significant role and that was not accounted by the code due to the poor resolution of the radiation calculation. In conclusion, velocities are slightly underpredicted with LES and overpredicted in the fresh air flow for RANS. It has to be pointed out that ambient humidity was not known, radiation pa- rameters and properties are subjected to high uncertanties and therefore the simulation was conducted *on the safety side*, meaning that emissivity and assorbance of partecipating bod- ies to radiative thermal exchange was assigned in order to get those overprediction, avoiding what in design crite-

ria evaluation could lead to dangerous underpredictions; the neutral plane (smoke layer level) is quite well predicted in both RANS and LES cases.

3.4 NUMERICAL ANALYSIS OF DISCRETIZETION ERRORS

Since the only recommended method for discretization error estimation is the Richardson extrapolation method upon which the Grid Convergence Index (GCI) is computed [22]. This methodology is applied to ensure that results won't be affected too much by grid resolution errors and it is very useful to assess grid generation for further simulations. The method is well known and aims to verify for the three grids applied in this case (1=coarse, 2=medium, 3=fine) that were chosen so that the ratio between the cell dimentions is around 2. In order to assure grid indipence according to the method one have to assure that Equation 24 is true.

$$GCI_{32} = GCI_{21} * r^p \tag{24}$$

where

$r_{32} = r_{21} = 2$ ratio between grid dimentions

p local or global order of accuracy

The global order of accuracy is calculated according to Equation ; the GCI does refer to a physical variable, and was computed for the averages of velocity and temperature on the door centerline.

$$\frac{1}{ln(r)}|ln|\epsilon_{32}/\epsilon_{21}| \tag{25}$$

where

r ratio between grid dimentions

ϵ estimated error

The discretization errors calculated are reported in Table for the LES simulations and in Table for the RANS simulations.

	ϕ =Mean Temperature [K]	ϕ =Mean X-Velocity [m/s]
ϕ_1	338	0,14
ϕ_2	355	0,12
ϕ_3	350	0,22
p	1,92	2,69
err_{21}	5%	3%
err_{32}	1%	83%
GCI_{21}	**2%**	**3%**
GCI_{32}	**1%**	**19%**
$GCI_21 * r^p$	**8%**	**17%**

Table 3: Discretization errors calculated for LES simulations according to the Grid Convergence Index method for global accuracy determination.

	ϕ =Mean Temperature [K]	ϕ =Mean X-Velocity [m/s]
ϕ_1	354	0,08
ϕ_2	357	0,08
ϕ_3	353	0,16
p	0,43	3,61
err_{21}	1%	8%
err_{32}	1%	111%
GCI_{21}	**3%**	**1%**
GCI_{32}	**4%**	**12%**
$GCI_21 * r^p$	**4%**	**11%**

Table 4: Discretization errors calculated for LES simulations according to the Grid Convergence Index method for global accuracy determination.

Considering all the points of the door centerline where velocities and temperatures are calculated, the local order of accuracy for LES varies from 0.46 to 5.64 for temeprature and from 0.2 to 2.28 for velocity, whith a maximum discretization error of 9,6% for temperature and 55% for velocity. For RANS the local order of accuracy varies from 0.7 to 4.02 for temperature and from 0.24 to 7.78 for velocity with a pretty much higher maximum discretization error of 11% for temperature and 88% for velocity. High local discretization errors for U results are relative to a velocity near zero so corresponds to a maximum uncertainty of $0.33m/s$ for RANS and $0.18m/s$ for LES. For every case the 40% of the local points exhibited oscillatory convergence. Although it was reported that despite of promising results, the Richardson extrapolation in LES is not straightforward and the justification of its use is highly dependent on the applied grid resolution [8], there was not found better methods up to know to assess grid discretization error and forecast the better grid adaptation for cases of real interest which will be addressed in the present work.

4

VALIDATION AND ASSESSMENT OF A WATER MIST SPRAY

4.1 INTRODUCTION TO WATER MIST SYSTEMS

The interest in water mist as a fire fighting technology aroused because of its potential as a replacement for environmentally harmful halon-based systems and because of its efficacy. In facts, much of the research that has been carried out concentrates on nautical applications, since the system was firstly massively applied it maritime applications because of the less amount of water required. Then the use of water mist systems spreaded from such applications to include the protection of buildings, with a particular interest for road tunnel, since it is demonstrated that would be an effective strategy in suppressing pool fires, with particolar reference to large fires. In fact surfactant enhanced water mist systems have been proposed for small fires[17], since water mist systems are effective with large fires, as typical for tunnel design fires, while the small fire scenario is more challenging because a small fire may not be able to generate enough vaporized water to displace sufficient oxygen. The definition of water mist refers usually to the NFPA 750, where it is defined as a water spray where the 99% of the total volume is occupied by droplets with a diameter below $1000\mu m$. But in general water sprays need to be described with more than a characteristic diameter in order to be modeled and so measurements are required. The characterization of industrial water mist nozzles is of primary importance in order to achieve good confidence in prescribing input values for numerical simulations and validating numerical models that may be very useful in optimizing fire protection strategies at design stage. The main

phenomena that are involved with its effectiveness as a fire-fighting agent (oxygen dilution, gas phase cooling, fuel cooling, attenuation of radiation, disruption of air flow and influences on combustion reactions) are directly connected to the quality of the spray and the ventilation systems characteristic. The main problem in the design of such systems, is to verify the effectiveness of the strategy adopted that usually requires full-scale tests. These are however too much expensive often unsatisfying. These aspects were also investigated with numerical simulations and experiments, but there are few example in literature of characterizations and assessment of such models that might be useful to address investigations where there is a lack of data: for instance the influence on smoke stratification. Measurements of droplet velocities, diameters and water mass flux were carried out on a full cone spray from a high-pressure single fluid system at different operative pressures. Relevant results were obtained with Phase Doppler Anemometry (PDA) while Particle Image Velocimetry, Laser Tomography and High Speed camera that have also been used by other authors don't seem very promising since the higher uncertainty involved Husted [21], B. P. Husted [7]. The water density apparatus proposed originally by Holmstedt et al. [35]and modified and adapted also by others, is one of the most promising and interesting technique to have direct informations about the spray densities, since for optical techniques that kind of measurement for water mist sprays seem very difficult to assess . Experiments have not been conducted on the full nozzle spray but on the single injectors, in order to understand the implications and differences due to a single point injecton (or equivalent fixed parcel positioning used sometimes to avoid numerical difficulties [Hart [20]].

4.2 EXPERIMENTAL SET-UP

Phase Doppler Anemometry (PDA) techniques measure particle size and particle velocity at the same time. The method only measures at a point but with very high resolution in time. The underlying theory for the measurement is based on light scattering interferometry and the Doppler effect. Measurements are made in the volume of the intersection of two incoming laser beams and are conducted on single particles as they move through the sample volume, see figure 14 Particles scatter light from both laser beams and generate an optical interference pattern. The frequency of the pulsation of light intensity is proportional to the velocity of the particle. Each detector is mounted at different angles and converts the optical signal into a Doppler burst. The phase shift between the Doppler signals from two different detectors is a direct measure of the particle diameter. PDA is specifically designed for measuring particle size and velocity, with processing of measurements being carried out online. With the Dantec Classic PDA instrument used in this study, the results can be presented after post- processing. Characteristic diameters of droplets can be calculated as mean diameter, surface weighted mean diameter, volume weighted mean diameter, as well as mean velocities of all droplets. A single measurement for one position would typically consists of about 100000 samples. PDA is the only measurement technique that provides corresponding values of velocities and droplet sizes. To avoid dense spray regions, where there may be too much particles in the measurement volume, the first measurement point is chosen at 250 mm from the nozzle. The droplets are expected to be reasonably spherical and sufficiently far from the break-up region. The spray axis was chosen horizontal, assuming gravitational effects are negligible within the measured range. PDA measurements were conducted on a spray generated only by one operating orifice of a standard industrial nozzle operated at different pressures (50 bar,

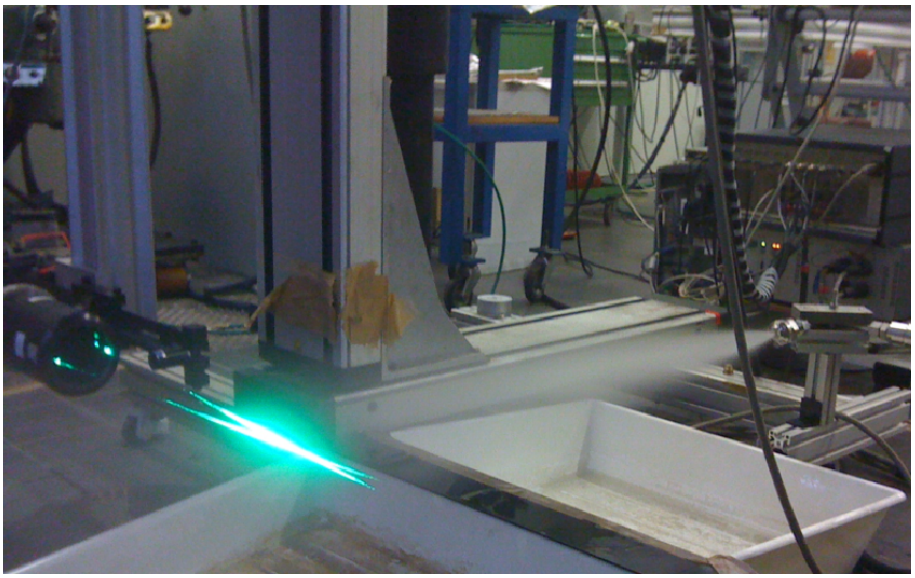

Figure 14: PDA Experimental setup

100 bar, 150 bar) by a variable speed volumetric pump. The operating orifice is mounted in the central position, with respect to a common nozzle, with stoppers closing the other orifices, thus disregarding the effects due to sprays interactions.. The activity is focused on single fluid water mist injectors and we report some data for a representative nozzle, thus results are referred to both the central C injector and the lateral L injector separetley. The influence of spray angles on the nozzle was investigated by some authors [41], and it was found that may affect the spray behaviour due to an increased coalescence, that of course should be avoided in advance by a correct nozzle design. The mean droplet diameter D_{10}, which is chose as the reference diameter to prescribe the initial droplet size distribution, is reported in Table and for the two orifices. Results shows that the sprays are quite similar, but they differ for mass flow rates.

p [bar]	t [s]	m [g]	f [kg/min]
150	17.5	1355	4.65
100	22.4	1382	3.70
50	30.5	1305	2.57

Table 5: Measured flow rates f, at different operating pressures for single injector C.

p [bar]	t [s]	m [g]	f [kg/min]
150	37.5	1446	2.31
100	40.6	1349	1.99
50	50.5	1080	1.28

Table 6: Measured flow rates f, at different operating pressures for single injector L.

4.3 EXPERIMENTAL RESULTS

4.3.1 *Water flow rates*

Water flow rates were calculated at the three different pressures considered in order to overcome the application of the K-factor reported on the technical specifications of the product since the K-factor is a parameter which may vary significantly at different operating conditions of the nozzle. The calculated values are reported in Table 5for the central injector and in Table 6 for the lateral one.

4.3.2 *Cumulative distributions*

Statistical corrections were done to treat sensitivity of data due to the particular class diameters to obtain the continuous cumulative distributions illustrated in Figure 15and data were not area averaged, so results are directly comparable with Malvern measurements which

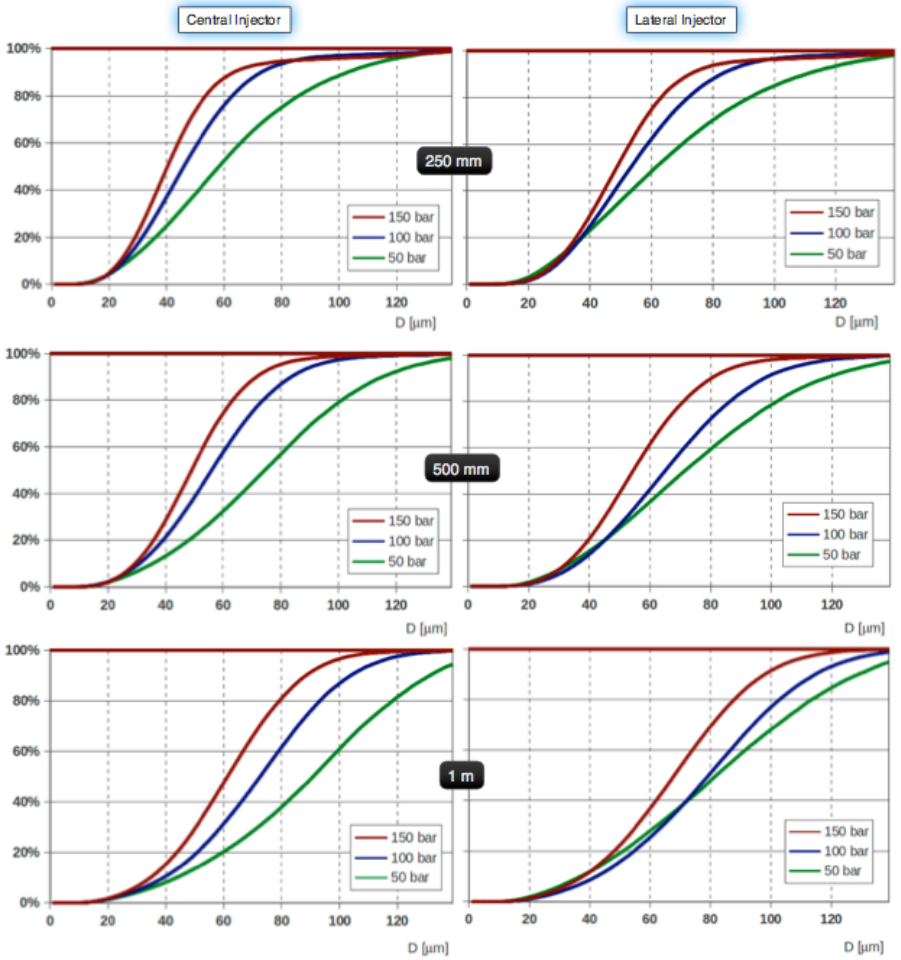

Figure 15: Continuous cumulative distributions obtained from experimental data for the central and lateral injector

may be available to futher comparisons, and used for water mist characterization purposes [36, 40].

4.3.3 *Representative diameters*

For a certain distribution of droplet dizes $f(D)$, it is possible to calculate many representative diameters according to equation 26.

$$D_{pq} = \left[\frac{\int_0^\infty D^p f(D) dD}{\int_0^\infty D^q f(D) dD} \right]^{\frac{1}{(p-q)}} \tag{26}$$

where

p	**x**	$\mathbf{D_{10}}$	$\mathbf{D_{20}}$	$\mathbf{D_{30}}$	$\mathbf{D_{32}}$	$\mathbf{D_{0.9}}$
$[bar]$	$[mm]$	$[\mu m]$	$[\mu m]$	$[\mu m]$	$[\mu m]$	$[\mu m]$
150	250	26.1	28.8	31.5	37.9	63.6
150	500	32.0	35.3	38.2	45.3	71.7
150	1000	32.4	37.7	42.4	54.2	88.4
100	250	25.9	29.5	33.0	41.6	73.1
100	500	30.6	35.2	39.3	49.8	83.7
100	1000	33.0	39.8	46.0	62.2	103.8
50	250	24.2	29.1	34.4	48.6	103.2
50	500	29.6	36.3	43.1	61.4	115.3
50	1000	30.1	39.1	47.9	73.0	131.1

Table 7: Representative diameters at different distance from the orifice and at different operating pressures for the central injector (C).

D_{10} Arithmetic Mean Diameter

D_{20} Area Mean Diameter

D_{30} Volume Mean Diameter

D_{32} Sauter Mean Diameter

Other useful representative diameters are theas volumetric mean diameters, defined as average maximum diamater that a certain distribution of droplet has respect of a certain fraction of its total volume. The calculated values are reported in Table 7for the central injector and in Table 8 for the lateral one. Measurements are reported as velocity and mean diameter profiles comparing central and lateral injectors for the operative pressures tested and reported in Figure 16 for the 50 bar case, in Figure 17 for the 100 bar and Figure 18 for 150.

p	**x**	$\mathbf{D_{10}}$	$\mathbf{D_{20}}$	$\mathbf{D_{30}}$	$\mathbf{D_{32}}$	$\mathbf{D_{0.9}}$
$[bar]$	$[mm]$	$[\mu m]$	$[\mu m]$	$[\mu m]$	$[\mu m]$	$[\mu m]$
150	250	32.5	35.6	38.5	45.4	72.5
150	500	34.8	38.6	41.9	50.1	80.3
150	1000	34.6	40.6	45.9	59.5	98.1
100	250	33.5	37.1	40.4	48.7	82.6
100	500	36.7	41.7	46.3	57.8	97.7
100	1000	37.0	44.1	50.7	67.9	114.7
50	250	28.6	33.2	38.4	51.8	110.2
50	500	32.5	38.1	44.2	59.9	117.8
50	1000	30.6	37.7	45.2	65.9	129.0

Table 8: Representative diameters at different distance from the orifice and at different operating pressures for the lateral injector (L).

4.3.4 *Radial profiles*

Radial profiles are illustrated in Figures 16,17and 18, so comparisons may be done with numerical results. It has to be pointed out that during experiments the spray was not perfectly symmetric, and thus this divergence was corrected for further comparisons with simulations.

4.4 VALIDATION OF A WATER MIST INJECTOR MODEL

4.4.1 *Size ditributions*

The most important parameter for the correct simulation of the water mist injector is in prescribing a well-fitted size distribution. In fact instead of using analytical droplet size distributions, an empirical method is adopted, based on a simple Rosin-Rammler distribution (equation 27, which is one of the most widely used. It can how-

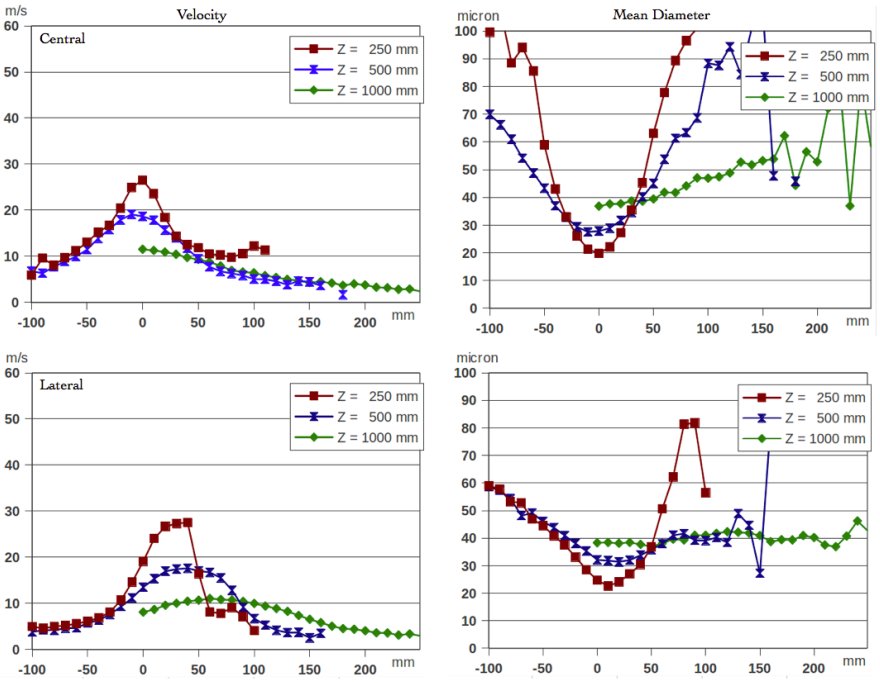

Figure 16: Comparisons of average velocity and mean diameter profiles of central and lateral injector operating at 50 bar

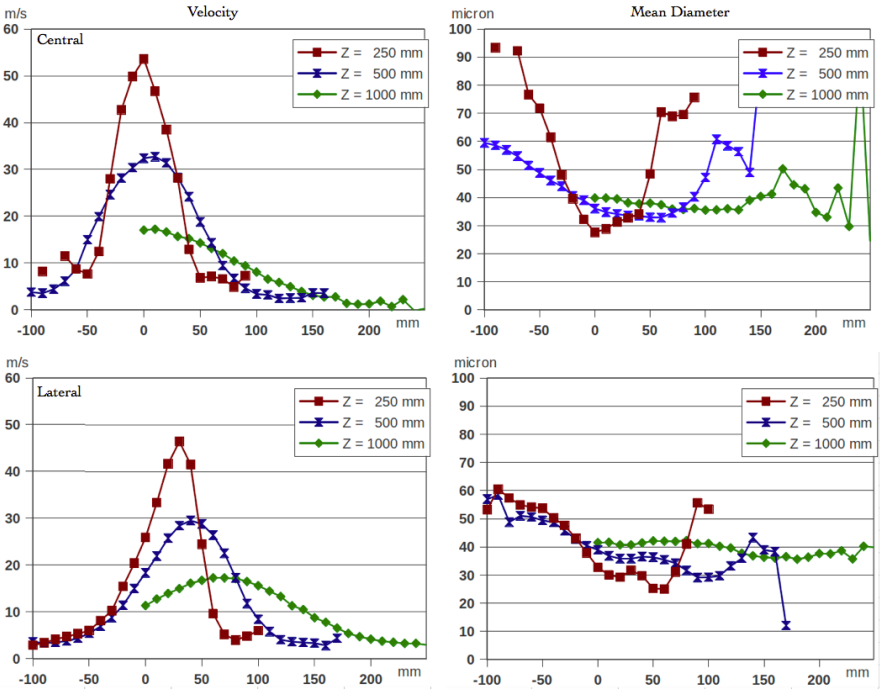

Figure 17: Comparisons of average velocity and mean diameter profiles of central and lateral injector operating at 50 bar

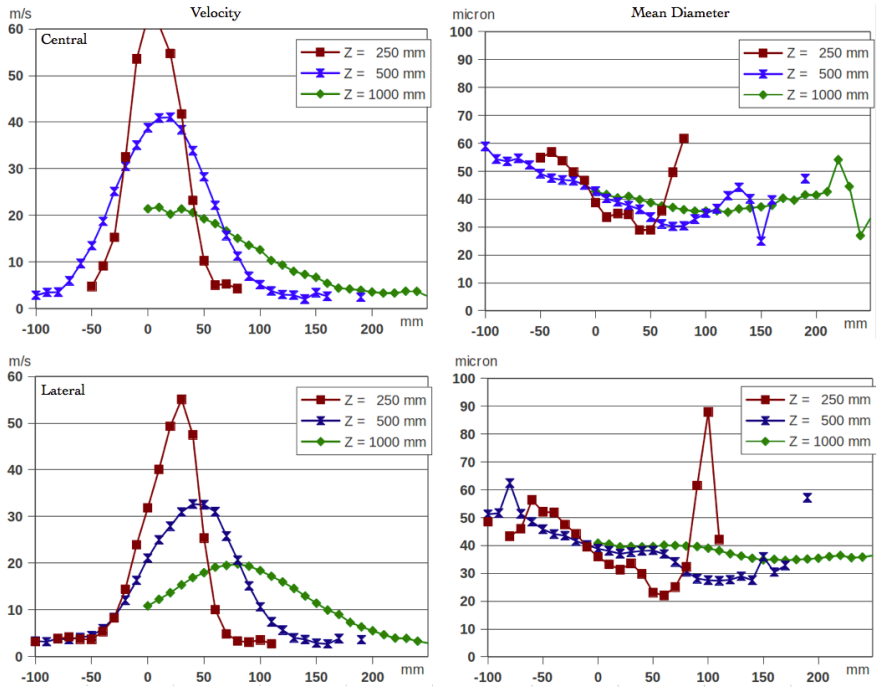

Figure 18: Comparisons of average velocity and mean diameter profiles of central and lateral injector operating at 50 bar

ever be difficult to determine the values for the model parameters, particularly for the more complex distributions which may be generated within the model so in this analysis secondary break-up was neglected, since it is considered of a low influence.

$$p(d) = e^{-\left(\frac{d}{\overline{d}}\right)^n} \tag{27}$$

where

$p(d)$ is the probability of the droplet to have the diameter d

d is the droplet diameter

$\overline{d}$ is the average diameter

n is a measure of the spread of drop sizes

In Figure 15 are illustrated the measured droplet distributions, while the prescribed one is illustrated in Figure [RIF] obtained with a Rosin-Rammler distributions of mean diameter 54 and exponential factor 1.2, that is used to model the spray initial distribution. The fit cannot be done solely based on the derived cumulative volume at 250 mm

from the nozzle, because at that point break-up does matter and at the orifice the distribution should be slightly different, so a trial and error approach is applied. Since the model proposed does have to set boundary conditions upstream the region where measurements were conducted, an estimation of the inlet velocity has to be done based on Bernoulli balance equation with a proper correction coefficient for the orifice head loss. These simulations are also used to evaluate different evaporation rates obtained by a single-injector water mist spray in different ambient air conditions in terms of temperatures and air humidity. The spray is modeled in the Lagrangian-Eulerian form previously described, with standard Ranz- Marshall heat exchange correlation for determining the evaporation rate, assuming that the gravitational forces effect within the measurement region are neglecTable. Under the simplest modeling assumptions, the droplets small scale contribution due to collision, coalecence and break-up phenomena are neglected and the prescribed diameter distribution and inlet velocity of droplets is prescribed starting from the available experimental data.

4.4.2 *Numerical set-up*

A *reactingCloud* (according to OpenFOAM™ 1.7 version) class with a full cone injector of an angle of around 15° with 500k parcels per second. Simulations were conducted until steady state conditions were reached and the water evaporation rate is predicted at different ambient temperatures in order to check the behaviour of the model. Two different grids were applied to give evidences of the grid dependency of the Lagrangian procedure, and results are shown in comparison at different nozzle distances for diameter and velocity radial profiles. Although there are no available experimental results, also the effect of different ambient air humidity is verified. To assure consistency of the numerical results versus the PDA measurements, different numbers of parcels (up to 1.5 millions of droplets per second) and different

grids have been tested in order to assure convergence in terms of radial profiles and evaporation rate estimations. The evaporation of droplets is evaluated within a region of 3 m from the nozzle, sufficient for a complete resolution of the spray behaviour. The comparisons between experimental measurements and simulations are presented for average diameters in Figures 23,24 and 25 at different distances from the orifice and in Figures 26, 27 and 28 for average velocities. Simulations were carried out for two different adapted hexadral meshes, a fine grid of a approximately 7mm of lenght and a coarse grid of 10 mm of lenght; boundary conditions are set as open boundaries (InletOutlet) at sides and bottom. An adiabatic wall is set at top patch; buoyancy is considered in both Eulerian and Lagrangian fields, the radiation model is applied although negligible at low temperatures and different air humidities are evaluated, that of a dry and a wet. Results are shown at the operative pressure of 100 bar with a flowrate of around 2 l/min, assigning therefore a theorically inlet velocity of droplets of 140 m/s according to Bernoulli energy balance equation, with a distribution described by a Rosin Rammler of $n = 2.1$ and a reference diameter of $x = 54\mu m$ for the central injector and of $n = 1.9$ and $x = 45\mu m$ for the lateral one and are illustrated respectively in Figures 20and 21. Droplet dispersion due to turbulence can be accounted based on the Stokes number estimation as described before and it is of low importance as the critical Stokes number of 1 is diffcult to reach for small water droplet as water mist one, even at high velocities. To assure that secondary break-up may be neclected the Weber number is estimated for different droplets dimaters at different velocities typical of droplets around the spray cone and is illustrated in Figure 19, pointing out that the break-up region may occour only in the first region of the spray, nearby 500 mm from the orifice, as also reported in experiments, for example comparing the 50 bar central injector profiles with the 150 bar (respectively Figure 16 and 18). Another aspect involving water spray simulations is about the droplet-wall interaction because of the impact on solid surfaces. Since it was

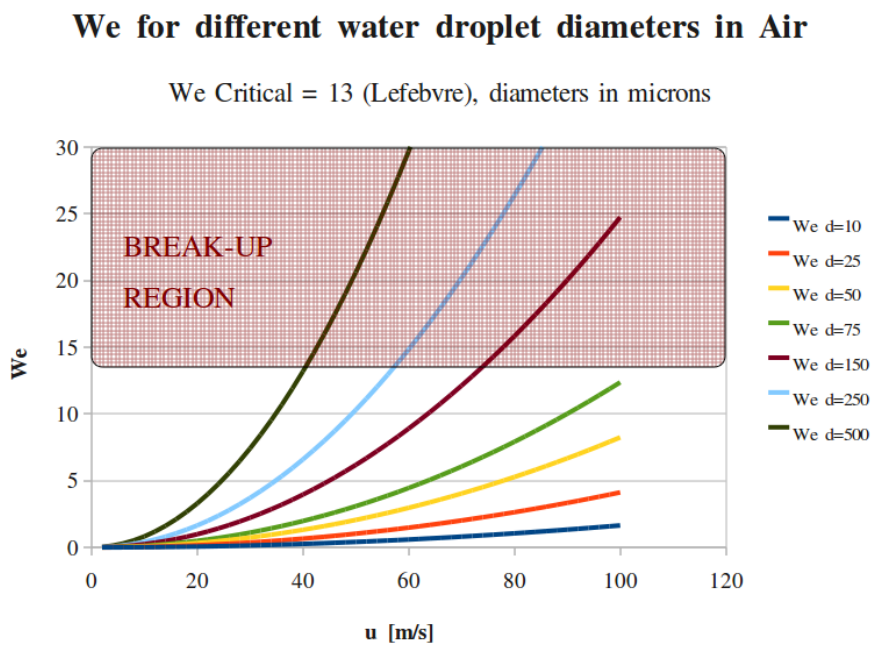

Figure 19: Weber number for water droplets of different size at different velocities

an important phenomena only at floor, where due to gravitational force and the presence of a water pool may lead the droplet to simply remain attached to the wall, evaporating, or to splash into the pool. Since a pool model was not applied yet, wall interaction was treated without a liquid film model to scrutinize the combined effect to heat transfer, and the focus of the application is on the evaporation that occur in the gas phase. For vertical and horizontal surfaces where film and pool formation are negligible, the behavior of the impacted droplet onto the heated surface depends on the surface temperature and can be described by the classical boiling curve. Since the surface properties are affected to great uncertainty and the wall rougthness is generally modeled just to account for head losses generated by turbulent dissipation enhancement due to friction, but it sot resolved due to meshing and computational contraints, the behavior of the droplets in these simulations was not affected only by the thermal exchange with the surrounding gas not with the surface.

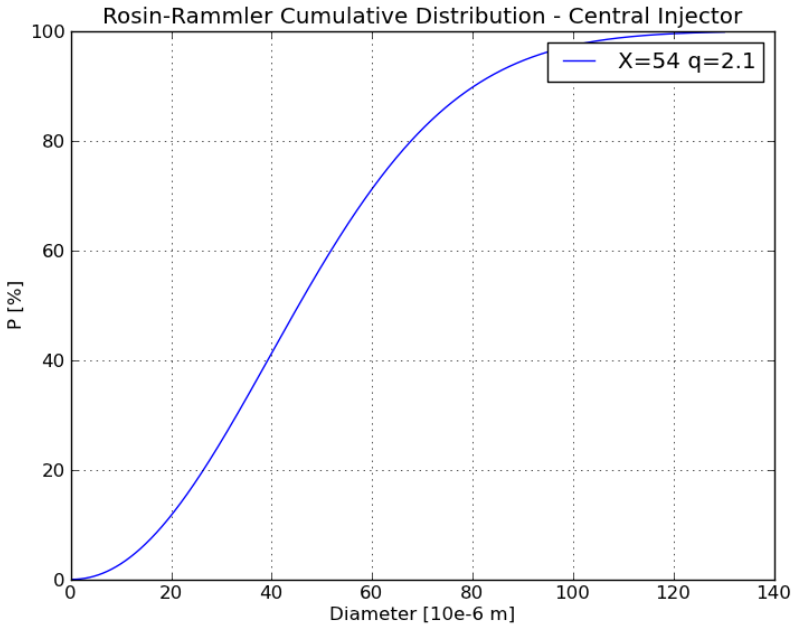

Figure 20: Prescribed cumulative Rosin-Rammler distribution for central injector

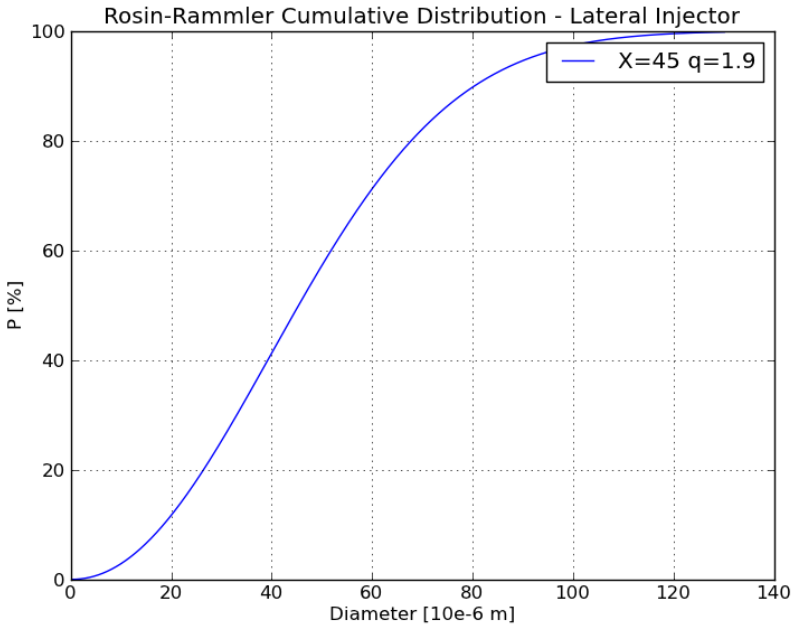

Figure 21: Prescribed cumulative Rosin-Rammler distribution for lateral injector

4.4.3 *Results*

Experimental results show that the numerical modeling of the spray is in good agreement, in terms of velocity (well reproduced at 1 meter from the nozzle) and diameters of the droplets (well reproduced within 500 mm from the nozzle). On this basis the evaporation rate estimated in different ambient condition shows that the influence of air humidity is important, giving a reduction of the 30% of the evaporation rate due to diffusion (which is the leading mechanism at low temperature differences), and so that cannot be neglected. More analysis are needed of course to assess better the simulation parameters, to evaluate the influence of droplet small scale phenomena and to take into consideration the influence of multi-injector configurated nozzles. In fact they are the most common ones and are very challenging from an experimental point of view to be characterized. The effect of droplet distributions on evaporation rate and of ambient humidity is very important and should be investigated experimentally to assure a good validation of numerical simulations, therefore future works are oriented to get more experimental results, in particoular at different ambient conditions.

The evaporation rates calculated from the simulations in steady state conditions show that the grid resolution has a strong impact of the spray, and the more the evaporation takes place, the more results are affected by mesh resolution, due to the coupling between the two phases. The values are reported in Table 9and in Figure is shown the trend, to evidence such divergence. In order to assure convergence the optimal grid resolution has found to be around 5 mm. Since the spray model is applied to forecast evaporation rates in real fire scenario, this assessment is of primary importance.

Grid	T_{amb} [K]	Rel. Hum. [%]	Tot. Parcel in domain [-]	Ev. rate [g/s]
Fine	300	0	140425	3,3
Coarse	300	0	129597	3,6
Fine	300	50	120171	2
Coarse	300	50	129114	2,3
Fine	350	0	133670	7,6
Coarse	350	0	121662	8,2
Fine	350	50	114038	6,8
Coarse	350	50	121519	7,7
Fine	400	0	125735	12,3
Coarse	400	0	116181	13,3
Fine	400	50	109026	11,5
Coarse	400	50	115847	13,2

Table 9: Simulations carried out to validate and assess the single injector model

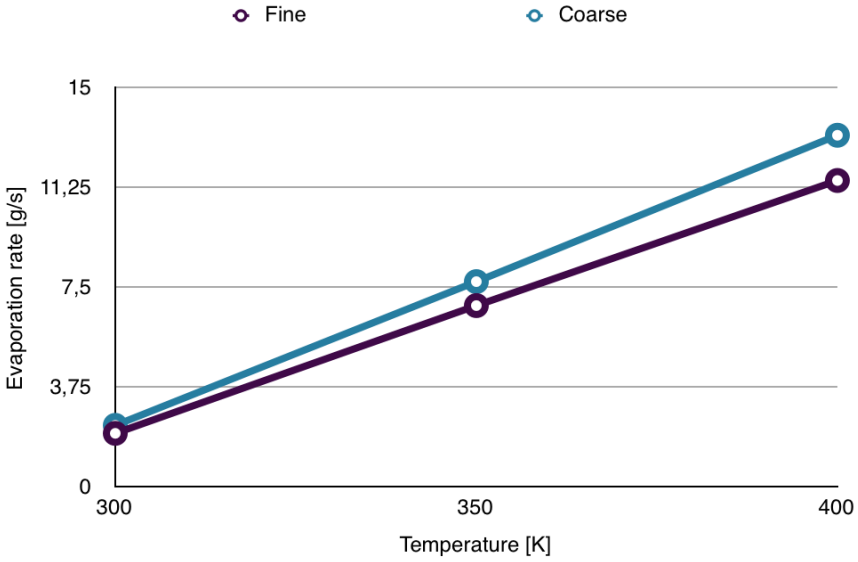

Figure 22: Evaporation rate comparisons between fine grid (5mm) and coarse grid (7mm) for a wet atmosphere

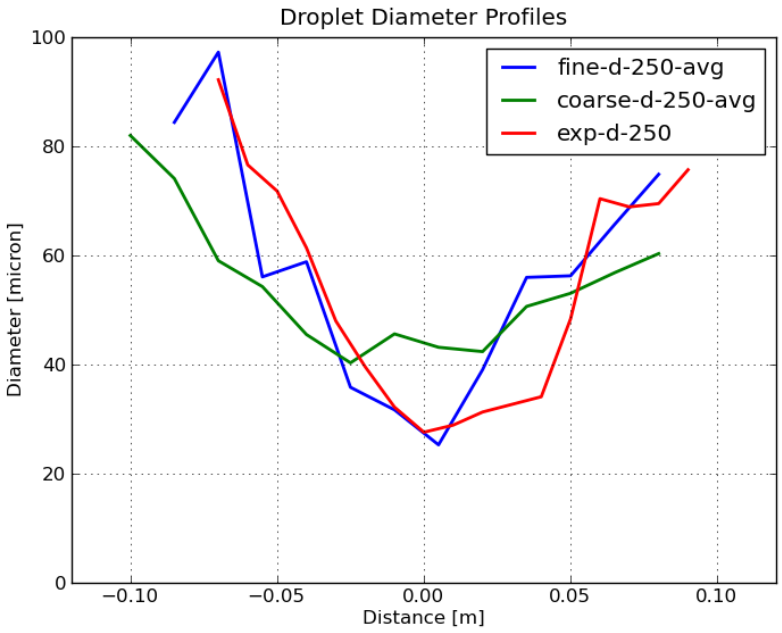

Figure 23: Mean droplet diameter comparisons at 250 mm from the orifice for the central injector

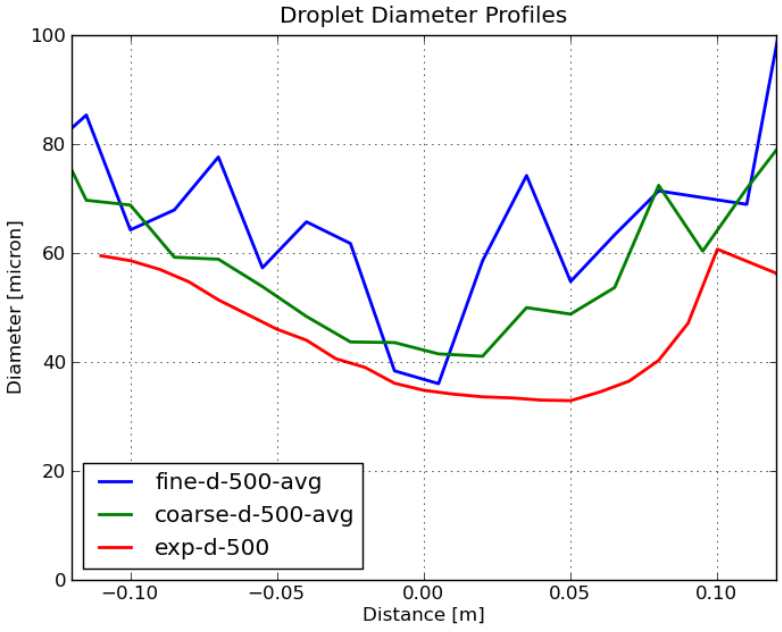

Figure 24: Mean droplet diameter comparisons at 500 mm from the orifice for the central injector

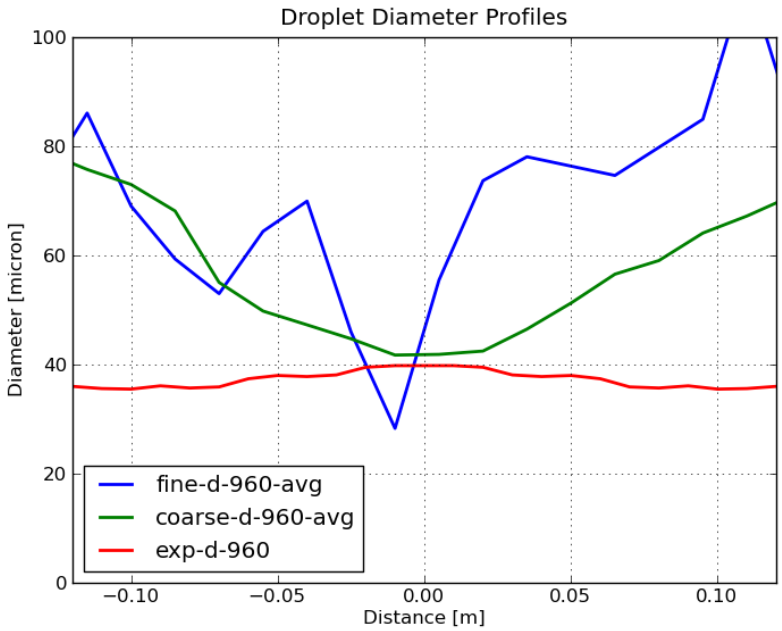

Figure 25: Mean droplet diameter comparisons at 1000 mm from the orifice for the central injector

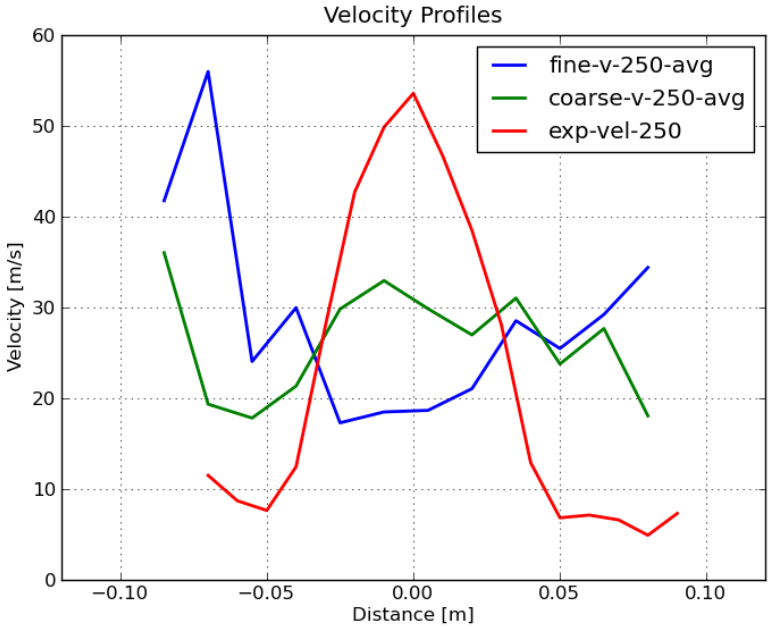

Figure 26: Average droplet velocities comparisons at 250 mm from the orifice for the central injector

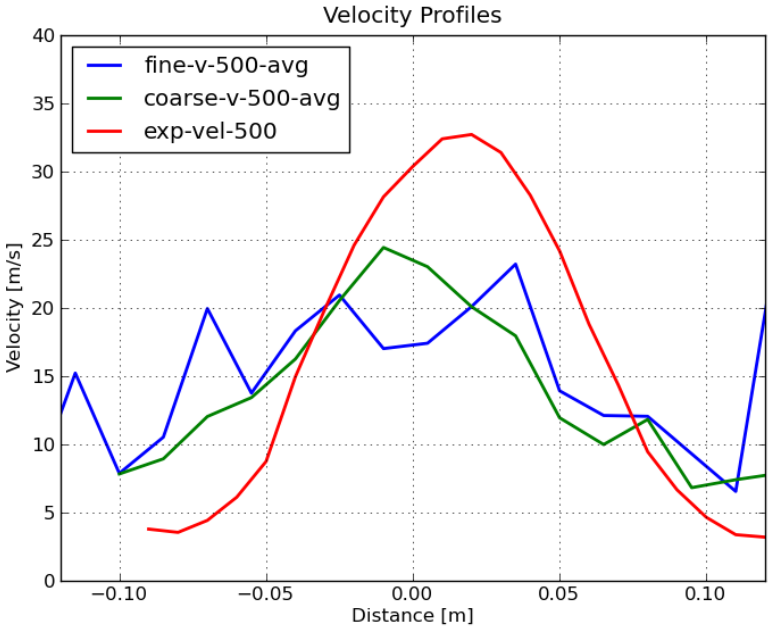

Figure 27: Average droplet velocities comparisons at 500 mm from the orifice for the central injector

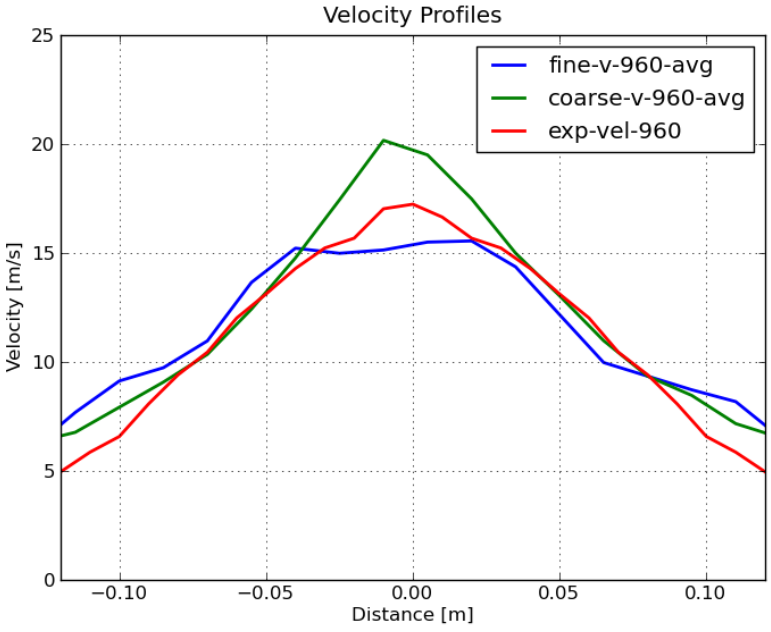

Figure 28: Average droplet velocities comparisons at 1000 mm from the orifice for the central injector

4.5 ASSESSMENT OF A WATER MIST SPRAY FOR FIRE SIMULATIONS

The behaviour of droplets inside the spray is dependent on the spray characteristics, and the spray dynamics associated to the evaporation rate is dependent on the volume fraction of the dispersed phase generated. For the validation of the spray models, it is necessary to measure the local droplet sizes, velocities and temperatures at different ambient air conditions. Since this could not be done, an assessment was carried out, based solely on simulations, to evaluate the optimal numerical set-up.

A water mist nozzle contains multiple active nozzles, and the air flow associated with a single injector will have an influence on adjacent ones. Spray patterns may be very different so the dispersion of droplets in the domain affecting dramatically the results. Since usually water mist model are simulated as a single equivalent injector comparison are presented for different conditions that may be help to figure out what behavior the spray may have in order to optimize the number of parcel needed to reproduce the spray with respect to evaporation, which is considered the most relevant phenomenon. This activity is of primary importance, since in a typical tunnel fire scenario, hundreds of nozzles may be operated simultaneously making necessary to optimize computational resources. The simulated cases are reported in Table 10. Two different kind of nozzle simulation are investigated, the most common single point source injector and the most similar to reality multi-injector one. The single point source injection is often used because spray model were adapted from sprinkler nozzles, that usually holds a single orifice. The multi-iniector model may avoid a manual parcel positioning for initialiazion, which is more difficult to assess from a statistical point of view, since a different total numebr of parcel may be assigned to a given position to accurately reproduce the radial concentration estimated. The single

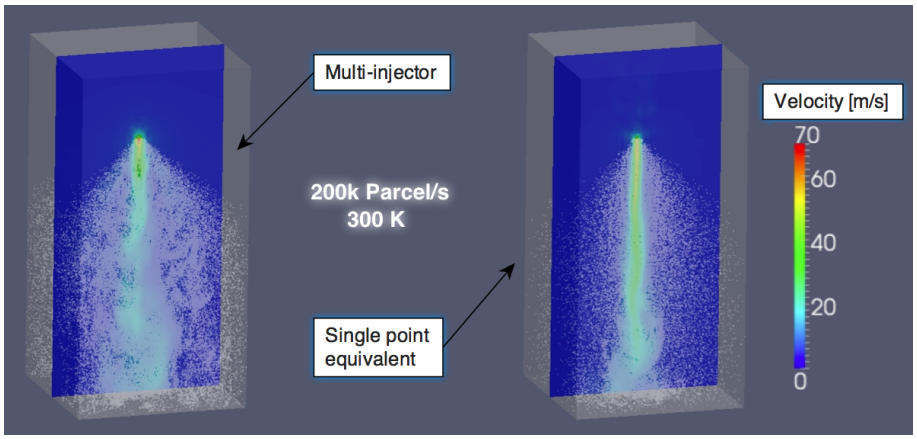

Figure 29: Comparisons between a multi-point injector and a single point equivalent injector at 300 K

equivalent injector model is compared to the multi-injector in order to account for differences, since at first attempt it may be a reasonable simplification. Of course the differences are not negligible and evidence of this is given in Figure 29for 300K and for 450 K of ambient air temperature, to compare them when evaporation is important. It is important to point out that in the fire scenario droplets are subjected to different flow regimes, and the one studied here is focused on the high Reynolds number one close to the nozzle. Where mist play a significant role as a flooding agent is also at low Reynolds number regimes, and further experimental investigation need to be carried out to assess the model in that conditions. These problems affect suppression investigation, where the low Reynolds droplet seem to be the more prone to be caught into flames and evaporated. This was also investigated experimentally to find out if, with theoretical analysis, scaling relationships could be extended from high to low drop Reynolds number conditions, for whose a proper scale factor may be proposed [43].

Concentration distributions and nozzle flows, velocities and diameters are compared for two particular number of parcel per second for the multi-injector nozzle and the equivalent one, described with a single point source injection. The aim of this assessment is to un-

Case	Parcel/s	Point Source	Temp. [K]	Tot. Parcel	Ev. rate [g/s]	Avg Conc. [ppm]
1	50k	Single	300	26245	48.2	3.4
2	100k	Single	300	48324	52.8	3.5
3	200k	Single	300	104689	54.2	3.25
4	50k	Multi	300	38499	111.6	3.2
5	100k	Multi	300	87324	82.4	4.5
6	200k	Multi	300	171992	79.6	4.7
7	50k	Single	450	18458	246.8	1.5
8	100k	Single	450	39340	112.6	1.6
9	200k	Single	450	78330	68.5	1.6
10	50k	Multi	450	20789	276.8	1.2
11	100k	Multi	450	40115	275.3	1.2
12	200k	Multi	450	87314	274.3	1.2

Table 10: Simulations carried out to assess the complete nozzle description

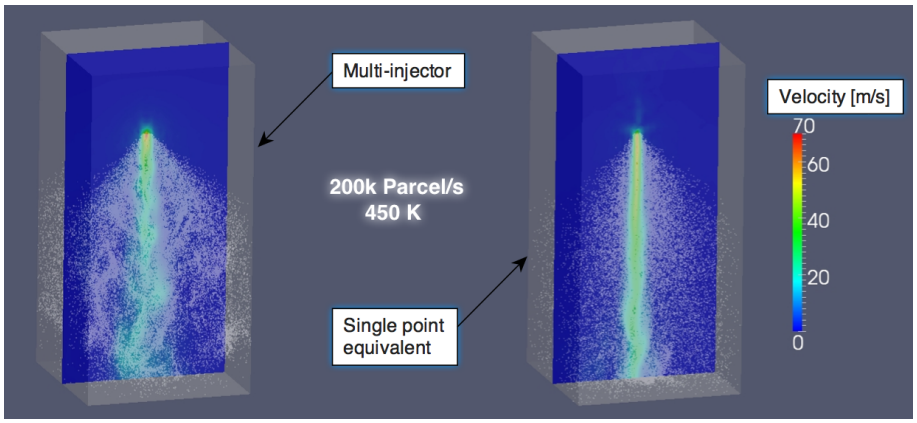

Figure 30: Comparisons between a multi-point injector and a single point equivalent injector at 300 K

derstand the optimal number of droplets per second that was found in 200k, for a representative temperature value for fire scenario. This number is referred of course to a single nozzle and not to the total nozzles eventually operating in the scenario of interest. The assessment should also involve investigations about turbulence parameters, in order to verify that mixing is resolved with sufficient accuracy but it was not possible to made experimental measurements on the entire spray. Of course the average concentrations are almost the same, since they are imposed and differences are due to numerical noise. It is important to point out that the variation of optimal water droplet size on flame inhibition and suppression was investigated numerically [10]and an optimal diameter for water droplet dimeter was found in between 6 and 20μm, which is likely to happen with the average diameters measured for the water mist nozzle considered in this analysis. Although suppression phenomena are not considered, they play a significant role, and should be considered for futher work. From the serie of comparisons velocities, droplet diameter distribution and volumic concentration are illustrated in Figures 31, 32 and 33 with a proper resolution to show the different spray pattern obtained, for averages on a vertical plane passing through the ideal center of the nozzle. In Figures 34,35are illustrated the averages local values of velocity magnitude and volumic concentration for an orthogonal plane

at 250 mm of axial distance from the central orifice, in Figures 36and 37 at 500 mm of distance and in Figures 38 and 39at 1 m. Comparison with experimental results cannot be done because it was not possible to measure the complete spray resulting from a water mist nozzle, since the limitations of the experimental facility and the problems connected with laser measurements in dense region of the sprays. Nevertheless from numerical simulations it is possible to state that the single equivalent injection description won't be sufficiently accurate to describe the multi-injector water mist nozzle, even at 1 m from the orifice, so it not a way to take into account the global effect of the nozzle behavior in terms of characteristics of the dispersed droplet in the domain. In fact even with the same initial droplet size distribution and total angle of the cone, inside the spray cone velocities distributions are determined by the composition of multiple injections and thus they affect the water mist produced by the nozzle within the spray regions, leading to important consequences in the behavior of the fire scenario. Only the 100*bar* operating condition is compared because it is the nearest to common operating pressures for civil applications with deluge systems as the ones designed for tunnel fire fighting strategies, that will be investigated in the present work.

4.6 ACTIVATION MODEL

The activation model was implemented according to Equation 18, where C_1 and C_2 were set to 0 due to their low impact and the high uncertainty associated to their determination in order to activate the nozzle when the reference temparature for activation is reached. In absence of experimental data to evaluate the influences on activation, a simple activation estimation time in carried out in the Steckler room fire scenario simulated for the small compartment fire validation. With the RTI value assigned according to the technical sheet of

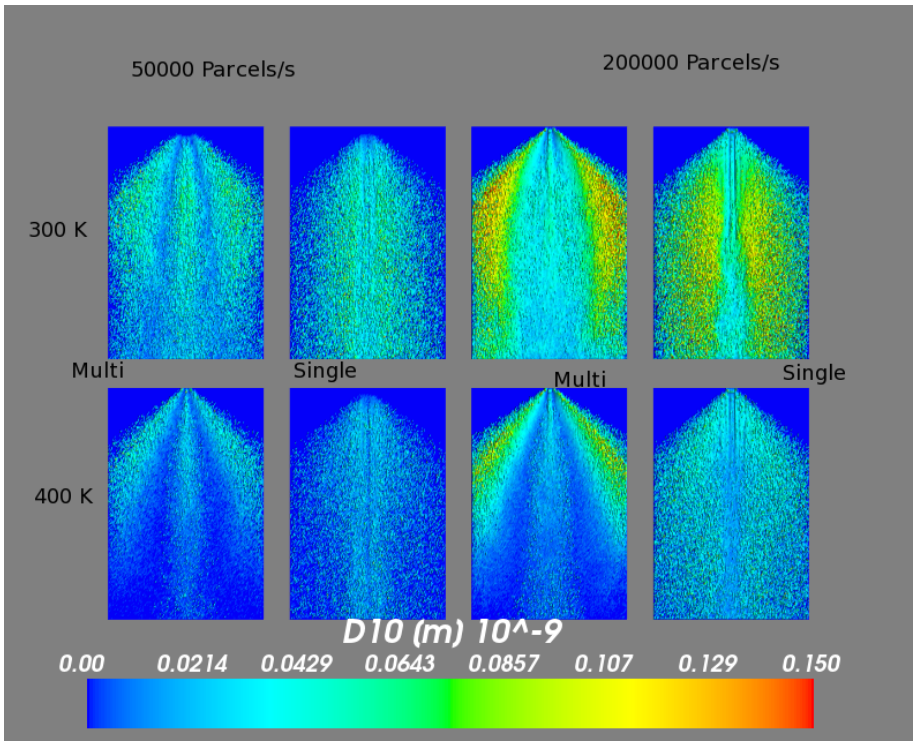

Figure 31: Comparisons of vertical mean diameters on the vertical plane

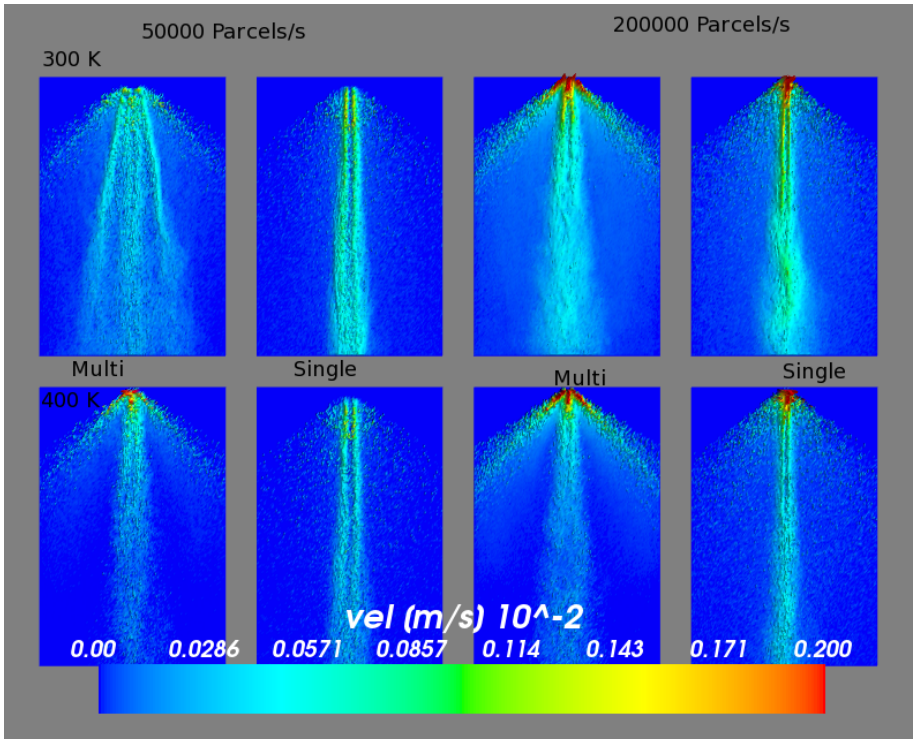

Figure 32: Comparisons of average velocities on the vertical plane

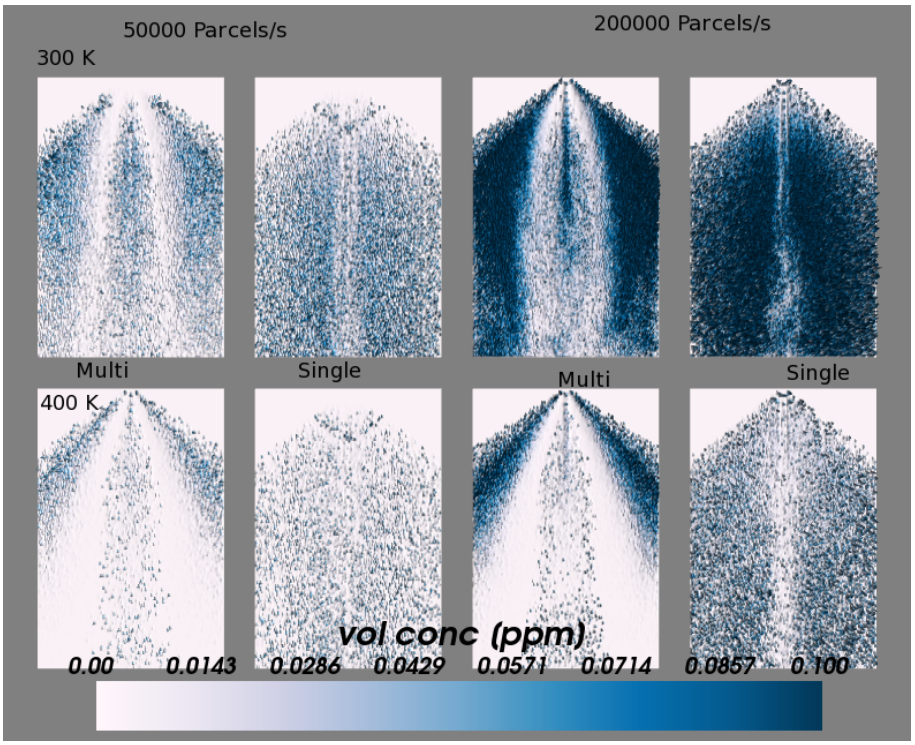

Figure 33: Comparisons of average concentrations on the vertical plane

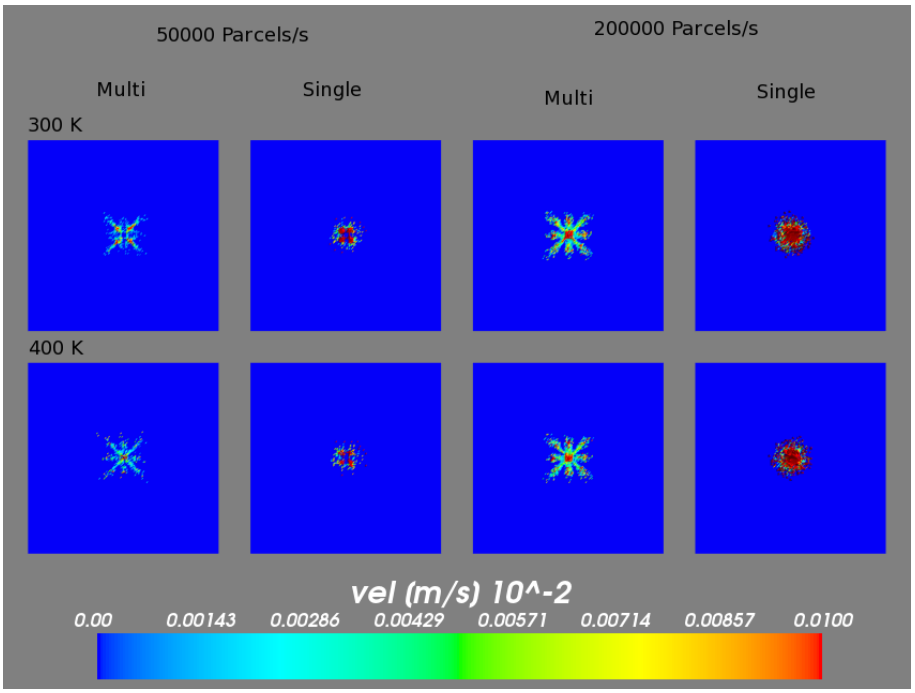

Figure 34: Comparisons of average velocities on the othogonal plane at 250 mm from the nozzle for the multi-injector model operating at 100 bar and the single-injector equivalent one.

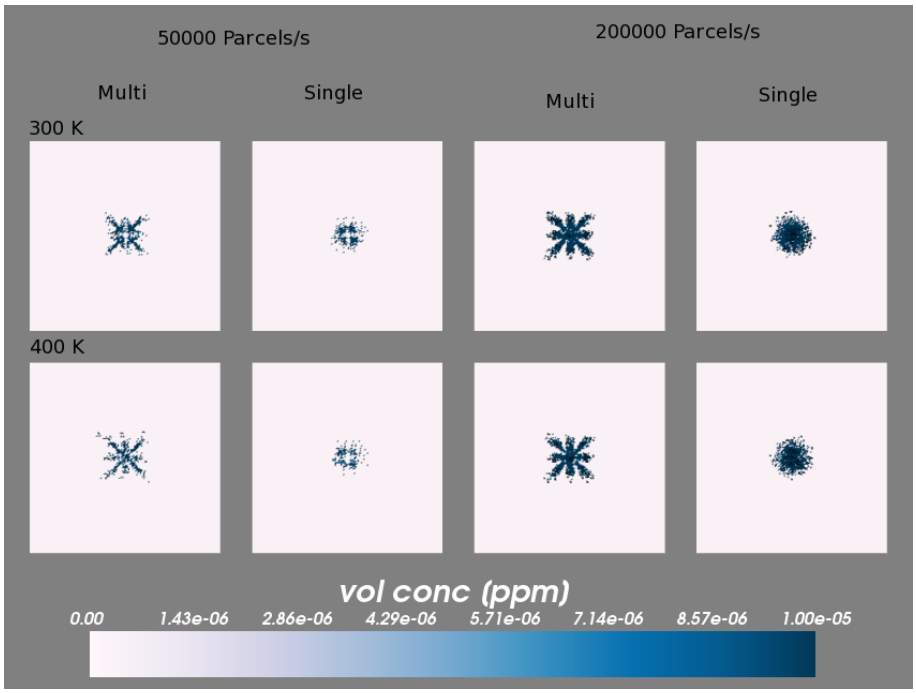

Figure 35: Comparisons of concentrations on the othogonal plane at 250 mm from the nozzle for the multi-injector model operating at 100 bar and the single-injector equivalent one.

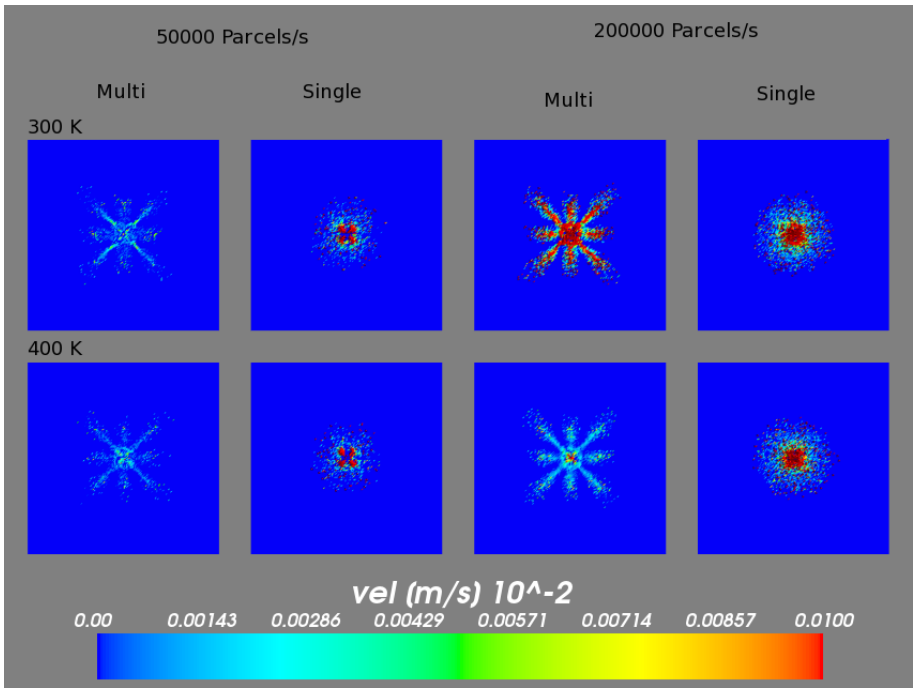

Figure 36: Comparisons of average velocities on the othogonal plane at 500 mm from the nozzle for the multi-injector model operating at 100 bar and the single-injector equivalent one.

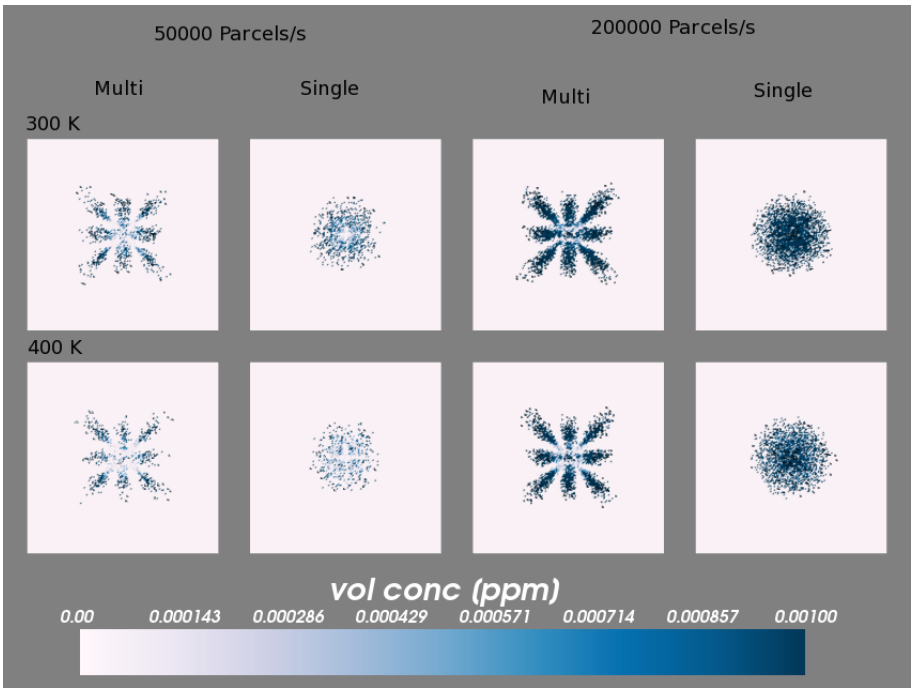

Figure 37: Comparisons of concentrations on the othogonal plane at 500 mm from the nozzle for the multi-injector model operating at 100 bar and the single-injector equivalent one.

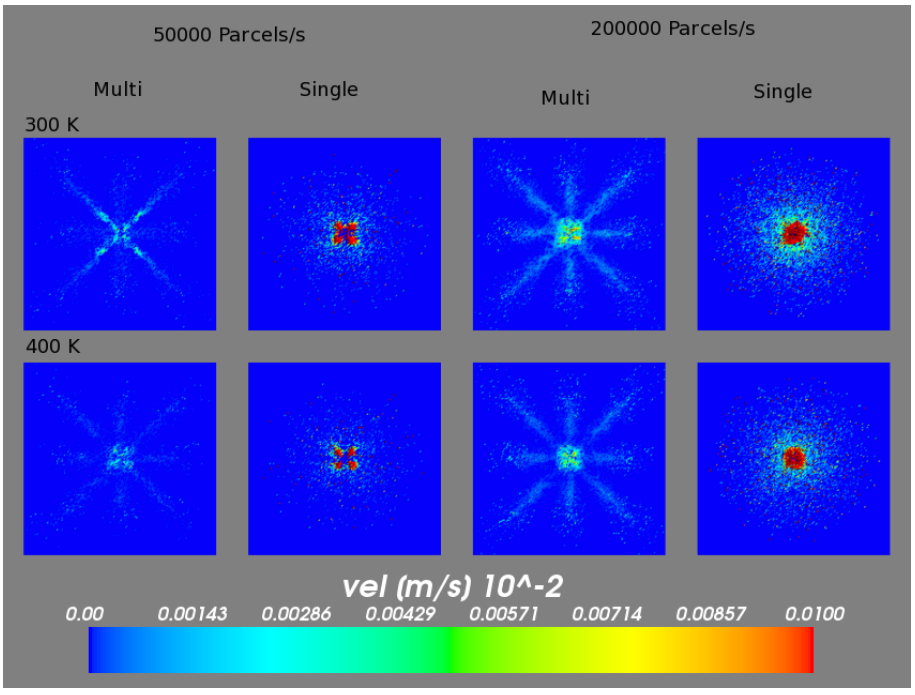

Figure 38: Comparisons of average velocities on the othogonal plane at 1 m from the nozzle for the multi-injector model operating at 100 bar and the single-injector equivalent one.

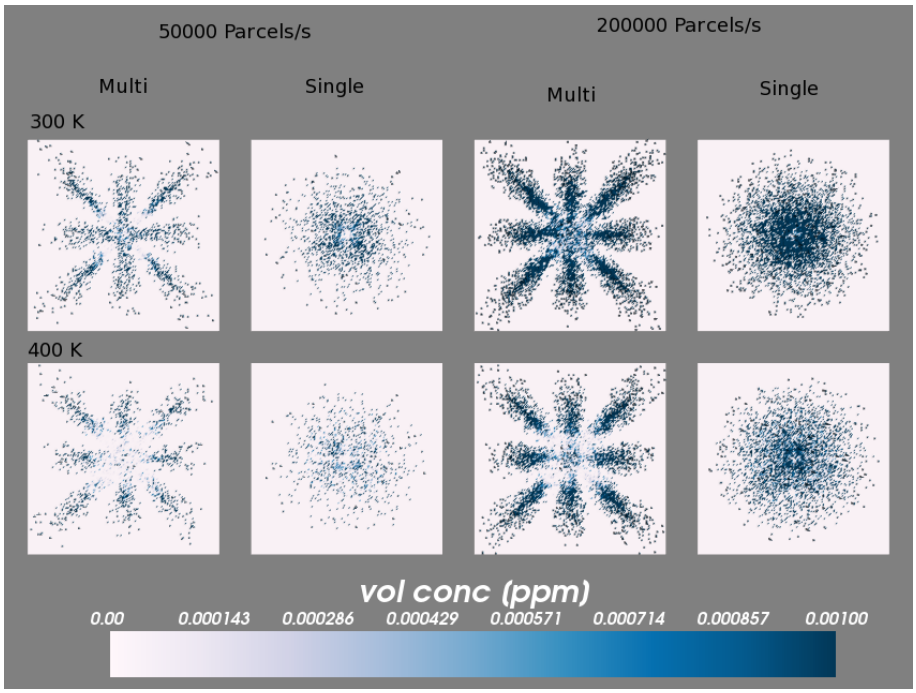

Figure 39: Comparisons of concentrations on the othogonal plane at 1 m from the nozzle for the multi-injector model operating at 100 bar and the single-injector equivalent one.

the nozzle, a 45 seconds response time was estimated, as shown in Figure 40.

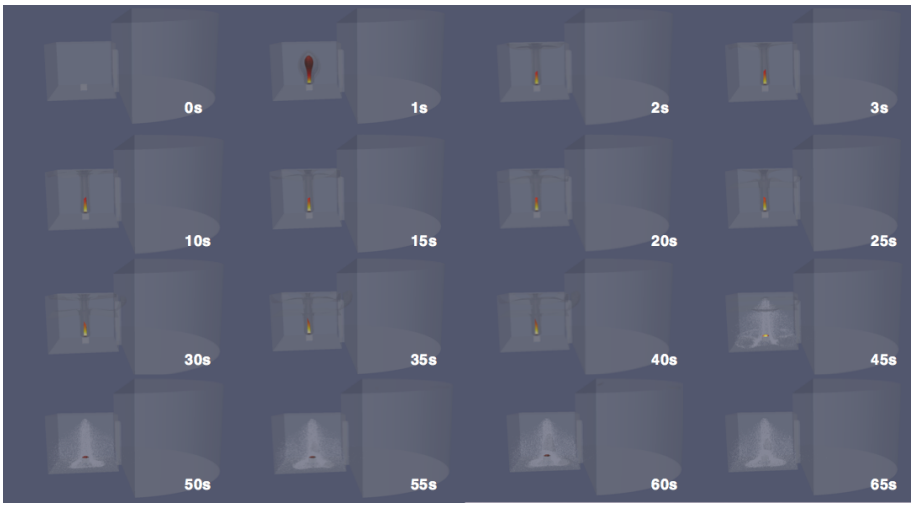

Figure 40: Activation sequence (water discharge starts at 45s) of a water mist nozzle for the assigned RTI factor in the validated compartment fire scenario.

Part III

CRITICAL ASSESSMENT

Although one of the main reasons of water mist systems design in compartment fires is for fire suppression purposes, it is very complex to address this objective in a predictive manner, due to the high uncertainty in combustion modeling. The first aplication deals with water mist in tunnel with the solely objective to investigate smoke confinement and stratification. The second application regards the protection of people during the egress from combustion products in subway emergencies with natural ventilation shaft. After the determination of a proper cross-section for the considered design fire, a detailed geometry of the scenario is investigated to assure that the solution provided meets the requirements.

5

NATURAL VENTILATION DESIGN FOR EMERGENCY STRATEGIES

5.1 DESCRIPTION OF THE PROBLEM

A code compliant tunnel ventilation system design can be investigated with numerical simulations to verify its performance. Because of design fires may vary significantly, many different fire sources may be investigated respect to their probability to occur.

The present application is about the analysis of the consequences of fires in subway line, with the intent to evaluate the efficacy of fire-fighting strategies in order to assure the prescribed safety level, with an emphasis on the egress of people during and emergency. Since natural ventilation shafts design for smoke extraction that protect exit paths from the spread of smoke are not well regulated, numerical simulations are carried out to evaluate the influence of the main parameter in order to figure out an optimal cross-section of the shaft for a reference design fire in a geometrical simplified domain.

Then, to assure that the cross-section of choice satisfies the criteria that the given strategy imposes, a detailed geometry is considered to forecast the when smoke enters the emergency exit in the given scenario. In this case the instant when the smoke gets to the exit door needs to be determined in a particular configuration of interest, under certain hypothesis. The scenario is set in an underground subway single line system, in a section of the tunnel between two stations, which has to be provided with an emergency exit, protected to prevent income of smoke by a natural or forced ventilation system which has to be properly designed. In order to get an overview of the macroscopic influence of the cross-section of the shaft, for the tunnel aspect ratio

considered and a selected design fire, a preliminary study was conducted with a simplified geometry, assuring that global head losses in the branches are resolved by properly calculated equivalent diameters.

The tunnel geometry considered was a section of 120 m of a common single track line, of approximately $20m^2$ of cross-section, containing a train 50 m long with a frontal area of approximately $6m^2$. A compartment connect the tunnel with the emergency stairs, which has a volume of approximately $70m^2$ and communicate with an opening of $1,8m$ of length and $2,1m$ of heigh. A $2\,MW$ fire is located at the center of the train, which in this case is right in front of the open emergency exit doors. Three different cross sections were considered, respectively of $0,1m^2$ (which is the minimum required value as stated in Italian regulations), $6m^2$ and $12m^2$ and ASET time is then estimated by monitoring the mass flow of the combustion products through the different branches and the average temepratures of the smoke layer at $1,2m$ of height on the door section. Two different possible elevation was considered, $-20m$ and $-30m$ tested for all the cross-sections of the ventilation shaft, under the hypothesis that the influence of the flow up and down the considered section was negligible. Even if important results for fire risk management regards indicators of the toxicity of smokes, whose may determine different time-to-incapacitation and time-to-death values, in this study the concentration of CO_2 was used to evaluate smoke danger. Moreover, there appears to be not so much informations on visibility and toxicity levels for fires under natural ventilation conditions.

5.2 NUMERICAL SET-UP

The simulated cases are reported in table 11 and they involve different cross-sections of the natural ventilation shaft and line elevation. The mesh was adapted in order to assure physical convergence of the

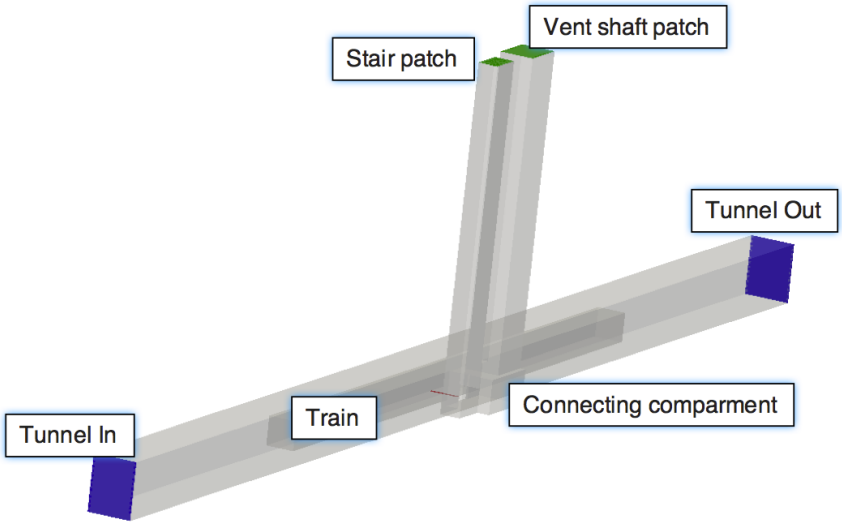

Figure 41: Simplified geometry for natural ventilation assessment of a subway emergency exit.

results and boundary conditions are reported in table 12. The turbulence model adopted in this case was the LES (One Equation formulation) with the EDM for combustion. In this cases the influence of the initial condition of air flow in the tunnel is neglected (as the one that may be induced by the piston effect) and a quiescient ambient has been considered as initial condition.

5.3 RESULTS

Simulations results are interpreted in terms of stairs and shaft flow rates, that are connected to the emergency exit and affect monitored average temperatures at $1,8m$ of height in the center line of the door that opens to the evacuation stairs. As it is possible to see from Figures 46 and 47, sjowing temperatures contours at 30, 60 and 90 seconds since the fire has started, the $6m^2$ and the $12m^2$ solutions are effective in keeping the stairs free from smoke, in the both cases of $-20m$ and $-30m$ elevation , while the $0,1m^2$, which is the minimum required value for such application for the current legislation in Italy, is ineffective in both cases.

Case	Ventilation shaft	Elevation	Design Fire
1	$0.1\,m^2$	$-30\,m$	$2\,MW$
2	$0.1\,m^2$	$-20\,m$	$2\,MW$
3	$6\,m^2$	$-30m$	$2\,MW$
4	$6\,m^2$	$-20\,m$	$2\,MW$
5	$12\,m^2$	$-30\,m$	$2\,MW$
6	$12\,m^2$	$-20\,m$	$2\,MW$

Table 11: Simulations carried out to assess the effectiveness of a natural ventilation shaft for an emergency exit in an underground scenario.

Patch	Type	Value
Fire	Mass flow rate (methane)	0.04 kg/s
Inlet Tunnel	U: pressureInletOutlet p: TotalPressure	-
Outlet Tunnel	U: pressureInletOutlet p: TotalPressure	-
Outlet Stairs	p: buoyancyPressure	-
Outlet Shaft	p: buoyancyPressure	-
Walls	Adiabatic	-

Table 12: Boundary conditions assigned to carry out the simulations for both the simplified and the detailed geometry.

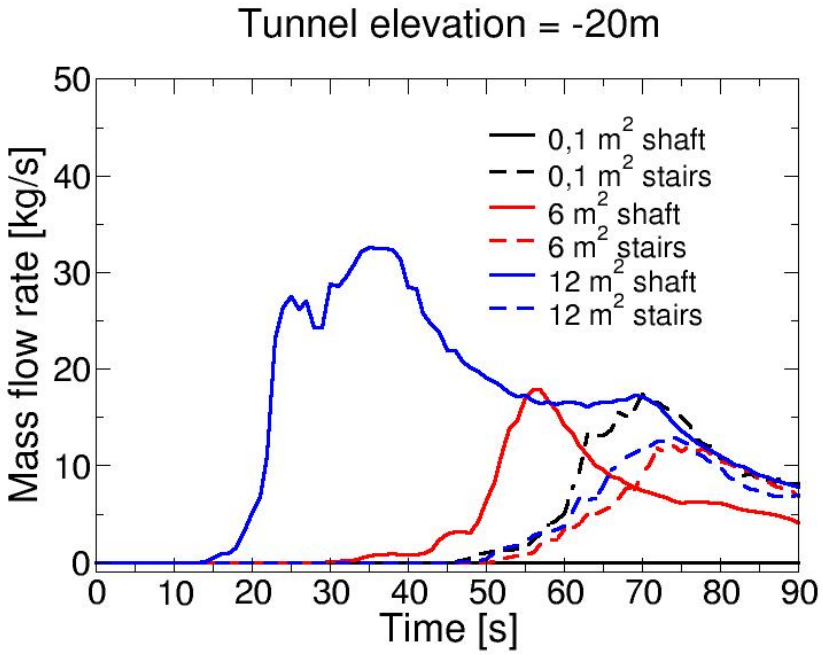

Figure 42: Comparisons of flow rates for cases at -20 m elevation that pass through the stairs and the extraction shaft.

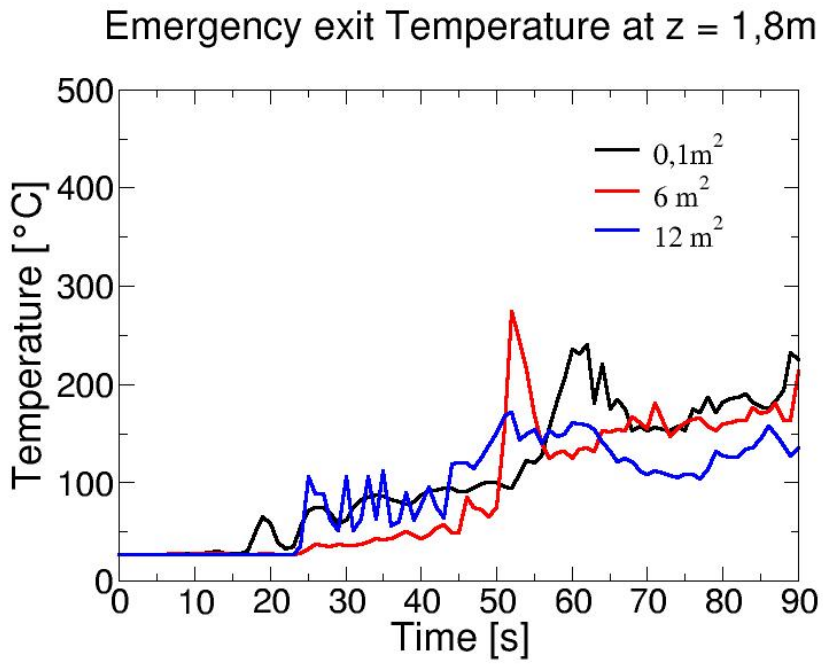

Figure 43: Comparisons of temperatures at z=1,8m on emergency exit door centerline for cases at -20 m of elevation.

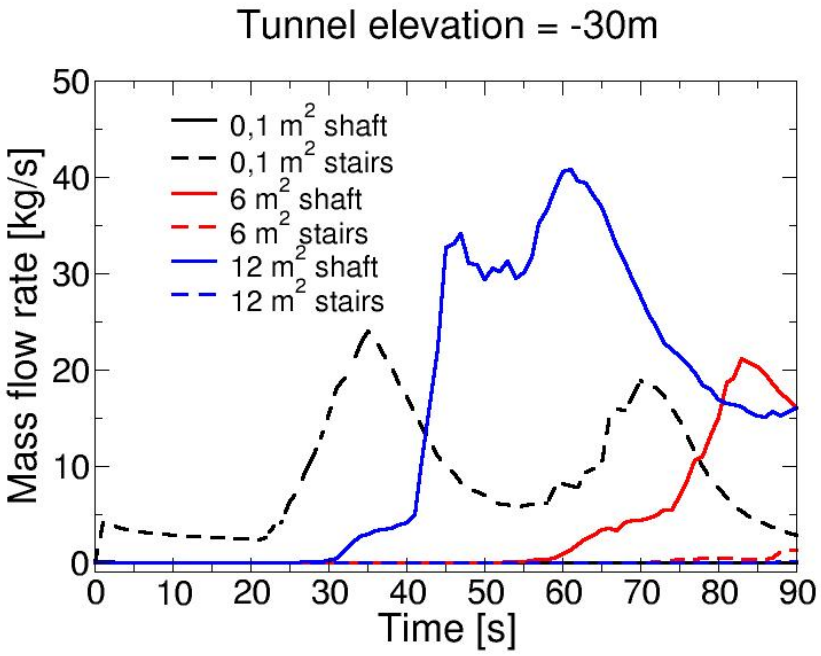

Figure 44: Comparisons of flow rates for cases at -30 m elevation that pass through the stairs and the extraction shaft.

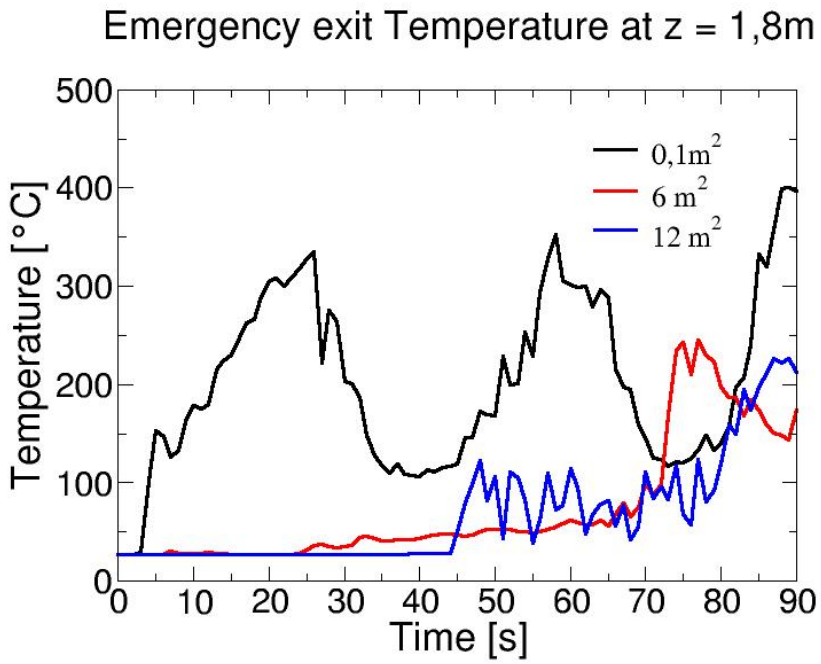

Figure 45: Comparisons of temperatures at z=1,8m on emergency exit door centerline for cases at -30 m of elevation.

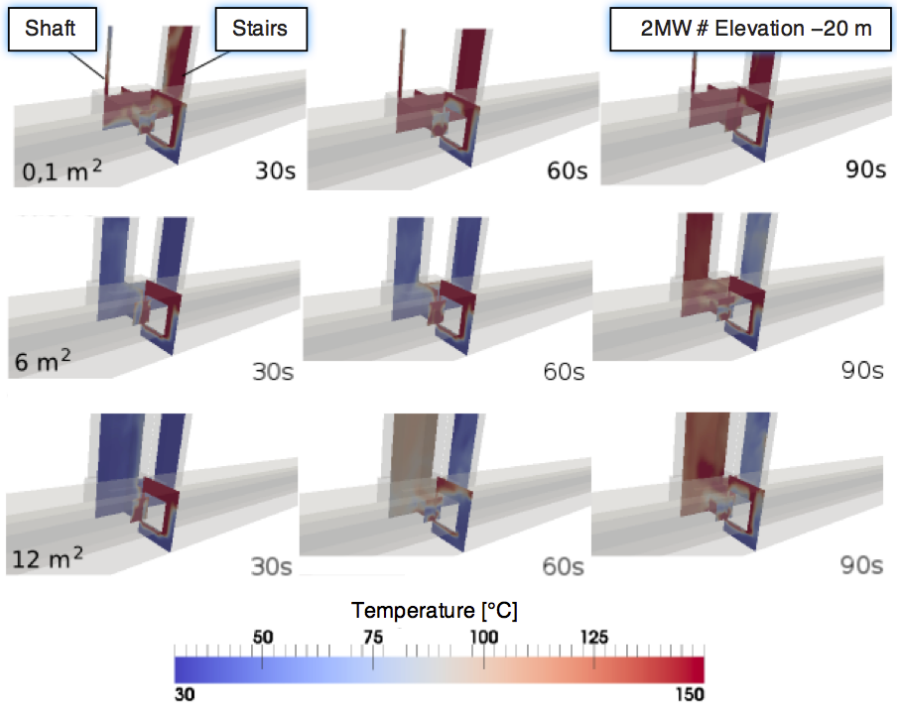

Figure 46: Comparisons of temperature contour in the connecting compartment for different cross-sections of the shaft at an elevation of -20 m.

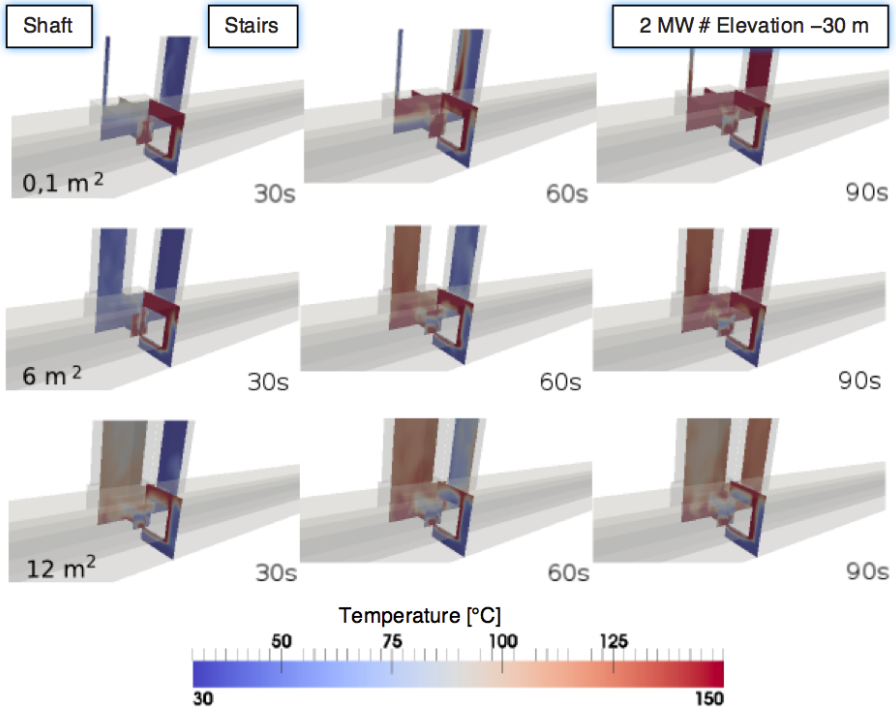

Figure 47: Comparisons of temperature contour in the connecting compartment for different cross-sections of the shaft at an elevation of -30 m.

The critical ventilation velocity for the given scenario is calculated with an iterative procedure illustrated in Figure 48 and the value estimated is 2 m/s, which is not compatible with the natural ventilation shaft cross-sections considered for the given design fire.

5.4 DETAILED GEOMETRY SIMULATION

5.4.1 *Objective of the analysis*

While these results may give a rough overview of the influence of the shaft cross-section, they still allow to make hypothesis on design parameters whose depend also on other constraints in complex buildings. It is then important to verify that the solution adopted meet the performance criteria defined by the risk assessment analysis that cover all the aspects connected to the emergency plan. For this purpose, a detailed geometry is investigated to calculate the ASET time, which in this application is defined as the time when the smoke starts to spread through the compartment without considering any minimum target of temperature, nor combustion products concentrations and thermal radiation fluxes in order to give a safety value of reference for the given scenario, whith the assuption that the fire reach the peak of 2MW when the train stops with the head at 100 m from the emergency exit, and the fire located at the center of the train. Further work need to be done in order to assess better the design fire properties, the roughness of surfaces, the different ventilation conditions that may occur in the tunnel, and so on. In fact a detailed description of the strategy may assure great accuracy, but it costs a great effort not only from a computational point of view. For example, even if it possible to account for the roughness of walls even with simple wall function treatment, only simple assumptions may be done about how to characterize surfaces, and for long tunnels, even a little difference in the roughness parameters of the model may lead to great differ-

	Back layer in steady state condition
0.5 m/s	
1 m/s	
1.5 m/s	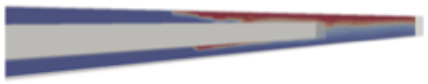
2 m/s	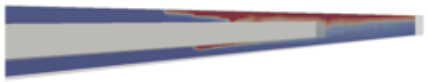

Figure 48: Determination of the critical velocity for the given scenario by imposing different boundary velocity values.

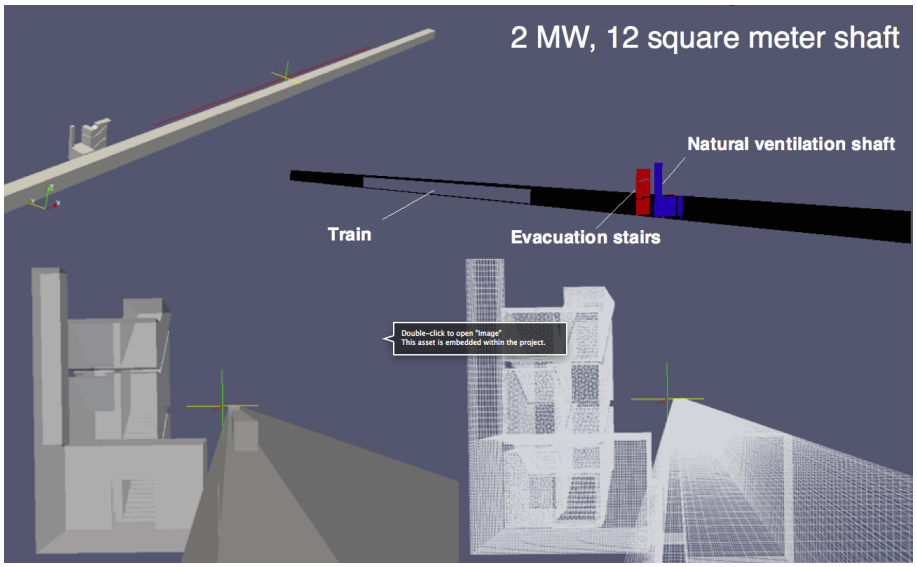

Figure 49: Description of the detailed geometry scenario for ASET Time estimation, with indication of fire location, grid resolution and tunnel extend.

ences in terms of global head loss determination. The present study did not address the impact of roughness on determining the ASET time of the particular scenario considered, but a value of 0.01 m of mean roughness was compared to the smooth wall solution, showing a 30% difference in maximum velocities values in the flow direction nearby the boundary layer of walls. So further investigations have to be carried out, with a previous understanding of the average properties of the surfaces, which may vary a lot in consideration of many factors.

5.4.2 *Results*

It is possible to verify from Figures 50, 51, 52and 53at 120 sec the smoke starts to enter the emergency compartment and thus 120 s was defined as the critical time for this kind of simulation, which is of course on the safety side, since smoke concentrations and temperatures have not yet overcomes maximum safety levels. These figures give the same information in different manner, since the objective of

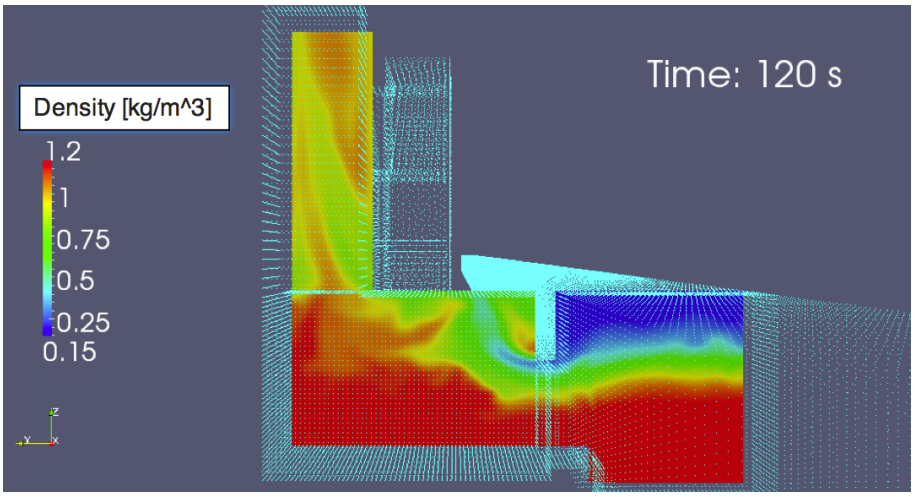

Figure 50: Air density contour at 120 sec nearby the exit door that is used to evaluate ASET time.

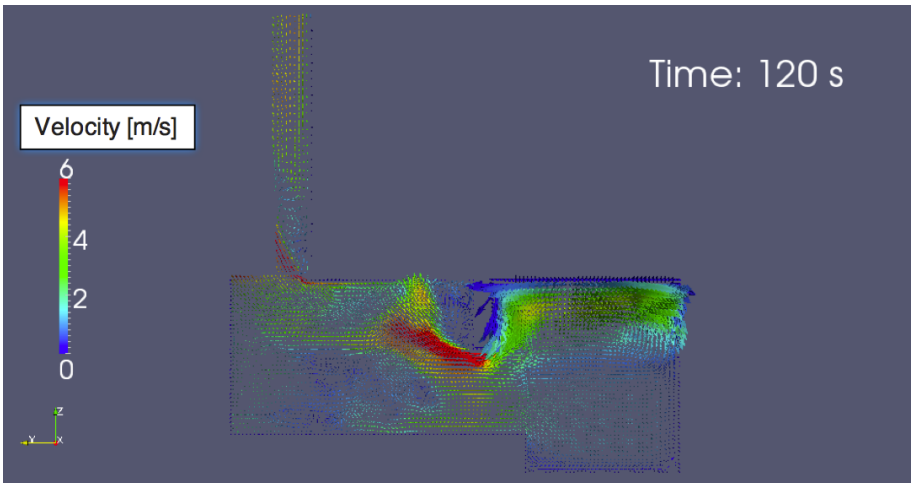

Figure 51: Velocity distribution at 120 sec nearby the emergency exit door.

the analysis just focuses on smoke propagation and not in the scrutinizing of different criteria (as radiative heat fluxes, combustion product concentrations and temperature averages or smoke layer heigh).

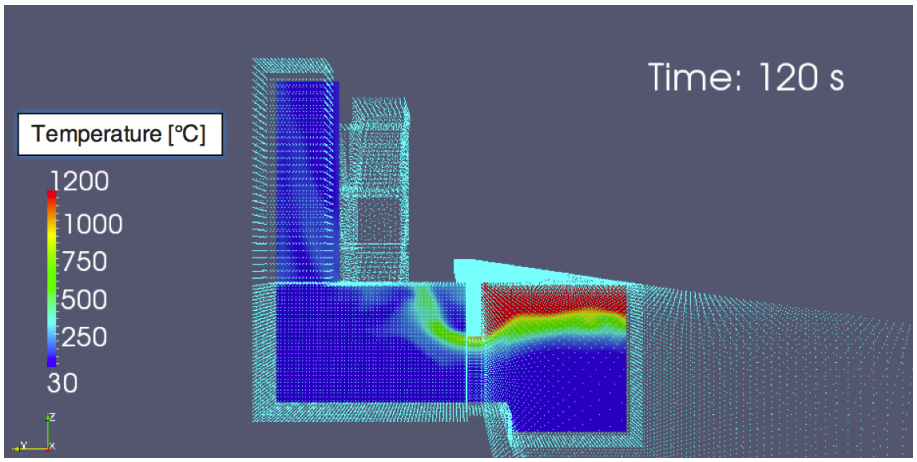

Figure 52: Temperature distribution at 120 sec nearby the exit door

Figure 53: Smoke distribution at 120 sec nearby the exit door (represented with carbon dioxide concentration)

6

WATER MIST FIRE-FIGHTING STRATEGIES AND SMOKE STRATIFICATION

6.1 LARGE-SCALE COMPARTMENT FIRE VALIDATION

In order to apply the water mist nozzle model, previously validated and assessed, to investigate fire fighting senarios, it is necessary in advance to validate a fire model of a tunnel fire. From literature, the 20 MW Memorial Tunnel fire case has been selected from the natural ventilation tests that were conducted, and a sensitivity analysis is carried out to find an acceptable grid resolution, while in the region where water mist nozzles operate, also contraint due to spray resolution are applied based on previous analysis.

6.1.1 *Description of the Memorial Tunnel Fire Tests*

Because of the lack of knowledge regarding the efficacy of fire fighting ventilation strategies in road tunnels, the Memorial Tunnel Fire Ventilation Test Program was started in 1982 and settled the base of full-scale experiments which rapidly increased in number after the Mont Blanc and the San Gottardo accidends, and still don't allow to set a comprehensive reference for system design. The Memorial Tunnel tests are very important because of the relatively high number of tests (98) that were conducted and measured so that it is possible to do comparisons with CFD simulations. The Memorial Tunnel was built in 1953, made up with bricks covering the surrounding dolomite rocks for 853m long and with a 3.2% upgrade from the South to the North portal. The cross-section of the tunnel is about , because the

ceiling was removed in the natural ventilation tests, in fact it could be destroyed by the fire quite soon and there is no need of the ventilation shafts.The original ventilation systems was in fact modified to allow the operations of different strategies such as transverse (both full and partial) and longitudinal ventilation with jet fans. Anyway the presence of the fan rooms located at each tunnel portal of the previous systems reduces the tunnel height at the entrance at approximatively $4m$, thus reducing the cross-section significantly as shown in Figure 55. The effectiveness of the different strategies to manage the smoke evolution over time essentially based on temperature and smoke concentration evolution were tested in case of different heat release rate powers: 10, 20, 50 and $100MW$. In the present comparison the $20MW$ test is considered, since it is a good value of reference according to many authors [30, 14, 24, 19].The program consisted in a series of full-scale fire tests conducted in an abandoned road tunnel in West Virginia (US). A wide range of different tunnel ventilation systems and configurations were operated in order to assess their performances in managing the smoke and temperatures produced by the fire within the tunnel, and to validate a fire model the natural ventilation test is the one of choice, because the phenomenon that drives the spread of smoke is of course the buoyancy effect. The tunnel was equipped with many instrumental devices so that results could be represented under a global description of the evolution of the fire until steady condition. Contours of velocities, temperatures, and combustion products concentrations along the tunnel are available at different time location, and without focusing on the early stage of the fire, data are compared at $5m$ to give evidence of a sufficient accurate description. An ambient air temperature of approximately $7°C$ was registered during the tests and no relevant relative pressure differences at portals were evidenced due to meteorological conditions, otherwise different reference pressures should be imposed. Wind velocity was considered negligible, so a stagnant air initialization was considered to be sufficiently accurate.

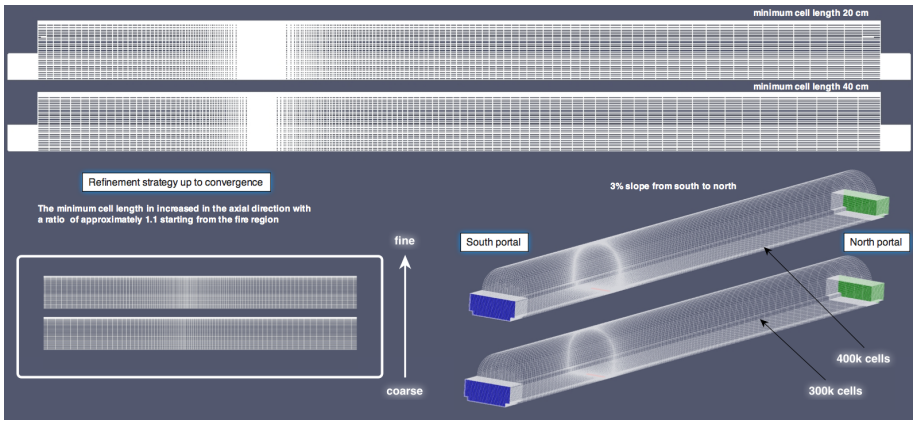

Figure 54: Memorial Tunnel refinement strategy adopted to assess a sufficient grid resolution with respect to the evolution of velocity and temperature profiles

Patch	Type	Value
Fire	Mass flow rate (methane)	0.04 kg/s
South Portal	U: pressureInletOutlet p: buoyancyPressure	-
North Portal	U: pressureInletOutlet p: buoyancyPressure	-
Walls	Adiabatic	-

Table 13: Measured flow rates f, at different operating pressures for single injector C.

6.2 NUMERICAL SET-UP

6.3 RESULTS

Results were compared in terms of temperatures and velocity profiles and were in good agreement since a minimum coarse grid resolution were established. A fine grid was then applied to assure grid independence. Contours of temperatures at 5 minutes since ignition are illustrated in Figure 56 and in Figure 57 to assure grid independence, for the portion of the tunnel that goes from the fire location to the North Portal. Also velocities are compared and were slightly over predicted, since in the model the walls were assumed smooth.

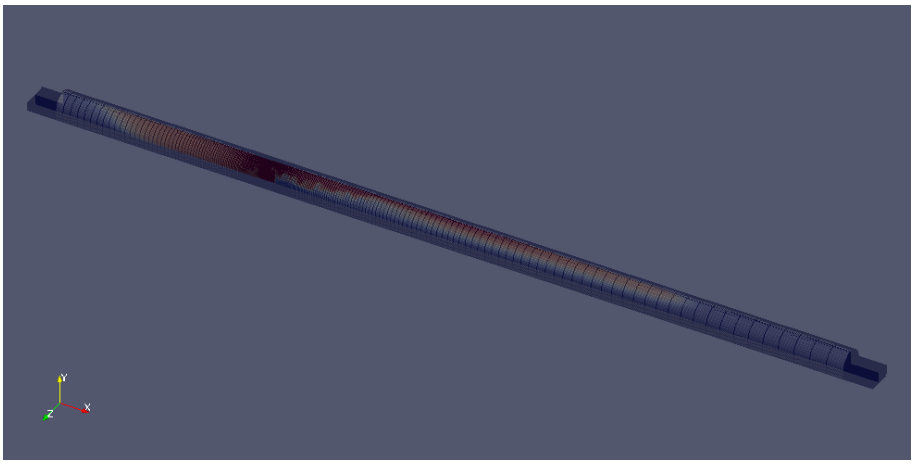

Figure 55: Memorial Tunnel adapted final mesh with 20 MW fire size at 120 sec since ignition, different grids were tested until global convergence was reached with an average 12 cm cell lengh nearby the fire source.

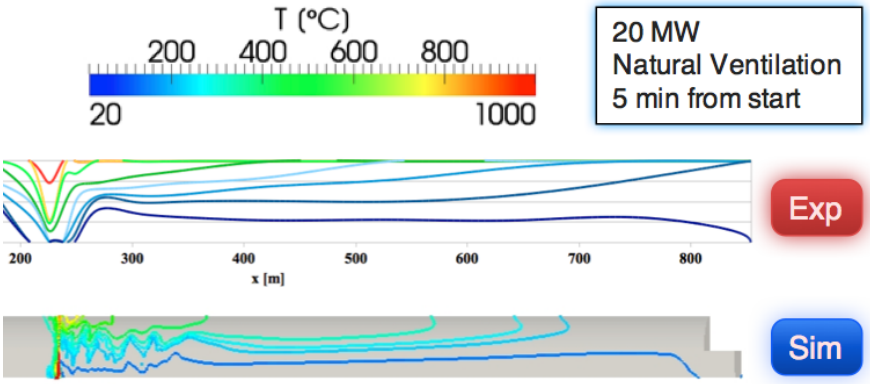

Figure 56: Comparisons of experimental data and simulations at 5 min since the fire has started for the 20MW natural ventilation case

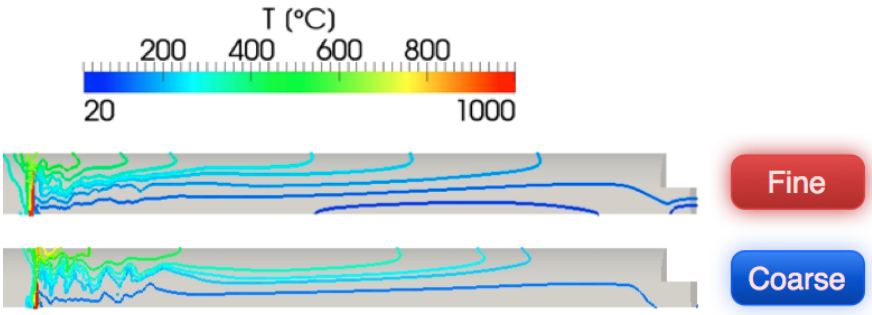

Figure 57: Comparisons of temperature contours between two different adapted meshes

6.4 DESCRIPTION OF THE SCENARIO

Water mist systems have been installed in several tunnel systems in Europe, such as portions of the A-86 tunnel near Paris, France, and the M-30 tunnel system near Madrid, Spain, among many others and also tested, since recent years also with test fires that are much larger than in the past, since it was demonstrated (after the serious fires that have occured mostly in Europe and North America) that the maximum rate of heat release is commonly comprises generally from 20 to 200MW, with the latter representing a common peak value of an uncontrolled compartment fire of an Heavy Goods Vehicle (HGV) . Criteria about how to design fire tests to evaluate system performance vary a lot between countries and many other factors, and experiments are difficult to carry out, so numerical simulations may give useful information of investigate better a given strategy when the desing of the system is proposed. It has to be noted that recently authors proposed an EE approach to such simulations, but with no indications about the quality of the simulation of the water mist spray described [16]. Investigations on water mist systems efficacy in fire-fighting strategy don't involve just fire suppression, since they affect the overall scenario with a particular emphasis on the effects on smoke destratification and visibility. In fact due to the high mixing generated by water mist Since it is very difficult to estimate visibility (as described in a previous section) and it may be sufficiently clear that in case of a deluge water mist discharge during a tunnel fire may lead to a very low visibility close to the water mist sprays because of its high effect on radiation absorption and scattering. What may be more interesting for a fire risk assessment analysis is the influences on smoke stratification, which have strong consequences on temperatures and combustion product concentration in the controlled volume, by causing air flow and smoke disruption and cooling. This has a positive effect on containing the smoke in a confined region, but may severely

downgrade the safety conditions within the operative area. These consequences can be controlled and design optimization may be carried out by numerical simulations, based on a previous assessment of the spray numerical set-up, described before. In this application the effects of water mist in a tunnel fire-fighting strategy are investigated to estimate temperatures and smoke product concentrations for 30 seconds after the water mist system has started, which is a time comparable with egress time and human resistance to high temperatures and high toxic concentrations. The smoke control by water mist systems has also been recently investigated experimentally not only for road tunnels, but also for subway station applications [4] but they do not seem to provide more information than numerical simulations, due to the extremely high costs and the consequent limitations that affect measurements, becouse of the limited spacial distribution that devices may cover and the limited number of variables that can be monitored simultaneously.

6.5 NUMERICAL SET-UP

The cases simulated refer to a typical water mist strategy which adopt a diluge zone system to control the smoke spread along the tunnel. Since the design need to take into account tunnel geometries and water mist system parameters, such as operating pressure, nozzle spacing, so then flow rates, spray patterns, droplet diameters, among many others, in this application the validated water mist nozzle was applied to a $100m$ zone control strategy, with 4 rows of nozzles with $10m$ of distance one from each other in the axial direction. Since the design fire and the tunnel characteristic are the one of the natural ventilation Memorial Tunnel case, in order to have a validated case to compare results, which has a very high ceiling due to the absence of the ventilation ducts, the nozzles are at $6m$ heigh which is the maximum heigh at which those nozzles are usually installed. Each nozzle

starts to discharge water at 30 s since the fire start, according to the assumptions at the base of the strategy and every nozzle operates at 80 bar, with a characteristic flow rate of around 20 l/min per each. To assure that the assessment of the nozzle model has given good results two determine in advance the required minimum numeber of droplets per seconds, a simulation was carried out doubling the number of droplets per second and results show that this doesn't affect the results, as osberved in terms of levels of temperatures and CO_2 concentrations. Many different scenarios should be investigated, in particular for different operational zones in order to minimize the total water flow and to assure a synergic integration with forced ventilation, depending on tunnel geometries, to optimize the nozzle locations, but this if out of the scope of the presented analysis.

6.6 RESULTS

In tunnel fire scenario the smoke stratification is of primary interest in determining the safety condition for people, in the early stage of the fire, when people are evacuating and have higher chances to survive [34]. Although recently have been published simulations about the prediction of soot and carbone monoxide [44], many different methodologies were proposed to evaluate the toxic potency for fire hazard analysis based on experimental data [15]. It is very difficult also to validate those data, since soot formation and unburt products depend on complex chemical reactions, and also a detailed description and properties of the materials involved in the scenario is needed. Temperatures are a measure of the overall mixing and evaporation effect, and they have been compared to assure that evaporation occurs without depending on droplet numbers. From Figures 58, 59 and 60togher with Figures 61, 62and 63it is possible to estimate the confinement effect on smoke propagation due to water mist supply. In this way it is possible to account for different temperatures and

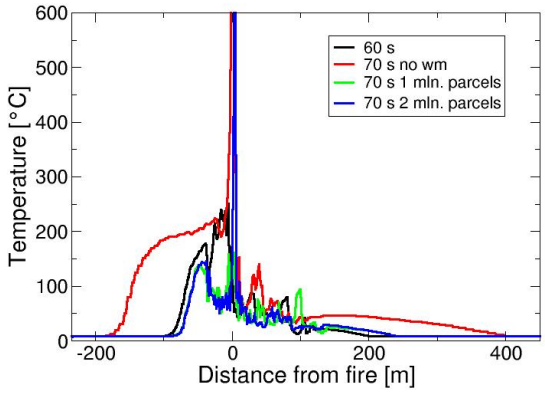

Figure 58: Comparisons of temperatures at z=1,8m on the tunnel center line at 70s for the free burn simulation and the two water mist simulations (2 and 4 M droplets per second respectively).

combustion product concentrations. The same results are provided in Figures 64, 65and 66for temperature peaks and in Figures 67, 68 and 69for CO_2concentrations. The design fire was validated against the Memorial Tunnel fire test for natural ventilations, and results always shows a comparison between the 2M and the 4M droplet per second case, in order to assure that results are parcel-indipendent for the objectives of interest.

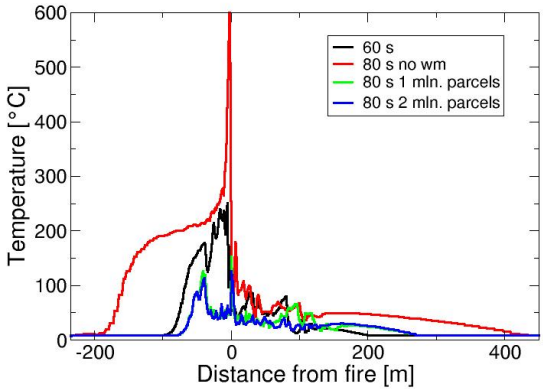

Figure 59: Comparisons of temperatures at z=1,8m on the tunnel center line at 80s for the free burn simulation and the two water mist simulations (2 and 4 M droplets per second respectively).

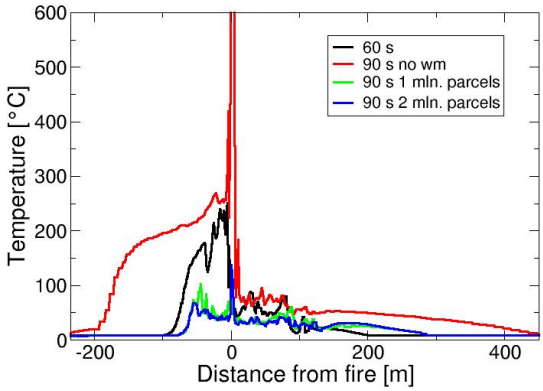

Figure 60: Comparisons of temperatures at z=1,8m on the tunnel center line at 90s for the free burn simulation and the two water mist simulations (2 and 4 M droplets per second respectively).

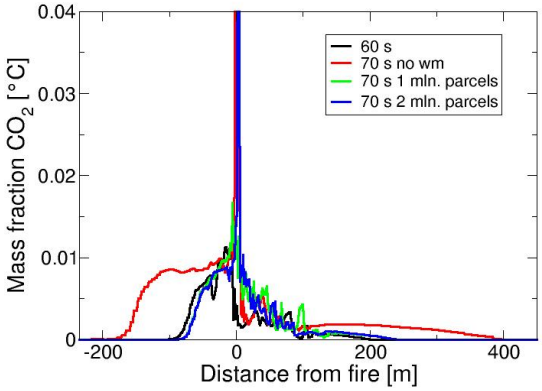

Figure 61: Comparisons of carbon dioxide concentrations at z=1,8m on the tunnel center line at 70s for the free burn simulation and the two water mist simulations (2 and 4 M droplets per second respectively).

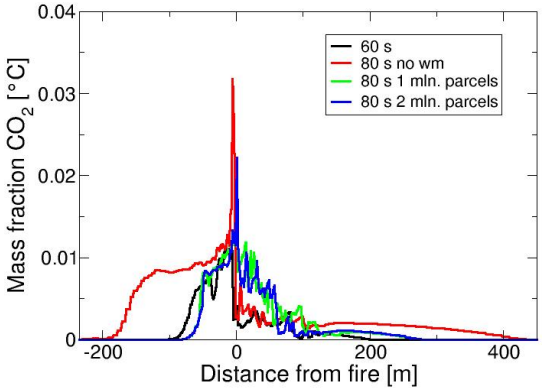

Figure 62: Comparisons of carbon dioxide concentrations at z=1,8m on the tunnel center line at 80s for the free burn simulation and the two water mist simulations (2 and 4 M droplets per second respectively).

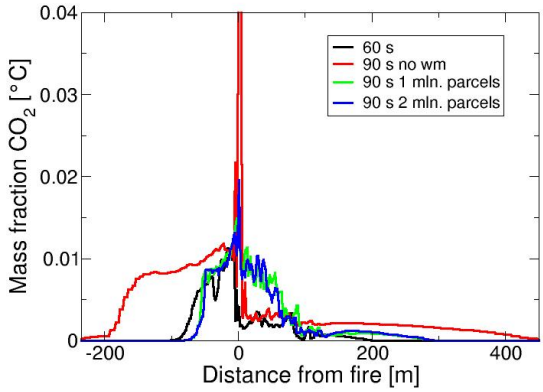

Figure 63: Comparisons of carbone dioxide concentrations at z=1,8m on the tunnel center line at 90s for the free burn simulation and the two water mist simulations (2 and 4 M droplets per second respectively).

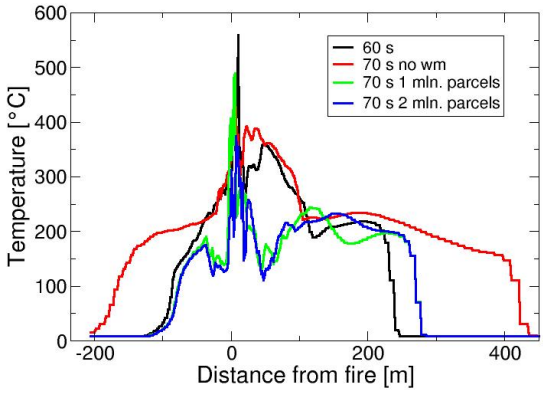

Figure 64: Comparisons of temperatures at z=1,8m on the tunnel center line at 70s for the free burn simulation and the two water mist simulations (2 and 4 M droplets per second respectively).

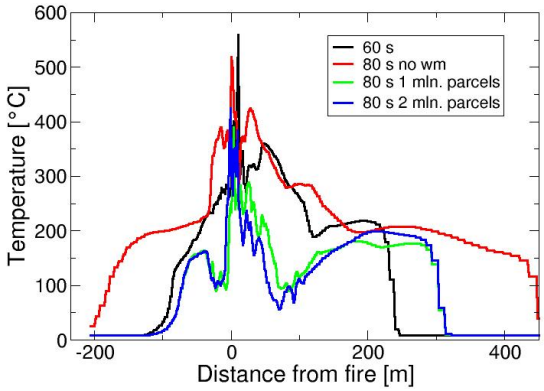

Figure 65: Comparisons of temperatures at z=1,8m on the tunnel center line at 80s for the free burn simulation and the two water mist simulations (2 and 4 M droplets per second respectively).

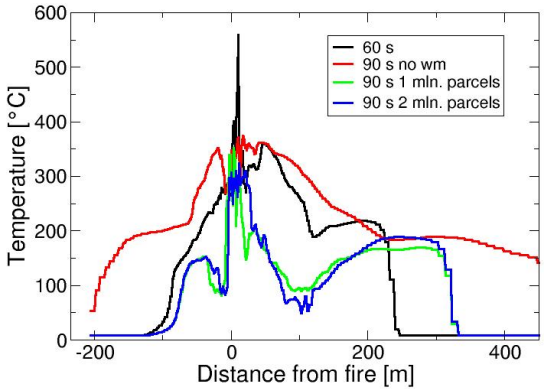

Figure 66: Comparisons of temperatures at z=1,8m on the tunnel center line at 90s for the free burn simulation and the two water mist simulations (2 and 4 M droplets per second respectively).

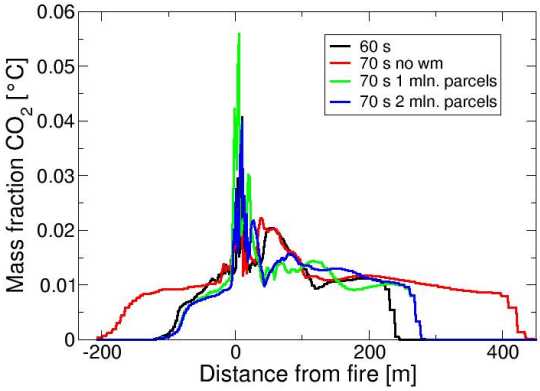

Figure 67: Comparisons of carbon dioxide concentrations at z=1,8m on the tunnel center line at 70s for the free burn simulation and the two water mist simulations (2 and 4 M droplets per second respectively).

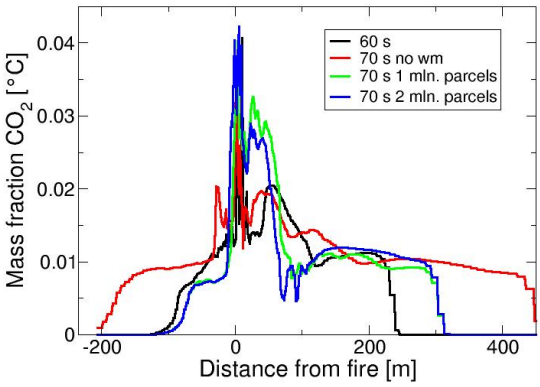

Figure 68: Comparisons of carbon dioxide concentrations at z=1,8m on the tunnel center line at 80s for the free burn simulation and the two water mist simulations (2 and 4 M droplets per second respectively).

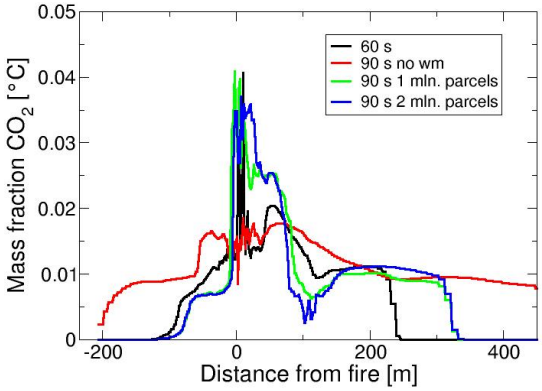

Figure 69: Comparisons of carbone dioxide concentrations at z=1,8m on the tunnel center line at 90s for the free burn simulation and the two water mist simulations (2 and 4 M droplets per second respectively).

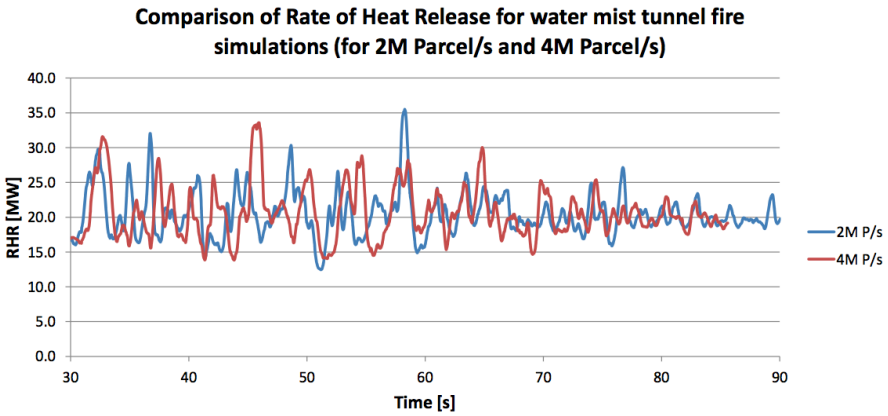

Figure 70: RHR comparisons since water mist discharge has started (+30s) for the 2M and the 4M Parcel/s cases.

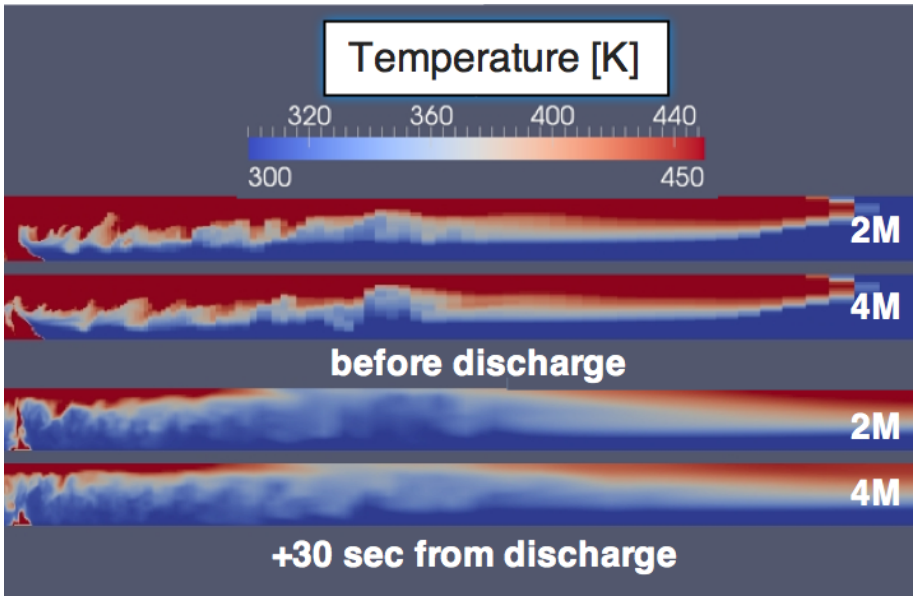

Figure 71: Comparisons of temperatures contour at 60 sec (just before erogation starts) and 30 seconds later between the two cases (2M of total droplets/s and 4M) for the right section of the tunnel (from the fire location to the north portal).

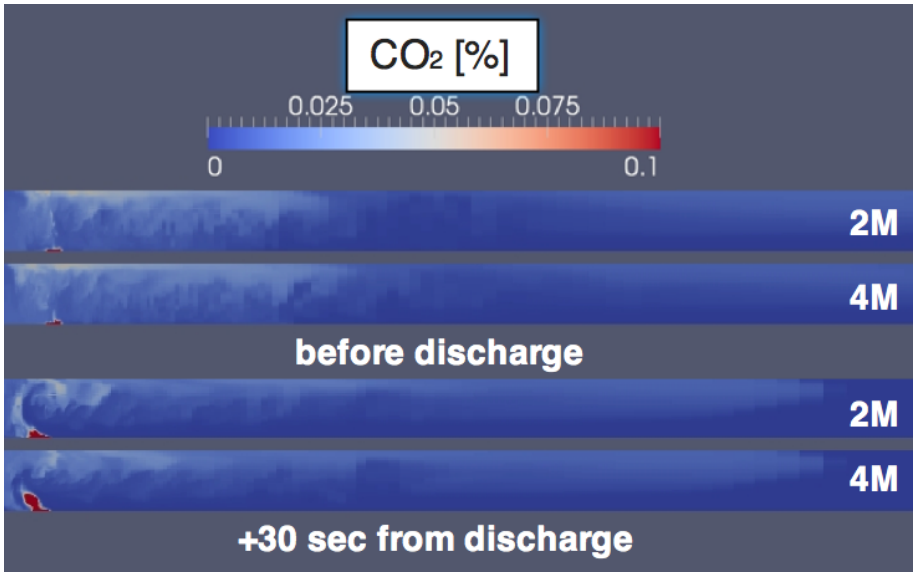

Figure 72: Comparisons of carbon dioxide contrentation contour at 60 sec (just before erogation starts) and 30 seconds later between the two cases (2M of total droplets/s and 4M) for the right section of the tunnel (from the fire location to the north portal).

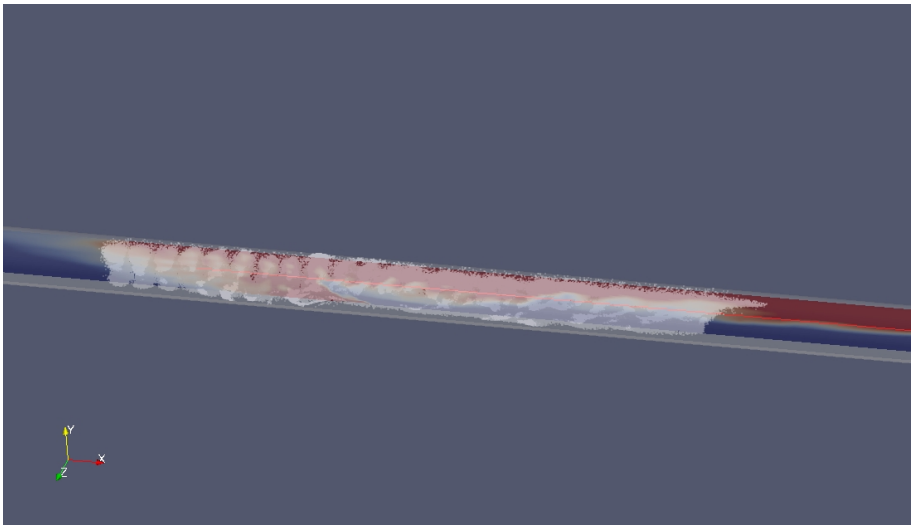

Figure 73: Water mist discharge visualization for 2M of droplets per second simulation after few seconds since erogation has started.

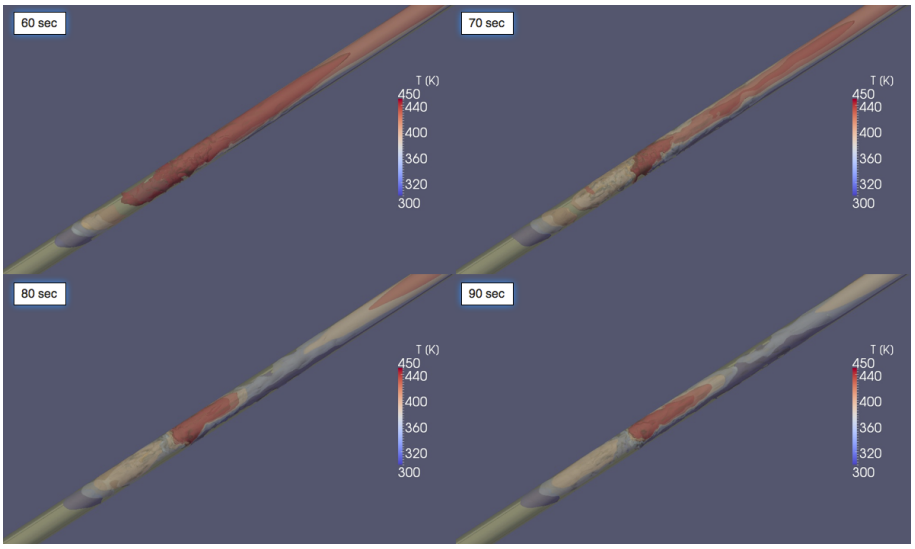

Figure 74: Temperature contours at different times since the fire has started (erogation started at 60s) showing the effect on smoke control due to air disruption and cooling effect by water mist.

7

CONCLUSIONS AND FUTURE WORK

During this research CFD methodologies are applied to assess a model to simulate fire scenarios for typical FSE applications with a focus on road and underground subway tunnels, because of their rapid increase in number in our cities and the high fire risk associated to them, due to the possible catastrophic consequences. The activity involved the validation and the assessment of this CFD methodologies, based on the most relevant literature about, and, since a comprehensive analysis of the most important implications of fire modeling to FSE applications is impractical, just a selection of the possible relevant scenarios has been investigated. Fire dynamics, smoke movement and water sprays simulations are belong to complex phenomena and need to be resolved with a proper numerical set-up and this set-up is strongly dependent upon the goals of the analysis. The applications shown in the present work try to minimize the uncertainties associated to simulation providing an assessment of the main parameter involved just with reference to smoke control and not focusing on fire suppression, nor fire control. In the simulations carried out in this work, a design fire was assigned and the total heat release rate was monitored and combustion always occur completely and within the expected fire region. Further investigations are needed if the fire fighting strategy significantly affect the combustion process and were out of the purposes of this research.

The application of the natural ventilation shaft design, to reduce the computational costs, followed an approach that involved a preliminary analysis in order to find the most convenient cross-section with a simplified geometry and then the verification of the selected criterion with a detailed analysis. This approach assured the maximiza-

tion of the accuracy of the result, despite the given computational resources available. Results shown that the standard requirement is unsatisfactory, and compare different solutions to allow to find out the best compromise.

About water mist systems application, the focus of the analysis carried out is about the stratification of smoke is on the consequences for people during evacuation, which occur in the early stage of the fire. It was found that the strong mixing due to water mist, needed to address fire suppression, should be alter significantly the estimation of ASET time for people along evacuation paths and should be investigated and related on system performance and design parameters.

In fact in tunnel evacuation the stratification of smoke in the early stage of the fire could be of primary importance of the evacuation of people. The results are parcel independent, in the sense that not only grid sensitivity analysis was carried out for wall boundary resolution, but also a spray (and then parcel) sensitivity analysis. This applying a methodology that first lead to scrutinize a water mist multi-injector model for fire simulations, and then to assure that the discretization parameters don't affect significantly the results with respect of the desired analysis. The CFD solver of choice is validated upon well established and documented small scale (Steckler et al.) and large scale fire test (Memorial Tunnel) and the numerical modeling was found in good accordance with the State of The Art in the filed. RANS simulations where compared to LES simulations with the final goal to understand pro and cons when applied to the same meshes, that produce reasonable results, and the average 30% less time consuming RANS approach was a little advantage despite the more realistic LES resolution of vortex that, due to the usual characteristics of design fires, are well resolved also with relatively large cells. Moreover, LES simulations allow a more detailed resolution of the transient behavior, that is of primary importance when assessing the ASET time for a given strategy. The boundary layer is often resolved with wall function, but for natural convection problems, it has evidenced that

a proper wall refinement may reduce a lot the total number of cells needed to assure the same accuracy. The wall boundary layer resolution is important in particular with reference to the roughness of the walls, which may have a strong influence on smoke movement because of the long geometries of tunnels, and that it is difficult to account for due to the high uncertainty associated in determining the model parameters for the complex geometries involved in FSE applications. Radiation plays usually an important role in a confined region of the scenario and for complex geometries it is difficult to carry on its calculation with a good accuracy, hence maybe its. Since the main focus of the activity was on smoke propagation and smoke temperature away few meters from the fire is often below values for a significant contribution of radiation, the combustion products were not described with a soot model and the account for participating media and toxic substances is avoided, hence the latter one may be correlated to the concentration of combustion products. The representative fire that better meet suite for design purposes is that of a fuel controlled combustion, imposed by prescribing a fuel mass flow rate according to the desired surface area specific heat release rate that describe its global thermal behavior. During the simulations the combustion occurred always in the expected regions and there no evidence of air controlled combustion, but scrutinizing forced ventilation strategies, this will be expect to happen, and this will complex much more the design fire description from a modeling point of view, requiring probably different assumptions than the ones adopted here. CFD methodologies are very powerful, and when used with a stronger support of experimental data it could have the potential to draw a comprehensive picture of the behavior and performance of fires and water mist systems for FSE applications. Although a significant effort is needed to model better design fires in order to address suppression investigations,valuable results have been achieved in terms of natural ventilation effectiveness assessment and water mist spray modeling for tunnel fire-fighting strategies also with a simple combustion mod-

eling, since design fire themselves are simplified representation of actual fires but allow a consistent description of the global phenomena. Of course it is important to assure that the fire characteristics are well resolved respect to the given hypothesis, in terms of the specific heat release rate of the surfaces involved in the combustion. The results provided are intended to be a first attempt in scrutinizing different solutions, because of the high numerical costs involved in such analysis and the necessity of a previous definition of the related risk and of the all connected aspects that determine the fire scenario. Nevertheless results refer to practical problems in FSE applications, which need to be accounted for with the Fire Safety Management does involve engineering because the main activities are concerned with solving problems, and often it is not possible to provide perfect solutions, but just to distinguish the better from the worst. The robustness of the solution provided has to refer to global and local quality aspects, and since quality is highly contextual, it is comprised of a large number of independent metrics and yet there are not well established rules to measure it or to define general criteria. Moreover, current research on CFD methodologies is in rapid development and the upcoming knowledge soon overcomes ongoing attempts, but, by Pareto's principle, it's still possible to wonder if just a few of those dimensions will give us a good indication of the total quality.

Part IV

APPENDIX

BIBLIOGRAPHY

[1] *Guide for the Verification and Validation of Computational Fluid Dynamics Simulations*, volume G-077. AIAA, 1998. (Cited on page 32.)

[2] *Standard Guide for Evaluating the Predictive Capability of Fire Models.* ASTM, E 1355-90. (Cited on page 7.)

[3] *Standard Guide for Documenting Computer Software for Fire Models*. ASTM, E 1472-92. (Cited on page 7.)

[4] *Experimental Study of Smoke Control in Subway Station for Tunnel Area Fire by Water Mist System*, 2011. The 5th Conference on Performance-based Fire and Fire Protection Engineering. (Cited on page 96.)

[5] S. Komori A. Fujita, R. Kurose. Experimental study on effect of relative humidity on heat transfer of an evaporating water droplet in air flow. *International Journal of Multiphase Flow*, (36): 244–247, 2010. (Cited on page 20.)

[6] A. Tamir A. Kitron T. Elperin. Stochastic modelling of the effects of liquid droplet collisions in impinging streams absorbers and combustors. *International Journal of Multiphase Flow*, 17:247–265, 1991. (Cited on page 23.)

[7] I. Lund G. Holmstedt B. P. Husted, P. Petersson. Comparison of piv and pda droplet velocity measurement techniques on two high-pressure water mist nozzles. *Fire Safety Journal*, (44):1030–1045, 2009. (Cited on page 46.)

[8] B.J.Geurtsand and J.Frohlich. A framework for predicting accuracy limitations in large-eddy simulation. *Physics of Fluids*, 14, 2002. (Cited on page 43.)

[9] M. Sommerfeld C. Mundo, C. Tropea. On the modelling of liquid sprays impinging on on the modelling of liquid sprays impinging on surfaces. *Atom. Sprays*, 8:625–652, 1998. (Cited on page 24.)

[10] H.K. Chelliah. Flame inhibition/suppression by water mist: Droplet size/surface area, flame structure, and flow residence time effects. *Proceedings of the Combustion Institute*, (31):2711–2719, 2007. (Cited on page 67.)

[11] C.T. Crowe, T.R. Troutt, and J.N Chung. Numerical models for two-phase turbulent flows. *Annu. Rev. Fluid Mech.*, 28:11–43, 1996. (Cited on page 17.)

[12] Dougal Drysdale. *An introduction to fire dynamics*. Jhon Wiley ans Sons Ltd, 1999. (Cited on page 11.)

[13] J.K. Dukowicz. A particle-fluid numerical model for liquid sprays. *Journal of Computational Physics*, (35):229–253, 1980. (Cited on page 23.)

[14] E. Migoya et al. Determination of the heat release rate inside operational road tunnels by comparison with cfd calculations. *Tunnelling and Underground Space Technology*, (26):211–222, 2011. (Cited on page 92.)

[15] V. Babrauskas et al. A methodology for obtaining and using toxic potency data for fire hazard analysis. volume 31, pages 345–358, 1998. (Cited on page 97.)

[16] A. Kaiss A.C. Fernandez-Pello B. Porterie F. Nmira, J.L. Consalvi. A numerical study of water mist mitigation of tunnel fires. *Fire Safety Journal*, (44):198–211, 2009. (Cited on page 95.)

[17] M. Pabon G. LeFort, A. W. Marshall. Evaluation of surfactant enhanced water mist performance. *Fire Technology*, (45):341–354, 2009. (Cited on page 45.)

[18] L.G. Gibilaro, R.I.D. Felice, and S.P. Waldram. Generalized friction factor and drag coefficient correlations for fluid-particle interactions. *Chem. Eng. Sci.*, 40:1817–1823, 1985. (Cited on page 19.)

[19] A. Lönnermark H. Ingason. Heat release rates from heavy goods vehicle trailer fires in tunnels. *Fire Safety Journal*, (40):646–668, 2005. (Cited on page 92.)

[20] R. A. Hart. *Numerical modeling of tunnel fires and water mist suppression*. PhD thesis, University of Nottingham, 2005. (Cited on page 46.)

[21] B. P. Husted. *Experimental measurements of water mist systems and implications for modeling in CFD*. PhD thesis, Department of Fire Safety Engineering, Lund University, Sweden, 2007. (Cited on page 46.)

[22] P. J. Roache-C. J. Freitas H. C. P. E. Raad I. B. Celik, U. Ghia. Procedure for estimation and reporting of uncertainty due to discretization in cfd applications. *Journal of Fluids Engineering*, 130(7), 2008. (Cited on pages 32 and 41.)

[23] G. Hu I. Celik, J. Li and G Shaffer. Limitations of richardson extrapolation and some possible remedies. *Journal of Fluids Engineering*, (127):795–805, 2005. (Cited on page 32.)

[24] H. Ingason. Model scale tunnel tests with water spray. *Fire Safety Journal*, (43):512–528, 2008. (Cited on page 92.)

[25] J. Floyd H. Baum-R. Rehm W. Mell R. McDermott K. McGrattan, S. Hostikka. *Fire Dynamics Simulator (Version 5) Technical Reference Guide*. NIST, 2010. (Cited on page 25.)

[26] W.J. Rinkinen K.D. Steckler, J.G. Quintiere. Flow induced by fire in a compartment. Technical report, NBS, 1982. (Cited on page 31.)

[27] A.H. Lefebvre. *Atomization and sprays*. Taylor and Taylor and Francis, 1989. (Cited on page 21.)

[28] L.E.Kollàr, M.Farzaneh, and A.R.Karev. Modelingdropletcollisionandcoalescenceinanicing wind tunnel and the influence of these processes on droplet size distribution. *International Journal of Multiphase Flow*, 31:69–92, 2005. (Cited on page 23.)

[29] A. B. Liu, D. Mather, and R. D. Reitz. Modeling the effects of drop drag and breakup on fuel sprays. *SAE Paper*, (930072). (Cited on page 19.)

[30] Anders Lönnermark. *On the Characteristics of Fires in Tunnels*. PhD thesis, Department of Fire Safety Engineering, Lund University, 2005. (Cited on page 92.)

[31] Hjertager BH. Magnussen BF. On mathematical models of turbulent combustion with special emphasis on soot formation and combustion. Cambridge, MA, 1976. 16th Symposium (International) on Combustion. (Cited on page 11.)

[32] H. Y. Zhang nd Y. S. Zhang, B. Xu, and C. I. Mo. Extension of o'rourke droplet collision model: application to diesel spray of single-hole injector. *SAE Technical Paper*, 2006. (Cited on page 23.)

[33] P. J. O'Rourke and A. A. Amsden. The tab method for numerical calculation of spray the tab method for numerical calculation of spray droplet breakup. *SAE Paper*, (872089). (Cited on page 19.)

[34] Carlo Ortolani. *Combustione, fondamenti e applicazioni*. Città Studi Edizioni, 1998. (Cited on page 97.)

[35] G. Holmstedt P. Andersson. An instrument for determining the total water content in air when extinguishing fires. *Fire and Materials*, 23:187–192, 1999. (Cited on page 46.)

[36] P. Tartarini A. W. Marshall P. E. Santangelo, N. Ren. Spray characterization of high pressure water mist injectors: experimental and theoretical analysis. ILASS, 2008. (Cited on page 50.)

[37] J. Y. Poo and N. Ashgriz. Variation of drag coefficients in an interacting drop stream. *Exp. Fluids*, 11:1–8, 1991. (Cited on page 19.)

[38] *Large eddy simulation of fire plumes*, 2010. Proc. Combust. Inst. (Cited on pages 8 and 27.)

[39] P.J. Roache, K. Ghia, and F. White. Editorial policy statement on the control of numerical accuracy. *ASME Journal of Fluids Engineering*, 108(1), 1986. (Cited on page 32.)

[40] P. E. Santangelo. Characterization of high-pressure water-mist sprays: Experimental analysis of droplet size and dispersion. *Experimental Thermal and Fluid Science*, (34):1353–1366, 2010. (Cited on page 50.)

[41] S. Schurmann. Droplet sizing and characterization of water mist fire protection spray nozzles. ILASS, 2002. (Cited on page 48.)

[42] W. A. Sirignano. *Fluid dynamics and transport of droplets and sprays*. Cambridge University Press, 1999. (Cited on page 16.)

[43] H. Yu T. Jayaweera. Scaling of fire cooling by water mist under low drop reynolds number conditions. *Fire Safety Journal*, (43): 63–70, 2008. (Cited on page 65.)

[44] H.Y. Wang. Prediction of soot and carbon monoxide production in a ventilated tunnel fire by using a computer simulation. *Fire Safety Journal*, (44):394–406, 2009. (Cited on page 97.)

[45] W.R. Marshall W.E. Ranz. Evaporation from drops. *Chem. Eng. Prog.*, 48, 1952. (Cited on page 22.)

[46] M.Z.A. Bakar Y. Wu. Control of smoke flow in tunnel fires using longitudinal ventilation systems - a study of the critical velocity. *Fire Safety Journal*, 90, 2000. (Cited on page 26.)

[47] C. Zhu, S. Liang, and L. Fan. Particle wake effects on the drag force of an interactive particle wake effects on the drag force of an interactive particle. *International Journal of Multiphase Flow*, 20 (1):117–129, 1994. (Cited on page 19.)